Development of low-cost and portable detection platforms for bacterial detection

FRIEDRICH-SCHILLER-
UNIVERSITÄT
JENA

Dissertation

Kumulative

Zur Erlangung des akademischen Gradesd octor rerum naturalium

(Dr. rer. nat.)

vorgelegt dem Rat der Chemisch - Geowissenschaftlichen Fakultät der

Friedrich-Schiller-Universität Jena

Von Master of Science (M.Sc.) Sahar Ahmed Alhogail

geboren am 25.06.1973 in United States of America, Indiana

Gutachter:

  1…Prof. Dr. Jürgen Popp…………………………………….

  2…Prof. Dr. Wolfgang Fritzsche…………………………………….

  Tag der Verteidigung: 19.10.2022

Selbständigkeitserklärung

Ich erkläre, dass ich die vorliegende Arbeit selbständig und unter Verwendung der angegebenen Hilfsmittel,persönlichen Mitteilungen und Quellen angefertigt habe.

Sahar Ahmed Alhogail

Ort: Jena, Datum: Unterschrift des Verfasserin/des Verfassers

Erklärung zu den Eigenanteilen der Promovendin/des Promovenden sowie der weiteren Doktorandinnen/Doktoranden als Co-Autorinnen/-Autoren an den Publikationen und Zweitpublikationsrechten bei einer kumulativen Dissertation

Für alle in dieser kumulativen Dissertation verwendeten Manuskripte liegen die notwendigen Genehmigungen der Verlage für die Zweitpublikation vor.

Die Co-Autorinnen/-Autoren der in dieser kumulativen Dissertation verwendeten Manuskripte sind sowohl über die Nutzung, als auch über die oben angegebenen Eigenanteile der weiteren Doktorandin- nen/Doktoranden als Co-Autorinnen/-Autoren an den Publikationen und Zweitpublikationsrechten bei einer kumulativen Dissertation informiert und stimmen dem zu .

Die Anteile der Promovendin/des Promovenden sowie der weiteren Doktorandinnen/Doktoranden als Co-Autorinnen/Co-Autoren an den Publikationen und Zweitpublikationsrechten bei einer kumulativen Dissertation sind in der Anlage aufgeführt.

Name der Promovendin/   Datum   Ort
Unterschrift des Promovenden

Ich bin mit der Abfassung der Dissertation als publikationsbasierte Dissertation, d.h. kumulativ, einverstanden und bestätige die vorstehenden Angaben.

Name Betreuerin/   Datum   Ort
Unterschrift Betreuer

Name Betreuerin/   Datum   Ort
Unterschrift Betreuer

Acknowledgments

I would like to express my deep and sincere gratitude to my research supervisors, Prof. Jürgen Poppe, Prof. Mohammed M. Zourob, and Dr. Dana Cialla-Maye, Friedrich Schiller University Jena, for giving me the opportunity to continue my PhD degree by providing invaluable guidance throughout this research. Their dynamism, vision, sincerity, and motivation have deeply inspired me. It was a great privilege and honour to work and study under their guidance. I am incredibly grateful for what they have offered me.

I am extremely grateful to my family for their love, prayers, care, and support. I am very much thankful to my husband and my kids for their love, understanding, prayers, and continuous support to complete this PhD journey. Also, I would like to express my thanks to my mother and sisters for their support and prayers. My special thanks go to Prof. Mohammed for the keen support to complete this thesis successfully.

Table of contents

List of tables

List of abbreviations

COVID-19	coronavirus disease 2019
POC	point of care
STEC	Shiga toxin-producing *Escherichia coli*
MERS	Middle East respiratory syndrome
SARS	severe acute respiratory syndrome
ELISA	enzyme-linked immunosorbent assay
sELISA	sandwich enzyme-linked immunosorbent assay
FCM	flow cytometry
NAT	nucleic acid amplification test
PCR	polymerase chain reaction
DNA	deoxyribonucleic acid
NASBA	nucleic acid sequence-based amplification
RNA	ribonucleic acid
mRNA	messenger RNA
rRNA	ribosomal RNA
tmRNA	transferase messenger RNA
HIV-1	human immunodeficiency virus-1
FDA	Food and Drug Administration
CNTs	carbon nanotubes
MRI	magnetic resonance imaging
dsDNA	double-stranded DNA
μPADs	microfluidic paper-based analytical devices
LFAs	lateral flow assays

PADs	paper-based analytical devices
PDMS	polydimethylsiloxane
LFA	lateral flow assay
LFT	lateral flow test
HBV	hepatitis B virus
SPR	surface plasmon resonance
NALFAs	nucleic acid-based lateral flow assays
E. coli	*Escherichia coli*
CRISPR	clustered regularly interspaced short palindromic repeats
PGN	peptidoglycan
GlcNAc	N-acetylglucosamine
MurNAc	N-acetylmuramic acid
EPs	endopeptidases
LTs	lytic transglycosylases
P. aeruginosa	*Pseudomonas aeruginosa*
S. aureus	*Staphylococcus aureus*
AMPs	antimicrobial binding proteases
P. gingivalis	*Porphyromonas gingivalis*
LF	lethal factor
Aur	aerolysin
LPS	lipopolysaccharide
NOS	nitric oxide synthase
BSA	bovine serum albumin
FRET	Förster resonance energy transfer

SPI   papain inhibitory protein

PSA   prostate-specific antigen

BoNT/E-LC   botulinum neurotoxin type E light chain

List of figures

Publications

The following publications are considered for the thesis:

[SAA1] Rapid colorimetric sensing platform for the detection of *Listeria monocytogenes* foodborne pathogen. Sahar Alhogail, Ghadeer A. R. Y. Suaifan, Mohammed Zourob.

[SAA2] Rapid and low-cost biosensor for the detection of *Staphylococcus aureus.* Ghadeer A. R. Y. Suaifan, Sahar Alhogail, Mohammed Zourob.

[SAA3] Paper-based magnetic nanoparticle-peptide probe for rapid and quantitative colorimetric detection of *Escherichia coli O157:H7*. Ghadeer A. R. Y. Suaifan, Sahar Alhogail, Mohammed Zourob.

[SAA4] Simple and rapid peptide nanoprobe biosensor for the detection of *Legionellaceae.* Sahar Alhogail, Raja Chinnappan, Majeda Alrifai, Ghadeer A. R. Y. Suaifan, Floris J. Bikker, Wendy E. Kaman, Karina Weber, Dana Cialla-May, Jürgen Popp, Mohamed B. Alfageeh, K. Al-Kattan, Mohammed M. Zourob.

[SAA5] On site visual detection of *Porphyromonas gingivalis* related periodontitis by using a magnetic-nanobead based assay for gingipains protease biomarkers. Sahar Alhogail, Ghadeer A. R. Y. Suaifan, Sergio Bizzarro, Wendy E. Kaman, Floris J. Bikker, Karina Weber, Dana Cialla-May, Jürgen Popp, Mohammed Zourob.

[SAA6] Rapid colorimetric detection of *Pseudomonas aeruginosa* in clinical isolates using a magnetic nanoparticle biosensor. Sahar Alhogail, Ghadeer A. R. Y. Suaifan, Floris J. Bikker, Wendy E. Kaman, Karina Weber, Dana Cialla-May, Jürgen Popp, Mohammed M. Zourob.

1. Motivation

Infectious diseases are the leading cause of mortality and morbidity in most developing countries and rank between the second and the sixth position as a cause of concern in other parts of the world. Human history has witnessed many pandemics leading to mass death. For instance, the outbreaks of the Black Death (bubonic plague), cholera, smallpox, and, recently, COVID-19, resulted in millions of demises. The COVID-19 pandemic emphasizes the importance of developing point-of-care (POC) diagnostics test.

Over time, clinical microbiology played a key role in helping clinicians diagnose such diseases. Anton van Leeuwenhoek invented the microscope in 1683, and since then, a new world of living organisms has been unveiled [1]. Subsequently, the Gram staining assisted in dividing the enormous collection of bacteria into different groups based on stain interaction, the shape of the organism, and their source. Furthermore, the acid-fast stain facilitated recognizing mycobacteria, while the Albert stain supported the presence of *Corynebacterium diphtheriae.* These developments helped in administering specific antiserums and developing particular treatments at the beginning of the 20th century [2].

The consolidation of the germ theory of diseases by Louis Pasteur and Robert Koch in the late 1870s was one of the most remarkable turning points in biological and medical history. Moreover, the advent of electron microscopy in the 1930s made it possible to detect the anatomy of microorganisms, enabling the visualization of nucleoids, ribosomes, cell walls and membranes, and flagella to provide a specific diagnosis of pathogens. In 1928, Frederick Griffith, a British physician, started the molecular diagnosis of bacteria through DNA. From the second half of the 20th century, major breakthroughs and significant developments took place in diagnostic medical microbiology, which reflected broadly on medical practices and saved millions of lives.

In medical practice, identifying the disease-causing pathogens as early as possible is crucial in fighting the infection and saving lives. Infectious pathogens are present everywhere around us, in food, water, soil, air, etc. The old-fashioned microbiology techniques (plating, culturing, and biochemical assays) are time-consuming and need highly trained personnel, who may not be available in developing countries or even in rural areas of the developed world. Conversely, although being sensitive and precise, modern microbiology relies on high-tech, costly equipment that requires heavy investments and may not be affordable in many parts of the world. Hence, the ideal microbiology diagnostic tool should be highly sensitive, specific, easy to operate, and affordable to provide a point-of-care (POC) diagnosis technique. Moreover, any such device should have a short turnaround time to give results promptly. Since specific

environments are the primary source of particular virulent pathogens, a portable diagnostic tool that provides on-site, accurate, and quick diagnosis will have a major role in preventing and curing severe diseases and outbreaks. Recognizing a source of infection and aborting an outbreak is vital for public health.

Bacterial diseases have caused devastating health issues in human history. Until the mid-20th century, pneumonia, caused by a bacterial infection, was probably the leading cause of death among older people. Improved hygiene, disinfectants, clean food handling, vaccines, and antibiotics have substantially reduced the mortality rates from bacterial infections. On the other hand, several novel bacterial infections have emerged in the recent past, including toxic shock syndrome, Lyme disease, campylobacteriosis, Legionnaires' disease, and new infections of *Escherichia coli* 0157:H7, *Helicobacter*, and *Bartonella* [3]. Thus, the virulence and pathogenicity of bacteria are changing rapidly [4]. Consequently, bacterial infections still cause numerous community health issues, hospital-acquired diseases, and foodborne ailments.

The United States reported data on foodborne diseases in 2019. Since 2015, a total of 25,606 infections were reported that together led to 5,893 hospitalizations and 120 deaths. The organisms associated with the infections were found to be *Campylobacter*, *Cyclospora*, *Listeria*, *Salmonella*, Shiga toxin-producing *Escherichia coli* (STEC), *Shigella*, *Vibrio*, and *Yersinia* [5]. Likewise, periodontitis affected 5–15% of the global adult population [6].

Since the 1970s, around 40 infectious diseases have been reported as endemic, such as the Middle East respiratory syndrome (MERS), severe acute respiratory syndrome (SARS), Ebola, chikungunya, swine flu, avian flu, Zika, and recently, novel coronavirus disease (COVID-19) most happened in low-income countries with poor resources and lack of technology skills. Providing rapid, low cost, highly sensitive and specific and easy to conduct diagnostic test will be of great benefit to the humanity.

2. State of the art

Various bacterial detection methods have been developed to date. Bacterial culturing and plating are the oldest and gold-standard methods for the recognition of bacteria and pathogens. However, cultural isolation is labor-intensive, relatively expensive, time-consuming to perform, and has constraints such as contamination by the overgrowth of undesired, rapidly multiplying microorganisms. Moreover, microbial identification by culture methods followed by biochemical analysis may take up to 10 days to confirm positive samples of certain pathogens [7] [8].

Because of the limitations of culture-based techniques of bacterial identification, other methods, such as immuno-based techniques, were adopted. Among these approaches, the enzyme-linked immunosorbent assay (ELISA) is the most commonly used technique. ELISA is a quick, convenient, and safe test that can detect a very low concentration of an antigen through a highly specific antibody. Multiplex ELISA can be used to identify multiple antigens/antibodies simultaneously [9]. The sandwich enzyme-linked immunosorbent assay (sELISA) has a detection limit of 10^2 cfu/mL of *Salmonella typhi* (*S. typhi*) following enrichment [10]. For quantifying a component or structure of cells by optical means, flow cytometry (FCM) is also a potential technique. FCM is a costly and sophisticated technique that requires highly trained personal and ongoing maintenance with warm-up laser calibration[11].

Nucleic acid analysis methods are advanced techniques that are widely used for the clinical diagnosis of infectious diseases. In all amplification methods, a purification step is required to purify and concentrate the genetic material from the raw sample because certain components in the clinical sample can inhibit amplification [12] [13].

Polymerase chain reaction (PCR) has been widely used for diagnosis due to its incredible sensitivity and specificity. Nevertheless, some of its limitations include the need for high-quality DNA, nonspecific binding of the primer to other similar sequences on the template DNA, the requirement of an electrically powered thermocycler, and an optimized experimental setup [14].

Isothermal amplification-based techniques are methods of great interest to researchers. Nucleic acid sequence-based amplification (NASBA) is used to amplify RNA, such as messenger RNA (mRNA), ribosomal RNA (rRNA), transferase messenger RNA (tmRNA), and single-stranded DNA (ssDNA), using isothermal conditions, i.e., a constant temperature from 37 to 42 °C.

NASBA can produce up to 10^9 copies within 90 min. Therefore, it is a sensitive diagnostic tool that can determine gene expression and cell viability [15]. Moreover, on-chip real-time NASBA

commercial kits that do not require sample preparation are also available. Hepatitis B virus has been detected with NASBA at 0.4 ng. Moreover, its use has also been approved by the Food and Drug Administration (FDA) for the molecular detection of hepatitis C and HIV-1 [16] [17].

2.1 Nanosensors in medical diagnostics

For the effective treatment of a disease, diagnosis is the first step that helps in reducing complications and disease mortality [18]. Traditional biosensors, which detect structural and compositional deficiencies in human secretions, are made of microparticles. They usually have limitations, such as time-consuming, lack of precision, and the requirement of a large number of samples [19] [20] [21]. To overcome these problems, nanomaterials can be utilized as an alternative for the rapid and accurate diagnosis of certain diseases.

Nanosensors have a wide range of advantages, the main one being their high penetration ability [22]. Nanoparticles have a large surface-to-volume ratio due to their extremely small size, which enhances the detection sensitivity even at femto, atto, and zepto scales [23]. Nanoparticles have several properties that make them ideal candidates to be utilized as rapid diagnostic tools. These properties include an enhanced surface reactivity, specific electrical and magnetic characteristics, and a flexible structure and shape, which can easily be transformed to enhance their function [24] [25]. Their surface can also be tailored to enhance their affinity and binding patterns with specific analytes [26]. Furthermore, nanoparticles can be molded into a variety of shapes, such as nanotubes, nanowires, nanocantilevers, and thin films, positively affecting the sensitivity and stability of these sensors [27] [23].

A variety of nanoparticles can be used as biosensors, which provide advantages over conventional methods. These nanoparticles include (1) metals and metal oxides [28] [29], (2) carbon-based materials such as nanotubes [30], (3) photonic crystal materials [31], (4) nano/microgels [32], and (5) nanomagnetic particles [33].

Metal and metal oxide nanoparticles are widely used for different purposes. The most commonly used metal particles include Au, Ag, Cu, Co, Pd, and Pt [34]. They provide advantages such as high sensitivity, improved selection, and high-end stability. These particles have various applications, ranging from the diagnosis of different diseases and the detection of pathogens in different media to the detection of toxic chemicals in environmental samples and the detection of hazardous gases [35]. Carbon-based nanoparticles, such as carbon nanotubes (CNTs), graphene, and nano/mesoporous carbon, have a wide range of applications in environmental control and biomedicine. CNTs are most commonly used for medical diagnosis as they have high sensitivity, specificity, and affinity for different biomolecules, thus providing excellent and quick diagnosis [36] [37].

Photonic crystals consist of materials with different dielectric constants, allowing them to control the movement of photons, resulting in the reflection of specific wavelengths. They have a wide range of applications in biosensing, biomarker detection, displays, bioconductors, and solar cells [38] [31]. They are favored over other biosensors due to their high sensitivity, specificity, and real-time monitoring [39]. They can be coupled to other sensing techniques for improved diagnosis, better drug delivery, and tumor screening [40] [31]. Nanogels are a special type of material with biomedical applications. They come with several advantages, such as high sensitivity, improved stability and solubility of the injected drug, target identification, intracellular delivery of drugs, protection from enzymatic and chemical degradation of drugs, low cytotoxicity, a large surface area, and a large amount of drug encapsulation [41] [42].

Magnetic nanoparticles are a special type of particle with numerous applications in biomedicine and medical diagnostics. They have unique properties, such as a large surface area, binding affinity with ligands, stability and resistance to different body fluids, and easy access to the target site [43]. They have a range of applications, such as drug delivery, immunoassays, biosensor development, cellular labeling, and, most importantly, magnetic resonance imaging (MRI) [33]. The challenges with these particles include their agglomeration, toxicity, blood circulation time, stability under different physiological conditions, surface charges, and resistance to oxidation [44] [33]

Biosensors have three structural components: (a) a bioreceptor (b), a transducer, and (c) a signal processor [45]. The bioreceptor binds to the target compound associated with a specific disease, generating a specific type of signal. The bioreceptor can be an antibody, a protein, an enzyme, a cell, a nucleic acid, or a whole organism [46]. These signals are modified by the transducer and transmitted to the signal processor, which gives an actual report about the number and nature of biomolecules present [47]. Nanoparticles can be used for the enhancement of the sensitivity of all these components. A variety of nanomaterials can be used for designing nanobiosensors. These materials include (1) metals and metal oxides [48] [29] [49], (2) carbon-based materials such as nanotubes [50] [30], (3) nanocomposites [51], (4) magnetic nanoparticles [52], and (5) nanochannels [53].

Sensors can be classified either on the basis of signal production (bioreceptor) or on the basis of the different methods employed for signal transduction (transducer) [54].

The signal production of a bioreceptor is an important element of a biosensor that must be specific and sensitive to the target analyte [55]. Biosensors can be classified into five groups: enzyme-based sensors, immunosensors, DNA/nucleic acid sensors, cell-based sensors, and biomimetic sensors.

Enzyme-based sensors were the very first type of sensor to be developed. These sensors work on the principle of binding to and catalyzing the analyte. An enzyme is capable of detecting a specific

analyte from a mixture [56]. These biosensors have high sensitivity due to enzyme–substrate specificity, which makes them ideal candidates for applications [57]. Enzyme-based sensors have few limitations, such as sensitivity to pH, temperature, the presence of inhibitors, and substrate concentration [58].

Immunosensors are antibody-based sensors with high specificity. Every antibody has two heavy chains (H) and two light chains (L). Each chain has a constant and a variable region. The variable portion is antigen-specific. Immunosensors are composed of antigens and use the binding ability of antibodies. These sensors are stable and versatile [59] [54]. Immunosensors play a significant role in various areas, such as clinical chemistry, food quality, and environmental monitoring [60]. These sensors can be utilized for the early detection of different diseases, especially cancer [61].

DNA/nucleic acid sensors utilize ssDNA sequences to bind to target sequences, thereby forming dsDNA. This reaction results in a biochemical reaction that makes it easy for the transducer to amplify the signal, resulting in rapid detection [54]. The working principle of these sensors is binding to complementary sequences present in a sample. They have high specificity and can be regenerated by denaturation to reverse the binding [62]. An optical biochip was designed for the detection of bacteria with a detection limit of 8.25 ng/ml [63]. The major advantage of DNA-based sensors is specificity.

Cell-based sensors contain whole cells that are utilized as sensing elements. These elements detect changes in internal and external cellular conditions and produce a specific type of response. They can also monitor different growth parameters [64]. Microorganisms can also be used as a biosensor. In contrast to other types of sensors, these sensors are resistant to various harsh conditions. As evident from previous studies, these types of sensors can be used for different purposes, such as clinical chemistry, food quality, environmental control, drug detection, and pharmaceutics [65] [66] [67].

Biomimetic sensors are synthetic compounds that function as natural biosensors. These include aptasensors, which have aptamers as sensing elements [56]. Aptamers are considered artificial nucleic acid ligands. They act like antibodies and can detect a larger range of targets than other types of sensors [68].

Bioreceptors based on transduction can be classified into four types: electrochemical, optical, piezoelectric, and colorimetric bioreceptors.

Electrochemical biosensors are gradually becoming more popular due to the rapid improvement in sensitivity and design [69]. These sensors provide some advantages over other types of sensors, such as high sensitivity, rapid detection, low price, simple design, and less complex instrumentation [70]. Electrochemical sensors are subdivided into four major groups: amperometric, potentiometric, impedance, and conductometric sensors.

7

Optical-based sensors are widely used in different fields. The most commonly used optical sensors include surface plasmon resonance, chemiluminescence, fluorescence, and optical fiber sensors. The advantages of these sensors include flexible detection, in vivo detection, and easy signal reading. The common limitations associated with them are signal bleaching, a high probe concentration, and less scattering ability [71] [72].

Piezoelectric sensors work on the principle that a vibrating crystal resonates at a natural frequency. The transducer is made of piezoelectric material, such as quartz coated on the surface of the bioreceptor [73]. Calorimetric-based sensors have been used in the clinical field, the food industry, and environmental monitoring [74] [75]. This method is favored due to its high stability, enhanced sensitivity, and possibility of miniaturization.

Smart nanobiosensors have personalized health wellness management. This type of diagnosis, which can detect analytes at low concentrations, is extremely useful in evaluating the effectiveness of a treatment. Thus, affordable, intelligent diagnostic tools are required, especially for outbreaks and epidemic states. Smartphones with advanced nanotechnology in conjunction with microfluids have been developed for viral detection. Such smartphones have been developed for Zika virus, hepatitis B, and hepatitis C, with high sensitivity [76]. One of the most common oncogenic viruses, the human papilloma virus, has been detected using a smartphone with DNA-based target hybridization without the amplification steps [77]. Nanosensors can provide rapid medical diagnosis, with higher sensitivity and specificity than conventional methods. Due to their many advantages and spectacular properties that simplify the design, these sensors use a smaller sample volume.

2.2 Paper-based detection methods

Paper-based sensors have been used in a variety of analyses for a long time. They have been studied for various applications as early as the 1800s [78]. Over time, they have emerged as one of the core subjects in medical research as scientists strived to manufacture sensing platforms using paper-based materials [79].

Paper-based biosensors can be categorized into three subgroups: dipstick assays, microfluidic paper-based analytical devices (also termed microPADS or μPADs), and lateral flow assays (LFAs). Among these, the dipstick assays exhibit a remarkably simple design [80]. This biosensor category is based on the principle of blotting the test substance onto a paper that already contains pre-stored reagents. Well-known examples of this group are pH strips for measuring the pH value and urinalysis dipsticks for detecting metabolic products. Nevertheless, these biosensors do not offer a wide range of compatibility with different biological substances. Moreover, another downside of this strategy is that it is not possible to develop highly sophisticated assays, which are often required in diagnostic applications.

Microfluidics technology was developed to overcome the limitations of the relatively simple paper-based biosensors. The μPAD biosensors have brought about a plethora of developments in paper-based biosensor applications [81]. Several modifications to μPAD technology have been introduced to detect target samples using electrochemical- [82], optical- [83], chemiluminescence-, and fluorescence-based approaches.

Paper-based analytical devices (PADs) use cellulose as the primary substrate for the point-of-care diagnosis. The PADs make extensive use of polydimethylsiloxane (PDMS) as a structural component. PDMS offers several advantages, such as flexibility, easy handling, and low cost, and therefore PDMS plotting is considered a promising method of constructing μPADs [84]. Most μPADs target different body fluids, such as uric acid, lactate, glucose, and choline, as biomarkers [85]. Enzyme-based μPAD biosensors provide rapid, accurate, and robust diagnosis for clinical purposes. However, because of the use of enzymes as constituents, these biosensors are heat sensitive and require special storage conditions to avoid thermal denaturation.

Lateral flow assays (LFAs) are deemed to be the gold-standard detection tools among the three types of paper-based biosensors. These biosensors have numerous applications in clinical diagnostics, and they are considered an exceptional strategy for detecting diseases. LFAs can employ a wide range

of biological samples, including urine, sweat, and saliva. Moreover, serum, whole blood, plasma, and other body fluids can also be used. LFAs are used in various fields, such as the food industry, veterinary medicine, quality control, and the monitoring of environmental hazards. Hence, these sensors are already employed for detecting diseases, pathogens, compounds of interest, hazardous chemicals, and environmental pollutants [86].

LFAs have established their significance as detection tools, and the current research focuses on improving their performance and sensitivity. In this research, LFAs have been combined with different analytes, giving rise to multiple types of LFAs, such as nucleic acid-based, antibody-based, and enzyme-based LFAs. Antibody-based LFAs are particularly worth mentioning for detecting different microbes. The principle of immune LFAs is similar to that of ELISA. Both techniques use secondary antibodies attached to labels, such as fluorescent molecules, gold nanoparticles, and quantum dots, to identify analytes, enabling the visual detection of color changes upon binding with the target. In recent developments, certain other materials, including carbon, latex, colloidal gel, and up-converting phosphor particles, have also been employed for developing lateral flow tests (LFTs).

Nanoparticles have emerged as promising candidates for labels in the fabrication of rapid diagnostic kits for better diagnosis and treatment of medical conditions [87]. Moreover, immune-based assays have also become popular as detection tools. Many immune-based lateral flow assays have already been introduced to detect disease-causing agents and are commercially available and used for point-of-care diagnosis. These assays can detect bacteria, microbial toxins, and viruses. One prominent and recent example is the coronavirus 2019 (COVID-19) detection kit, which targets both antigens and antibodies. This technique offers a cost-effective and rapid diagnosis of COVID-19 at distant locations and far-flung health facilities [88]. Other examples include C-reactive protein diagnosis kits, which identify target proteins in the blood, plasma, and serum [28]; brucellosis detection kits, which identify specific anti-brucella antibodies [26]; and antigen-based detection kits for detecting infection with *peste des petits ruminants* from feces and nasal swabs [27]. Furthermore, LFTs have also been developed to detect biological warfare agents, Avian influenza viruses, and bacterial contaminants, such as *Escherichia coli* O157:H7, *Bacillus anthracis*, *Yersinia pestis*, and *Francisella tularensis* [89].

LFT sensors are typically immobilized onto the surface through chemisorption or physisorption. The interaction between the reagent and the analyte takes place at the transducer surface via antigen–antibody reaction, protein–protein interaction, or nucleic acid hybridization. The detection setups utilize electrochemical, optical, piezoelectric, magnetic, mechanical, or thermal mechanisms of analyte detection. These biosensors consist of three vital components: a bioreceptor, a transducer, and a detector. The bioreceptor specifically detects the target biomarker. The transducer utilizes different

transduction mechanisms to modify the biochemical events into a readable signal, while the signal processor or detector processes and quantifies the results [90].

Recently, these biosensors have seen tremendous improvements, and the available versions can be divided into hand-held diagnostic units and compact bench-top systems [91].

One of the variations of LFAs, protein-based LFAs, has shown promising clinical diagnostic applications. Xua et al. (2015) reported an LFA biosensor for detecting hepatitis B virus (HBV) antigens in serum. The assay is based on a protein microarray using surface plasmon resonance (SPR) as a biosensor to detect HBV serum antigens. Systematic optimization of different parameters, such as the printing buffer, protein immobilization time, and concentration of the capture proteins, was used for performance evaluation. Under optimized conditions, the biosensor detected five different biomarkers of HBV simultaneously in half an hour employing just a 20 µL sample. In contrast, traditional diagnostic methods such as ELISA and PCR detect only one biomarker in four hours. Thus, it is evident that biosensors offer a significant advantage over traditional methods of clinical diagnosis [92].

A nucleic acid-dependent version of LFAs has also been introduced in recent times. The nucleic acid-based LFAs (NALFAs) work on the principle of DNA hybridization with complementary sequences found in the DNA of the target pathogen. The DNA is coated onto the surface of nanoparticles (NPs), often gold, e.g., DNA–AuNPs. This type of biosensor uses a colorimetric signal transduction mechanism, producing different colors upon the successful binding of the probe to the target DNA sequence. In the recent past, the use of CRISPR-Cas in LFAs was also reported. These paper-based LFAs employ CRISPR-Cas coupled with isothermal amplification of DNA for identifying target DNA. This approach provides excellent specificity and sensitivity. The sensitivity of this technique can be further enhanced, and the sample preparation can be simplified by using sequence-specific cleavage of reporter groups from amplified DNA. Nevertheless, the adoption of such improvements would require the additional processing of samples with enzymes [93].

A novel diagnostic method based on a simple paper strip LFA for the rapid detection of *Escherichia coli* (*E. coli*) nucleic acids in human feces has also been developed [94]. The biosensor exploits 23S rDNA–gold nanoparticles (AuNP) probes. The key advantage of this method is that it does not require PCR for DNA amplification or any special instrumentation for sample preparation. The assay employs colorimetric transduction, which allows visual detection of target DNA without any extra equipment. Furthermore, nucleic acid-based LFAs have also been developed for the rapid and accurate detection of different strains of *Listeria* spp., especially *Listeria monocytogenes* in food samples [95]. A wide variety of these biosensors are commercially available for the detection of various pathogens;

the most commonly employed detection platforms are for *E. coli*, *Helicobacter pylori*, influenza A and B viruses, HIV, tuberculosis, and malaria [96].

The paper-based biosensors have excellent properties for detecting pathogens. Furthermore, colorimetric target identification is possible with these sensors, making them an excellent choice for diagnostic purposes.

Paper-based biosensors have been applied in many fields, ranging from diagnosis of different medical conditions to food quality control and monitoring of environmental parameters. They offer simple, inexpensive, and portable detection tools for clinical diagnostics. Moreover, these sensors are easy to handle and portable and do not require complex instrumentation, thus presenting a significant advantage over other diagnostic approaches. Paper-based biosensors also offer superior sensitivity and detection limits compared with commonly used sensing methods [97] [90].

2.3 Proteases

2.3.1 Introduction

Protease enzymes are found in all life forms and are ubiquitously present in plants, animals, and microorganisms. Microbes, either bacteria or fungi, produce a variety of proteases, such as seryl, aspartyl, cysteinyl, and metalloproteases. Proteases have been characterized based on functional groups and the position of the peptide bond [98, 99]. Microbes produce intracellular proteases responsible for differentiation, protein turnover, and maintenance of the cellular protein pool within the cell. The extracellular category of proteases is important for the hydrolysis of proteins into amino acids and peptides outside the cell [100, 101].

Proteases are considered the largest functional group of proteins. They are essential for the proliferation, colonization, and attachment of bacteria to the host. They also play an essential role in destroying the host tissues, thus facilitating bacterial virulence. Bacterial infections trigger the activation of host protease cascades. Proteases even work under a wide range of pH values, from neutral to alkaline, based on their specificity of action. The proteolytic activity of proteases has been widely studied for different applications [102]. Proteases have gained interest not only due to their vital role in biological processes but also due to the many applications in different fields, such as medicine, nutrition, and agriculture. To list a few, the current applications of proteases include the development of photographic films, waste treatment, detergent preparation, and silver recovery [103]. These enzymes have been adopted in the medical field as diagnostic markers in periodontal diagnosis and wound infection treatment. Proteases have also been used as therapeutic targets in HIV and hepatitis C infection (Figure 1.1).

Figure 1.1: Application of protease enzymes in the medical, agriculture, and environmental sectors

2.3.2 Protease mode of action

The bacterial cell wall provides resistance to external pressure, offers protection from environmental threats, and determines cell shape and type. The cell wall consists of peptidoglycan (PGN), which is present in almost all Gram-positive and Gram-negative bacteria. PGN is a linear glycan heteropolymer chain containing alternating N-acetylglucosamine (GlcNAc) and N-acetylmuramic acid (MurNAc) units. This unique structure, known as (murein) sacculus, forms a mesh linked by β-1→4 bonds. It also supports other cell envelope components, such as proteins and teichoic acids [104] [105].

Protease enzymes, produced by bacteria, contribute to the proliferation and growth of the cell. During cell replication, the PGN sacculus expands through the coordinated action of degradative and synthetic enzymes. PGN peptides are hydrolyzed by proteases and released into the extracellular medium during the growth process, most of which are transported back to the cytoplasm for reuse, referred to as PGN turnover. After completing this process with endopeptidases (EPs) and lytic transglycosylases (LTs), monomeric 1,6-anhydro-muropeptides are produced and transported into the cytoplasm with the help of AmpG permease. Inside the cell, it serves as a substrate for NagZ b-N-acetylglucosaminidase and the AmpD amidase. Each generation of Gram-negative bacteria, such as *E. coli,* breaks down and reuses over 60% of the cell wall's PGN [106].

General and regulated proteolysis in bacteria is essential for cellular homeostasis, which relies on the high substrate specificity of the executing AAAþ proteases [107]. Moreover, Lon protease degrades unfolded or damaged proteins and has an essential part in regulatory processes and proteotoxic stress [108]. Furthermore, mitochondrial ATP-dependent protease is also crucial for homeostasis. Likewise, vegetative autolysins, such as LytD glucosaminidase, LytC amidase, and LytF (CwlE, YhdD) endopeptidase, have several important roles, including cell wall turnover, cell separation, protein secretion, mother cell lysis, antibiotic-induced lysis, and motility [109] [110].

2.3.3 Bacterial proteases as virulence factors

Bacterial proteases have been considered to be the most critical virulence factor for all bacteria. They play an important role in facilitating invasion, replication, and the establishment of infection [48]. Many bacteria secret proteases that attack host-associated proteins. Their actions involve degrading and splitting protein molecules into small fragments, leading to the inactivation or breakdown of proteins. The manifestations of the respective diseases attributed to microbial proteases are very complex and nonspecific. Also, bacterial proteases have been reported to affect the blood clotting system [111]. For

14

instance, the bacterial proteases of *Pseudomonas aeruginosa (P. aeruginosa), S. aureus, Proteus mirabilis,* and *Enterococcus faecalis* have been found in chronic wounds [112].

Proteases are classified into exoproteases and endoproteases based on where they introduce the cleavage, i.e., near or away from the carboxyl or amino-terminal portion in the targeted protein. Among the bacterial proteases, some are non-targeted and can degrade a wide range of proteins, while others are highly targeted. For instance, extracellular bacterial proteases degrade proteins of host tissues to provide nutrients to the bacteria. Thus, this type of protease aids in nutrient acquisition, helps establish an infection, and assists in evading and destroying the host immune defenses. They also help in the local and systemic spread of bacteria [113].

Some of the proteases interfere with immune functions, for instance, by cleaving proteins involved in the host immune defense, as in the case of ZapA from *Proteus mirabilis* [114]. In the case of an IgA1 protease secreted by pneumococci, the protease cleaves IgA into its inactive components, thus destroying the antibody molecules. Similarly, some proteases, such as Zn-metalloprotease, impair phagocytosis by changing the bacterial cell's surface proteins. Furthermore, some proteases act by inhibiting chemotaxis, thus obstructing the pathway of immune cells' communication [115]. Generally, bacterial proteases have an essential role in the intracellular regulation of biofilm production in various bacteria and can serve as antibiotic treatment for bacterial infection [116].

Bacterial proteases have a propensity for host tissue destruction either by direct breakage of the skin barrier or by indirect damage through the induction of an excessive and prolonged inflammatory response. Persistent secretion of proteolytic enzymes interferes with the host protease regulatory mechanism, leading to delayed healing of wounds [117]. *P. aeruginosa* invades the circulatory system with the help of bradykinin protease to establish infections in humans.

Numerous bacterial proteases, such as aerolysin (Aur), cysteine proteases, staphopain A, staphopain B, serine protease V8, and metalloprotease, are produced by *S. aureus*. These enzymes are involved in inactivating the complement system (a component of the host immune system) [118]. Moreover, some bacterial proteases have a neutralizing effect, such as antimicrobial binding protease (AMP) secreted by *P. aeruginosa* and LasB gingipin R secreted by *Porphyromonas gingivalis* (*P. gingivalis*).

Bacterial proteases also participate in the intoxication process, such as pertussis toxins, fragment A from diphtheria, and the metalloproteases in tetanus and botulinum neurotoxins [119]. *Bacillus anthracis* produces a zinc-dependent metalloprotease with a protease-specific activity that functions as a lethal factor (LF) [120]. Previous findings have also shown that bacterial proteases

contribute to host tissues' pathological process; for example, the secreted metalloprotease from *L. monocytogenes* is responsible for the activation of phospholipases [121].

In conclusion, the literature reveals that proteases secreted by pathogenic bacteria and host communication signals play an important role in pathogenicity [122].

2.3.4 Microbial protease pathogenesis

The manifestation of bacterial pathogenesis is strongly influenced by the host immune defense's strength and the microbial virulence factors. The severity of an infection is shaped by the virulence of the invasive microbes and the immune state of the host. For instance, virulent microbes can cause a severe infection in an immunocompromised patient, whereas the same virulent pathogens can be eradicated by an immune-competent host [123].

Protease accretion, which can cause direct tissue destruction, is the most classical pathogenesis mechanism for certain bacterial species. As in the case of open wounds and burnt skin, the accumulation of various bacterial colonies and the secretion of different protease enzymes hamper the healing process and delay recovery [124]. *P. aeruginosa* secretes various proteases, including LasA protease, elastase (LasB), protease IV, alkaline protease, cysteine protease, and metalloproteases. These enzymes were proposed to be important virulence factors in tissue degradation.

Microbial proteases also trigger host zymogen protease production, which is associated with critical clinical outcomes, especially in tissues, such as the cornea, with low blood supply and, consequently, lack of defense proteins and leukocytes[125]. The role of proteases and their inhibitors is pivotal in the degradation of tissues, as a balance between the two types of enzymes is crucial. The excessive production of protease inhibitors from hosts results in an increase in the bacterial invasion of connective tissues due to a translocation of the infection sites and changes in tissue properties [126]. Moreover, bacterial proteases have been found to influence or augment the infection of other causative agents as well. Serine protease from house dust mites is an example of a protease that enhances the deleterious effects of influenza virus infectivity and replication in the lung tissues of mice [127] [128].

Pseudomonas elastase generates bradykinin in the infected host via a Hageman factor-dependent pathway. Bradykinin (kinin), an endogenous nanopeptide, relieves severe pain and causes dilation of the vascular smooth muscles. Relaxation of endothelial muscle cells results in hypotension, shock, and increased extravasation [129]. Bacterial proteases are known to activate one or more steps

of the kinin release affecting the Hageman-factor-kallikrein cascade. Moreover, many microbial proteases inactivate various plasma inhibitors, such as α1-protease inhibitor and α2-macroglobulin. In addition to the extracellular proteases, the negative charge-carrying lipopolysaccharides (LPS) of the Gram-negative bacterial cell wall and the teichoic acid of the Gram-positive bacterial cell wall activate the Hageman-factor-kallikrein system because of the hypotensive effects of kinin production. Endotoxins also induce nitric oxide synthase (NOS), which appears to exhibit a relatively slow but significant effect on the relaxation of the vascular tone of the infected animal (thus causing hypotension).

Furthermore, bacterial proteases can activate the matrix metalloproteinase (collagenase), resulting in an exacerbation of tissue injury in the diseased animal. Many tumor cells or tissues excrete plasminogen activator and hence activate plasminogen. The plasmin, thus generated, activates procollagenases, as well as the Hageman-factor-kallikrein system, resulting in pronounced extravasation. Fluid accumulation in pleural and ascitic carcinomatosis is mostly due to the activated bradykinin-generating system.

Bacterial proteases induce shock in mice. The protease-elicited shock can be prevented by a soybean trypsin inhibitor that blocks the kallikrein-kinin cascade. Kinin antagonists and a kallikrein inhibitor have been employed for infectious diseases, such as septicemia, and in tumor pathology [130].

2.3.5 Diagnostic tests based on proteases as biomarkers

High specificity and sensitivity are essential requirements for a useful assay for diagnostic purposes. The widespread use, simplicity, reliability, and relatively low cost of the home-used pregnancy test make it an example of an optimal assay. The solid media screening technique is based on visualizing the microbial protease production using specific media supplemented with a particular substrate, such as skim milk agar, casein agar, gelatin agar, fibrin agar, elastin bovine serum albumin (BSA) agar, and hemoglobin [131]. This method has been used for the detection of *S. aureus* extracellular protease. A novel agar-based platform incorporating colorimetric visualization was used for this purpose; the strategy provided a detection limit of 10^2 cfu/mL [132]. Thus, extracellular proteases can be detected directly in the culture medium through this approach. It is a qualitative, simple, low-cost, and straightforward assay for assessing the presence of proteolytic activity of colonies of the microbe of interest. This technique also offers great freedom in substrate selection [133].

Another method is the fluorometric method, which is based on the use of fluorophore-conjugated substrate. It is a suitable technique for the detection of small quantities of microbial protease. Fluorometric methods are highly sensitive and provide excellent specificity. The proteolytic activity is detected by fluorescence emitted from the fluorophore after cleavage. Förster (fluorescence) resonance energy transfer (FRET) has been used to measure the proteolytic activity of protease by measuring the increase in fluorescence or the shift in wavelength resulting from the cleavage of the substrate labeled with fluorophore pairs (Figure 1.2). For detecting proteases, BODIPY dye is utilized as a fluorogenic substrate. The fluorescence emitted after the cleavage of the substrate is proportional to enzyme activity. The BODIPY dye is specific and highly sensitive and provides a wide range of detection [134] [135] [136] [137].
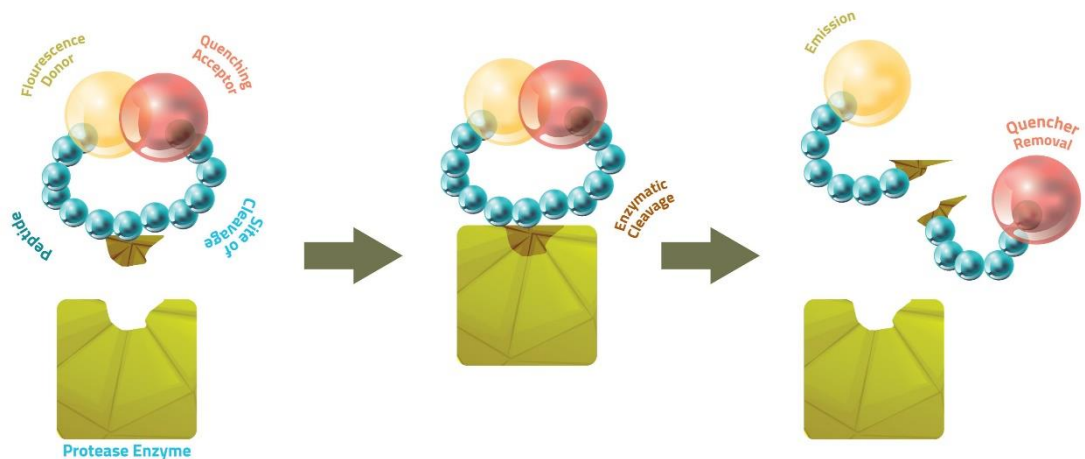
Figure 1.2 Fluorometric method for protease detection using peptide sequences from the FRET-substrate library. The proteolytic activity of protease is monitored by the increase in fluorescence or the shift in wavelength resulting from the cleavage of the substrate labeled with fluorophore pairs.

Kaman et al. [138] compared the FRET assay with other traditional methods for detecting *P. gingivalis* in patients' samples. The assay showed comparable results to those of the other methods utilized (culture-based as well as PCR). The technique was also studied for predicting virulence and pathogenesis of the protease enzyme secreted by *P. aeruginosa* [139]. Moreover, Zindel et al. [140] successfully employed this assay to evaluate the levels of *Streptomycin mobaraensis* papain inhibitory protein (SPI), which is secreted as an antagonist of bacterial growth.

Combinatorial use of FRET and real-time PCR, referred to as FRET-based real-time PCR, was developed to ameliorate sensitivity, specificity, and test duration. The approach has been successfully employed for diagnosing cutaneous *Leishmania* species [141]. Moreover, fluorescence-conjugated polymers have also been developed to increase sensitivity. Overall, FRET is a rapid and simple

technique. Further, it can be combined with molecular diagnostics, microarrays, real-time PCR, and live-cell imaging [142].

The proteolytic activity of proteases has also been detected using ultrasonic resonance within buffer systems. Born et al. compared its efficacy with the UV-visible/ninhydrin assay. The authors successfully measured protease activity during casein hydrolysis. The results were comparable to those of the other assay employed. This technology makes use of low-intensity, high-frequency ultrasonic waves to estimate different analytes. The technique is non-invasive, requires only a small amount of sample, and can provide continuous measurements. Nevertheless, this detection technology is relatively new and has not been adopted widely [143].

ELISA is an immunological and highly sensitive technique that has been implemented in several applications, such as clinical diagnostics and quality control studies. It is a quick, convenient, and safe technique that can detect a very low concentration of the target through a highly specific antibody. This strategy has also been applied to quantify protease enzymes. ELISA can successfully quantify proteases with a sensitivity of 4µg/mL using the sandwich assay. However, it has been withdrawn for detecting new protease enzymes as structural information of the enzyme is required before using ELISA [144].

Methods based on nanoparticles have also been used for protease detection. Typically, these approaches rely on immobilizing the enzyme substrate on the surface of the nanoparticles. The enzyme to be tested will induce changes in substrate composition, leading to variation in the media surrounding the nanoparticles [145] [146]. Nanoparticles have already been recognized as excellent microbe detection and drug therapy tools and are clinically approved [147].

Various types of sensing strategies can be used with nanoparticle-based biosensors. Gold nanoparticles (AuNPs), quantum dots, and surface-enhanced Raman approaches have been used for this purpose. Polymeric and silica-based nanoparticles are also used as sensing methods for in vivo and in vitro protease detection. These nanoparticles have the advantage of being highly sensitive and quantitative [147].

Protease estimation using electrochemical transduction involves an electrode decorated with a gold nanoparticle/carbon nanotube as an electrochemical sensor that detects the hydrolysis of a peptide substrate triggering an electrochemical current, which provides a sensitivity of as low as 6 pg/mL and a dynamic range from 1×10^{-2} to 1×10^{3} ng/mL. It is a low-cost and precise approach [148]. Another protease-based sensor was developed to detect botulinum neurotoxin type E light chain (BoNT/E-LC). This assay meets the requirements for point-of-care testing (POCT) [149]. Moreover, prostate-specific

antigen (PSA) was also detected using a monolayer of PSA substrate peptide conjugated with magnetic nanoparticles [150].

As mentioned in the literature, protease enzymes secreted from microbes are essential for many vital processes in microbes. Other vital processes include replication, the establishment of the infection by the role of proteases in the invasion, and the escape from host defense mechanisms. Thus, using a specific protease enzyme secreted from pathogens as a biomarker for infection detection is promising.

3. Aim of the work

The aim of this work was to fabricate a flexible, low-cost, colorimetric, instant, and easy-to-handle platform that could be employed for rapid diagnosis for side chair testing by a clinician or to carry out simple inspections in the field. Nanomagnetic particles were used to achieve these features. The designed platform can be used in various patient samples to screen illnesses. Moreover, it can be used for food sample analysis and water monitoring.

In this study, the attention was focused on the pathogen secretions rather than the antigen. Protease enzymes were chosen as biomarkers for each bacterium. To be able to accomplish our goals, the FRET technique was employed to identify the specific peptide sequence used for protease detection, specifically for each pathogen. Subsequently, these peptides were conjugated with nanomagnetic particles to develop a sensitive colorimetric sensor (Figure 1.3).

The sensing platform was generalized to detect several bacteria that cause foodborne diseases, such as *Listeria monocytogenes, Staphylococcus aureus*, and *E. coli* O157:H7. *Porphyromonas gingivalis* and *Pseudomons aeruginosa* were employed to test the sensor in the clinical samples. For testing the sensor as a field diagnostic tool, *Legionella* spp. were identified as water monitoring pathogens.

 The following objectives were proposed to achieve the aims of this project:

1.   To fabricate and standardize a sensor for bacterial detection.

2.   To design a specific peptide sequence to be used as a probe for the sensor and to develop a low-cost and portable sensing platform for identifying *Listeria*.

3.   To select a specific peptide substrate for water- and foodborne pathogens and to develop a low-cost paper-based sensing platform.

4.   To develop a rapid diagnostic tool for the detection of *Porphyromonas gingivalis* as a salivary diagnostic biomarker of periodontitis.

6.   To develop a smart and low-cost diagnostic tool for the detection of *Pseudomonas aeruginosa.*

Figure 1.3: Schematic diagram representing the steps involved in this project, including sensor fabrication, dipeptide library screening, functionalization of the nanomagnetic peptide sequence with nanomagnetic particles to form a complex, immobilization of the complex on the sensor platform, application of the enzyme, and colorimetric test results.

4. Own research results

The results of this research, reflecting the aims of the work involving the fabrication of the sensor and the testing of the sensor on different pathogens, are presented in this section.

4.1 Comparison of a D-amino acid and an L-amino acid paper-based sensor for *L. monocytogenes* detection

Dramatic progress has been made in the field of nanomaterial-based biosensors, particularly for biomedical and bioanalytical applications. Among these, magnetic nanobeads are of particular interest due to their large surface-to-volume ratio [23]. Moreover, these nanobeads easily separate or enrich specific analytes from complex matrices under the effect of an external magnetic field and provide a direct readout by the naked eye.

In this study, a novel diagnostic sensing probe for *L. monocytogenes* was reported. The strategy was developed based on the unique properties of magnetic nanobeads and provided specific detection by the naked eye. The biosensor peptide probe was prepared using a specific substrate to detect the proteolytic activity of the target microbe. This substrate was elongated with an Ahx-residue linker on both ends of the peptide. The Ahx-residue spacer enhances protease accessibility to the specific peptide cleavage site. The N-terminal of the peptide was coupled to carboxyl-terminated magnetic nanobeads. The cysteine residue at the C-terminal allows gold–sulfur interactions to construct a self-assembled monolayer (SAM) of magnetic nanobead–peptide complex on the surface of the gold sensor (Scheme 1 **[SAA1]**).

Further, the amount of the peptide substrate required for magnetic nanoparticle (MNP) functionalization was optimized. The detailed protocol steps of sensor preparation are shown in Scheme 1 **[SAA2]**. The sensing mechanism was based on the proteolytic activity of *L. monocytogenes* proteases on a specific peptide substrate, sandwiched between the magnetic nanobeads and the gold surface on top of the paper substrate. An external magnet fixed at the back of the sensor accelerates the cleavage of the peptide–magnetic nanobead moieties. This dissociation process reveals the golden color of the sensor surface that is visible to the naked eye, as shown in Scheme 2.1 **[SAA2]**.

L. monocytogenes is one of the most critical pathogenic agents causing foodborne diseases. A small undetectable number of microbes can multiply and become life-threatening, especially among

23

immune-compromised populations. Ready-to-eat foods are considered a source for the transmission of *L. monocytogenes*. Proteases are enzymes involved in bacterial growth, multiplication, and pathogenicity [102]. Therefore, developing this novel portable, low-cost colorimetric screening assay for detecting *L. monocytogenes* proteases using nanomagnetic particles is an important step. The proteases extracted from each *L. monocytogenes* bacterial concentration were applied to the D-peptide sequence. Figures 1a and 1b **[SAA1]** show the typical results before and after the addition of various bacterial protease concentrations, respectively. There was an evident correlation between the protease concentration and the appearance of the yellow area as a result of the cleavage of the black magnetic nanobeads. The second confirmation spot was formed by the accumulation of the black cleaved magnetic nanoparticles at the magnetic paper area. The gradual increase in the intensity golden background reflects the increase in the protease concentration. Figure 2 **[SAA1]** shows a linear relationship between the amount of cleaved magnetic nanobeads (appearance of the yellow color) and the concentration of the protease for various bacterial concentrations.

It is known that peptide substrates containing D-amino acids are specific and facilitate prokaryotic cleavages [151]. In this study, two peptide sequences were synthesized using D- and L-amino acids to compare the proteolytic activity of *L. monocytogenes*. The selected peptide sequence was then integrated with magnetic nanoparticles to construct a highly specific peptide sequence that can be explicitly cleaved by *L. monocytogenes* protease. Serial dilutions of *L. monocytogenes* were prepared to compare the detection limit (cfu/mL) for both D- and L-peptide sequences (Figure 2.1). The protease extracted from each bacterial concentration was applied to the peptide sequences containing D- and L-amino acids. Figure 2 **[SAA1]** shows the comparison of the percentage of the cleaved nanobead area for the D- and L-amino acid sequences as a function of various bacterial concentrations. The results indicate that the peptide sequence containing D-amino acids is highly specific, with a lower required detection concentration of 2.17×10^2 cfu/mL within 30 s than the sequence containing L-amino acids, which gave a higher detection limit of 2.1×10^3 cfu/mL in 2 h.

The detection limit of the D-amino acid probe sensor used in this study, without any preconcentration of the sample, is comparable to the detection limits of other reported methods [152]. For example, Moreno et al. (2012) detected *L. monocytogenes* using PCR with a detection limit (DL) of 7.4×10^2 after 7 h of culturing. Moreover, a colorimetric method using gold nanomagnetic particles combined with hyperbranched rolling circle amplification (HRCA) gave a detection limit as low as 100 aM for synthetic *hly* gene targets, and about 75 copies of *L. monocytogenes* can be identified [153]. Furthermore, Law et al. (2015) used a DNA microarray assay, and Sabat et al. (2013) used a next-generation sequencing (NGS) molecular method, to detect and identify *L. monocytogenes*. Both methods are highly sensitive and specific but laborious, costly, and unsuitable for field applications [154].
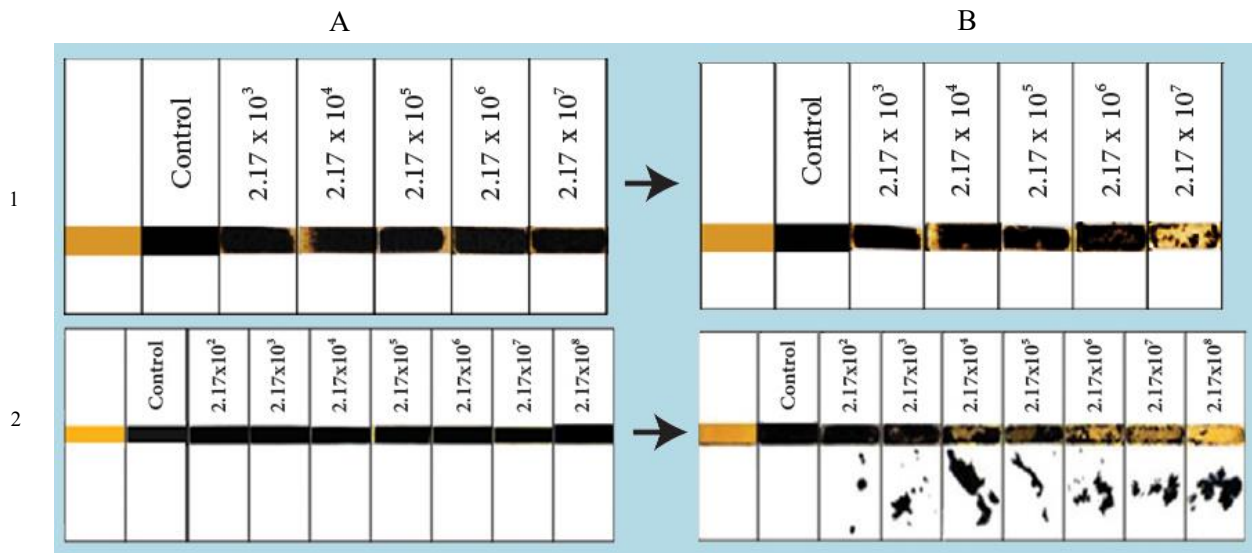
Figure 2.1: 1. *Listeria monocytogenes* sensor probe using L-amino acid conjugated to a colorimetric magnetic nanobead: (A) before and (B) after adding different concentrations of *Listeria monocytogenes* protease solutions. 2. *Listeria monocytogenes* protease sensor probe using D-amino acid conjugated to a magnetic nanobead: (A) before and (B) after adding different concentrations of *Listeria monocytogenes* protease solutions.

Table 1**[SAA1]** summarizes the detection limits for the most recently developed assays. The detection limit of the fabricated sensor is comparable to the detection limits of the other reported methods. Moreover, the novel sensor has a much shorter response time. The sensor was tested for specificity by using proteases extracted from other commonly associated foodborne bacteria. The proteases extracted from *S. aureus*, *E. coli*, *Shigella*, and *Salmonella* were used to check the cross-reactivity with the *Listeria*-specific substrate. The results indicated that cleavage occurred only with *Listeria*; with the other bacteria no cleavage was observed (Figure 3 **[SAA1]**). It can be concluded that the *Listeria* peptide probe is highly efficient and precise. In summary, in this study, a sensitive and flexible sensor for detecting *Listeria monocytogenes* was developed. This sensor was able to detect the target bacterial protease at a low concentration of 7.4×10^2 cfu/mL, indicating that it can successfully be used for monitoring food contamination and may have potential applications in the food industry. The sensor was created using the properties of D-amino acids. The following experiments were carried out to fabricate the sensor and validate it as a potential detection tool.

4.2   Evaluation of the sensor in a food matrix contaminated with *S. aureus*, *E. coli* O157:H7, and *L. monocytogenes*

Foodborne diseases are a significant health concern as they are responsible for the morbidity and mortality of many people each year, especially children. According to World Health Organization data, foodborne diseases cause around 420,000 deaths every year. *S. aureus*, *E. coli* O157:H7*, and *L. monocytogenes* are known as the common pathogens causing foodborne illnesses. Therefore, specific detection of these contaminants in the food matrix is crucial for limiting foodborne diseases [155].

Against this backdrop, this study aimed to develop a magnetic nanobead–peptide probe that would be cleaved specifically by the virulence proteases secreted by the pathogens *S. aureus*, *E. coli* O157:H7*, and *L. monocytogenes*. The biosensor peptide probes were prepared using the *E. coli* O157:H7-specific peptide substrate NH2-Ahx-KVSRRRRRGGDKVDRRRRRGGD-Ahx-Cys, the *S. aureus*-specific substrate ETKVEENEAIQK, and the *L. monocytogenes*-specific substrate CAhxNMLSEVERE-Ahx-COOH. These probes were then integrated with a gold-sensing platform via Au–S linkage to provide a specific and cost-effective strip-format diagnostic biosensor for qualitative and quantitative detection.

After the fabrication of the three sensors for each specific bacterium, proteolytic activity was detected. A color change occurs upon proteolysis of the peptide–MNP moieties, indicating the presence of the contaminant. To obtain an insight into the sensor's applicability for the quantitative detection of *S. aureus* and *E. coli* O157:H7, many biosensors were made for each pathogen and exposed to different protease solutions prepared from several bacterial pure broth culture concentrations. For *S. aureus*, the evaluated concentrations included 7.5×10^6, 7.5×10^5, 5×10^4, 5×10^3, 5×10^2, 75, and 7.5 cfu/mL. For *E. coli* O157:H7, the assessed concentrations were 1.21×10^6, 1.21×10^5, 1.21×10^4, 1.21×10^3, 1.21×10^2, and 12 cfu/mL. As demonstrated in Figure 2.2, a clear and proportional increase in the sensor's gold-colored area with the protease solution concentrations was obtained. The change was attributed to the proteolytic activity of the proteases, which resulted in the dissociation of the peptide–magnetic nanobead complex.

In parallel, ImageJ software (NIH, Bethesda, Maryland; http://rsb.info.nih.gov/ij) was used for analytically detecting and quantifying *S. aureus* and *E. coli* O157:H7. A standard curve was observed with an excellent R^2 value of 0.9557. The ImageJ software measures the size of the cleaved area (appearance of a golden color) in comparison with the total black area (before cleavage). Thus, the color threshold function needed to be tuned, as shown in Figure 2BII **[SAA2]** and Figure 1C **[SAA3]**. Blank

samples were tested for each sensor and showed no reaction as the sensor demonstrated no disruption of the SAM layer.
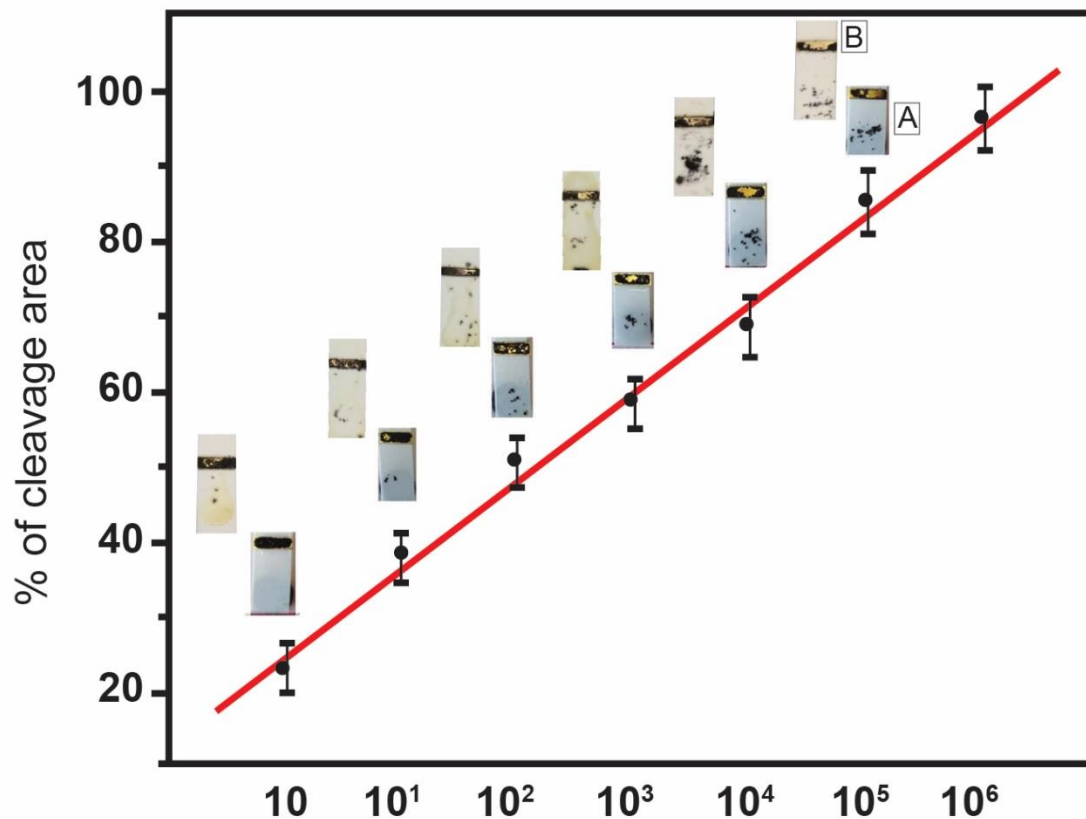
Figure 2.2: Proteolytic activity of different supernatant concentrations of **A** *S. aureus* and **B** *E. coli* cultures by a specific protease activity assay. Protease activity is determined in terms of units defined as the amount in micromoles.

4.2.1 Testing of the *L. monocytogenes* sensor with food samples

The stability of the *L. monocytogenes* sensor with a food matrix was one of the focuses of this research. Therefore, the sensor was tested against whole milk and a ready-to-eat meat supernatant to check whether the sensor shows any proteolytic activity in the food. Figure 4A **[SAA1]** (before adding the sample) and Figure 4B (B1, meat sample without inoculation) show that the food supernatant did not affect the sensor's performance. To evaluate the sensitivity of the sensor, fresh whole milk and ready-to-eat meat were spiked with colonies of *L. monocytogenes* and incubated at 35 °C for 15–18 h. The concentrations of the bacterial stock after 18 h were determined to be 13.8×10^7 cfu/g and 11.7×10^7 cfu/mL for the ready-to-eat meat and fresh whole milk, respectively. Serial dilutions were obtained from the stock concentrations, and a viable count of the spread dilution method was used to confirm the correct bacterial number. The sensor was then directly tested with the spiked samples (with and without

centrifugation). The detection limits of the amount of magnetic nanobeads cleaved by the protease on the sensor surface were similar regardless of whether the samples were centrifuged or not. The detection limit of the sensor in the spiked milk was 11.7×10^2 cfu/mL (B2 in Figures 4 and 5), and the detection limit in the spiked meat was 13.8×10 cfu/g (B3 in Figures 4 and 5 **[SAA1]** and Table 2.1). The results were obtained within 15 min without any pre-enrichment steps.

4.2.2 Evaluation of the *S. aureus* sensor with spiked food matrices

The feasibility of the sensor to detect *S. aureus* in contaminated food products and environmental samples was assessed by spiking 1.0 mL of different *S. aureus* concentrations (from 4.14×10^5 to 4.14 cfu/mL) into 9 mL of ground beef, turkey sausage, lettuce, and milk. The results are shown in Figure 2A **[SAA2]** and Table 2.1. Moreover, dust samples collected from different sites were suspended in sterile water and spiked with six different concentrations of *S. aureus*, ranging from 1.12×10^7 to 11.2 cfu/mL. The samples were then centrifuged, filtered, and exposed to the developed biosensor. The results are shown in Figure 3 **[SAA2]**. The results could be observed by the naked eye and revealed that there was a direct relationship between the golden sensor area and the bacterial concentrations.

Afterward, the biosensor was tested to ensure efficiency and stability over time. This evaluation was done by testing the ready-to-use immobilized strip sensors stored in empty Petri dishes at 4 °C. Every week, three sensors were used to detect the proteolytic activity of the known *S. aureus* protease solution. The negative control was also tested in parallel with each experiment. The biosensor exhibited adequate long-term stability of up to six months at room temperature. Moreover, a comparison of the sensor's response after less than six months and after more than six months of storage was also conducted (Figure 5A **[SAA2]** and Table 1).

For evaluating the specificity of the sensor, blinded clinical isolate samples (methicillin-resistant *S. aureus* [MRSA], brown and green *P. aeruginosa*, and *Candida albicans*) and standard pathogen (*P. aeruginosa* ATCC 2785) were applied on the fabricated *S. aureus* sensor. A positive readout by the naked eye was observed only for the MRSA clinical isolate, as shown in Figure 5B **[SAA2]**. Furthermore, the biosensor was exposed to a panel of food-contaminating pathogens, such as *L. monocytogenes* and *E. coli* 157. The results showed no disruption in the SAM layer of the tested pathogens and no significant change in the golden area of the sensor's surface, as shown in Figure 5B **[SAA2]**.

4.2.3 Biosensor-based detection of *E. coli*-spiked food matrices

The capability of the sensor to detect *E. coli* O157:H7 was determined with contaminated food products. For this purpose, a fresh primary bacterial culture (PBC) of *E. coli* O157:H7 was spiked into different food matrices, including ground beef, turkey sausage, lettuce, and milk. A positive and a negative control were prepared and tested to check the effect of food matrices on the sensor. The positive control and the spiked samples were allowed to incubate at room temperature for 2 h, after which *E. coli* O157:H7 was enumerated. The supernatant of the centrifuged spiked sample was examined with the developed biosensor. A clear and steady increase was observed in the sensing platform's gold-colored area in relation to the bacterial concentration.

The lowest detection limit of the developed biosensor was determined with different spiked food matrices. The biosensor displayed a detection limit of 30 cfu/mL in ground beef, turkey sausage, and lettuce samples, while the detection limit in milk was found to be 300 cfu/mL, as shown in Figure 3A, D **[SAA3]** and Table 2.1. Thus, the developed biosensor is suitable for detecting *S. aureus, E. coli* O157:H7*,* and *L. monocytogenes* in different food matrices.

The reported biosensor is suitable for use at the retail level as well as at home. The stability and specificity of the *E. coli* O157:H7 biosensor were determined, and it was observed that the platform offered good stability for up to six months. Moreover, different food-contaminating pathogens, including *L. monocytogenes, P. aeruginosa*, and *S. aureus,* were used to assess the specificity of the sensor. Hence, the biosensor was exposed to proteases of these pathogens. The assay showed no disruption of the SAM layer and no readout for color change by the naked eye for other pathogens. Thus, the specificity of the biosensor for *E. coli* O157:H7 was confirmed (Figure 2 **[SAA3]** and Table 1). All the experiments were conducted in triplicate.

The results indicated that the developed sensors for the detection of the foodborne pathogens *S. aureus, E. coli* O157:H7*,* and *L. monocytogenes* exhibited a low detection concentration, which reflects a high sensitivity, with great stability in the food matrix and high specificity. The sensors were able to obtain the results in a short detection time, within a minute. Thus, the sensor platform provides the detection of *S. aureus, E. coli O157:H7,* and *L. monocytogenes* and can be used as a potential point-of-care diagnostic platform in hospitals. Furthermore, it can be used for infection control in industrial food processing.

Sample	L.D.C	Matrix
L. monocytogenesis	11.77 x 10^2 cfu/ml	Milk
L. monocytogenesis	13.8 cfu/ml	Ground beef
Staphylococcus aurus	40 cfu/mL	Lettuce
Staphylococcus aurus	40 cfu/mL	Turkey
Staphylococcus aurus	40 cfu/mL	Ground beef
Staphylococcus aurus	40 cfu/mL	Milk
Staphylococcus aurus	100 cfu/mL	Dust
E. coli	30–300 cfu/mL	Lettuce
E. coli	30–300 cfu/mL	Turkey sausage
E. coli	30–300 cfu/mL	Meat
E. coli	30–300 cfu/mL	Milk

Table 2.1: Different applications of the colorimetric probe to food products spiked with *L. monocytogenesis, S. aureus,* and *E. coli*. The specific substrate peptide is bound covalently to the magnetic nanobeads test with different concentration of food spiked sample and **L.D.C** (low detection concentration) were detected.

4.3 The fluorescent resonance energy transfer assay and the magnetic nanoparticle-conjugated peptide probe as field diagnostic tools for the simple and rapid detection of *Legionella* spp.

Legionnaires' disease (LD), caused by *Legionella* spp., is a serious health problem due to the high mortality rate. Most cases are caused by *Legionella pneumophila*; however, other *Legionella* species have also been reported to bring about human disease [156]. Protease enzymes are involved in the growth, multiplication, and pathogenicity of *Legionella* spp. For instance, one of the virulence factors of *Legionella pneumophila* is metalloprotease, which is also called tissue-destructive protease or significant secretory protein. This protease inhibits the activity of neutrophil chemotaxis and the listericidal activity of human neutrophils and monocytes [157] [158]. Hence, the enzyme is crucial in the pathogenesis of Legionnaires' disease. In this context, this experiment aimed to exploit proteases for developing a novel portable, low-cost colorimetric screening assay for detecting *Legionella* spp. using nanomagnetic particles.

A fluorescence-based biosensing approach for simultaneously identifying multiple analytes was used in this assay. The FRET assay was employed for the detection of the protease-related proteolytic activity of different strains of *Legionella*. Furthermore, assembled peptides were selected as substrates and conjugated with nanomagnetic particles. The enzyme-specific peptide sequences were synthesized with terminal functionalization for the attachment to the capthonal group on the gold surface. The designed sensor uses nanomagnetic particles based on the proteolytic activity of the protease enzyme secreted by *Legionella* species and provides rapid colorimetric analysis. This sensor can be used in field detection and hospitals for regular water monitoring.

The *Legionella*-specific dipeptide substrates were identified by screening 115 fluorogenic peptides with the corresponding protease enzymes. The dipeptides containing FITC (fluorophore) and dabcyl (quencher) in C- and N-terminals were used as FRET pairs. In the sequences, the capital letter represents L-amino acids, and the small letter represents D-amino acids. The specific peptide was identified by incubating the culture supernatant of the six different *Legionella* strains (*Legionella pneumophila* ATCC 33155, *L. pneumophila* ATCC 33152, *Legionella micdadei* ATCC 33218, *Legionella anisa* ATCC 35292, *Fluoribacter bozemanae* ATCC 33217, and *Fluoribacter dumoffii* ATCC 33279). The peptidase produced by the substrate with the *Legionella* strains showed a significant

increase in the fluorescence intensity of the dipeptides L-L, F-F, W-W, and Y-Y, indicating that the peptide bonds between the dimeric peptides were cleaved efficiently by *Legionella* proteases.

The proteolytic activity of the protease-targeted dipeptides with L-amino acids is shown in Table 1 **[SAA4]**. It was observed that the primary cleavage site was the substrate with aromatic L-amino acids (tyrosine, tryptophan, and phenylalanine) except leucine-leucine (FITC-Ahx-L-L-K(Dabcyl)). Moreover, it was noticed that there was no proteolytic activity of the proteases with the dipeptides with D- and L-amino acids. Further, the results revealed that the proteolytic activity of *Legionella* species was stereo-specific. The *Legionella pneumophila* strain 33155 exhibited efficient proteolytic activity with F-F, L-L, and Y-Y and moderate activity with W-W. In contrast, the W-W substrate was cleaved efficiently in the presence of ATCC 33152 and ATCC 33279, which possessed moderate activity with the other three peptides, as depicted in Figure 2.3 (Figure 2C **[SAA4]**). *Legionella pneumophila* ATCC 35292 specifically digests Y-Y peptides, and its fluorescence intensity does not significantly increase in the case of the other three peptides, as shown in Figure 2.4 (Figure 2A **[SAA4]**). The substrate with F-F dipeptide was effectively cleaved by the *Legionella micdadei* ATCC 33218 strain, which showed moderate cleavage with the Y-Y peptide. However, there was no significant difference in cleavage between the L-L and W-W peptides (Table 2 **[SAA4]**). The specificity of the *Legionella* strains' cleavage of the substrates was tested in the presence of closely associated bacteria, such as *E. coli*, *Salmonella*, and *Campylobacter*. The change in the fluorescence intensities of each substrate (L-L, F-F, W-W, and Y-Y) was monitored in the presence of the respective bacterial culture supernatant. No significant change in fluorescence intensity was observed, indicating that *Legionella* specifically cleaves L-L, F-F, W-W, and Y-Y peptides. The substrates were stable in the presence of other bacterial proteases (Table 3 **[SAA4]**). The *Fluoribacter bozemanae* 33217 supernatant showed no significant effect on the cleavage of the FRET substrates, which might be explained by the significant phenotypic differences, as well as differences in the G+C content and DNA hybridization characteristics between *Fluoribacter dumoffii* and *Legionella* spp. Four D-based amino acids were designed and elongated with AHX to give proper space for the interaction. Then, conjugation was carried out with the nanomagnetic particles to develop a colorimetric sensor for visualizing the presence of bacteria in low or high concentrations. The results were comparable to those of the FRET assay.

Legionella pneumophila 33155*, Tatlockia micdadei* 33218*, Legionella anisa* 35292*, Fluoribacter dumoffii* 33279*,* and *Legionella pneumophila* 33152 were tested with the four sensors (Figure 2 **[SAA4]**). The proteolytic activity of the protease enzymes produced by the different *Legionella* species was visualized by the disassociation of the magnetic particles from the sensor area, resulting in changes in the sensor's background color from black to gold as cleaved particles trapped by the magnetic paper stabilized under the flexible plastic strip. All the five strains gave positive results. The biosensing methods were used for the quantitative detection of *Legionella pneumophila* 33155,

Tatlockia micdadei 33218*, Legionella anisa* 35292*, Fluoribacter dumoffii* 33279*,* and *Legionella pneumophila* 33152. Different concentrations of each strain, including 6×10^8, 6×10^7, 6×10^6, 6×10^5, 6×10^4, 6×10^3, 6×10^2, and 6×10 cfu/mL, were blotted onto the four functionalized gold sensors: Sensor 1 (Ahx-YY-AHX-C), Sensor 2 (Ahx-ww-AHX-C), Sensor 3 (Ahx-FF-AHX-C), and Sensor 4 (Ahx-LL-AHX-C). The lowest detection concentrations were obtained for *Legionella anisa* 35292 (6×10 cfu/mL) with Sensor 1, followed by Sensor 4 (6×10^3 cfu/mL), Sensor 2 (6×10^5 cfu/mL), and Sensor 3 (6×10^6 cfu/mL). For *Tatlockia micdadei* 33218*,* the lowest detection concentration was 6×10 cfu/mL with Sensors 1 and 3 (Table 4A **[SAA4]**).

The sensors were able to detect all the five evaluated strains of *Legionella*. The results showed a sensitivity of up to 6×10 cfu/mL. Sensor 1 (Ahx-YY-AHX-C) detected *L. anisa* ATCC 35292, *T. micdadei* ATCC 33218, and *F. dumoffii* ATCC 33279 with a detection limit of up to 60 cfu/mL. Sensor 4 (Ahx-LL-AHX-C) was able to detect both strains of *L. pneumophilia* with the lowest detection concentration of 60 cfu/mL.

The sensors were validated and tested against water to assess their stability. The results showed no reaction. Moreover, the sensors were also tested for specificity by using proteases extracted from other common waterborne bacteria. In this regard, proteases extracted from *E. coli, Campylobacter*, and *Salmonella* were used to check the cross-reactivity with different *Legionella* sensors, and no cleavage was observed, indicating the absence of proteolytic activity for the three types of bacteria on the biosensor platform (Figure 4 **[SAA4]**). Thus, it can be concluded that the *Legionella* peptide substrate is highly specific to *Legionella* spp.

To summarize, it can be concluded that the *Legionella* peptide substrate is highly specific to *Legionella* spp*.* and that the protease secreted by *Legionella* species can be used as a biomarker in water monitoring systems. It can also be used at home, for hygiene assessment protocols, and in air conditioning health systems.
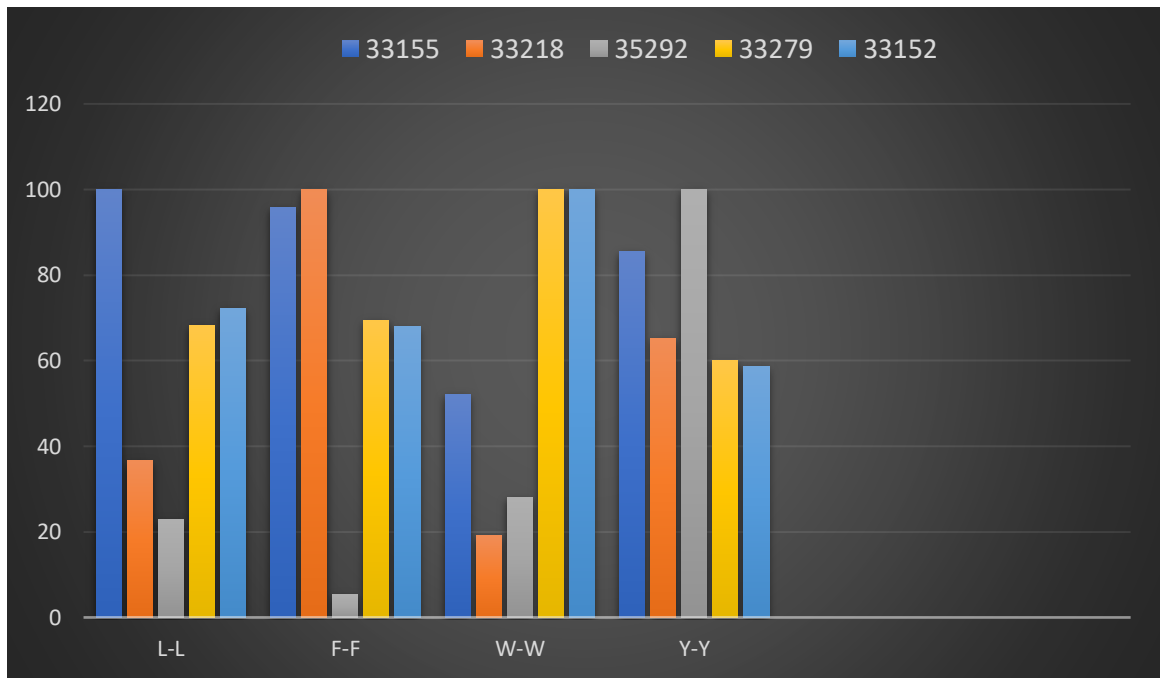
Figure 2.3: FRET-based cleavage efficiency of dipeptides by the supernatant of various *Legionella* strain cultures (6×10^8 cfu/mL). The Y-Y peptide substrate showed efficient to moderate proteolytic activity with *Legionella* spp. ATCC 33155, ATCC 35292, ATCC 33218, ATCC 33279, and ATCC 33152. In contrast, the W-W substrate was cleaved efficiently in the presence of ATCC 33152 and ATCC 33279. The substrate with F-F dipeptide was effectively cleaved by *Legionella micdadei* ATCC 33218 and ATCC 33155.

*L-L leucine, *F-F phenylalanine, *W-W tryptophan, *Y-Y tyrosin

4.4 A rapid diagnostic tool for the detection of *Porphyromonas gingivalis*-related periodontitis

Periodontal disease is a chronic oral disease. The pathogenicity of periodontal disease is represented by inflammation of the gum tissue and destruction of the bone-supporting structure of the teeth, leading to tooth loss. It has been established that gingipain proteases play a significant role in this disease. Therefore, *P. gingivalis*-specific gingipains are considered potential biomarkers for periodontal diseases. Based on this knowledge, a low-cost diagnostic tool for *P. gingivalis*-related periodontitis that measures gingipain protease activity was developed [135]. The proteolytic activity of *P. gingivalis* culture supernatant, and thus gingipain presence, was detected by placing the supernatant onto a functionalized gold biosensor. The cleavage of the specific peptide bond by the proteases leads to the dissociation of the peptide–magnetic bead moieties from the gold sensor surface. As a result, the golden color of the sensor is revealed, which can be observed by the naked eye (Scheme 1 **[SAA5]**).

To gain insight into the sensitivity of the *P. gingivalis* biosensor, a serially diluted *P. gingivalis* culture was prepared and exposed to the sensor's surface. The results are presented in Figures 2.4A and 2.4B, before and after the samples were exposed to the sensor's surface. A gradual increase in the visible gold-colored area was observed in proportion to the concentration of *P. gingivalis*. The change in sensor color is linked to the activity of the secreted proteases, which results in the cleavage of the peptide sequence. The designed sensor showed a detection limit of 49 cfu/mL within 20 s. Hence, this sensor was more efficient and sensitive than the FRET-based assay on which our peptide sequence sensor was based (see Kaman et al., 2012 **[SAA5]**). The promising characteristics were attributed to the use of magnetic nanoparticles, which, unlike organic fluorescent dyes, produce signals.

The biosensor for *P. gingivalis* detection is simple, cheap, and colorimetric, and its results can be observed by the naked eye. Hence, there is no need for readout instruments, making this biosensor applicable in the dentist's office. The feasibility of the constructed sensor for the diagnosis of *P. gingivalis*-related periodontitis was examined by using spiked saliva as an oral diagnostic fluid. Different *P. gingivalis* concentrations (4.5×10^6 and 4.5×10^7 cfu/mL) were spiked onto the purchased saliva in a 1:1 aliquot ratio and applied to the functionalized gold sensor. A steady increase in the visible gold-colored area in relation to the protease concentration was observed. The unspiked saliva sample was used as a negative control and showed no cleavage of the magnetic bead's peptide, no disruption of the SAM layer, and no significant change in the sensor surface's golden color (Figure 2c **[SAA5]**). The developed sensor is thus suitable for analyzing a patient's specimens at the collection site, enabling dental practitioners to perform an on-site test to identify the periodontal pathogen *P. gingivalis*.

To evaluate the performance characteristics of the developed sensor in a clinical setting, the sensor was tested with gingival crevicular fluid (GCF) samples of patients with *P. gingivalis*-related periodontitis. Accordingly, 27 specimens from patients diagnosed with *P. gingivalis*-related periodontitis were tested. The presence of *P. gingivalis* was confirmed by positive cultures and qPCR as described previously [135]. Notably, the golden color of the sensor surface was visible by the naked eye (Figure 3 **[SAA5]**). Hence, the results were encouraging and comparable to those of the culture testing. Likewise, the biosensor's specificity in the presence of other proteases, such as *Fusobacterium nucleatum* subsp. and *Tannerella forsythia*, was assessed. Figure 4a and Figure 4b **[SAA5]** show the results of the specificity test. The sensor showed no disruption of the SAM layer and no significant change in the sensor surface. These results confirmed that the developed sensor in this study was highly specific for detecting *P. gingivalis* and exhibited no cross-reactivity with other oral pathogens, so the sensor can be used as a side chair test in dental clinics for the initial evaluation of periodontitis.
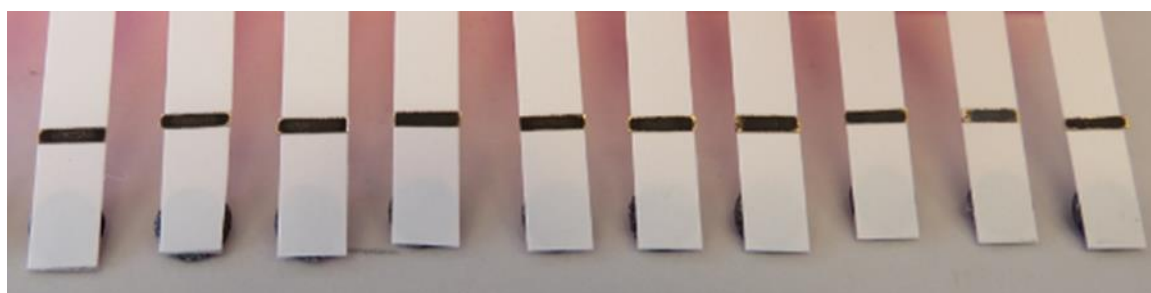
(A)
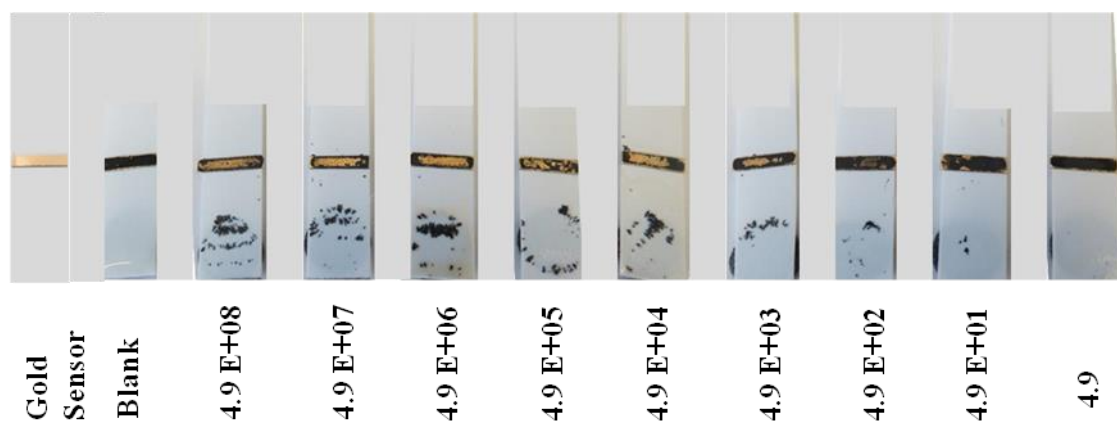
(B)

Figure 2.4: (A) The blank sensor before the application of the protease. (B) Colorimetric *P. gingivalis* protease sensor probe (specific for *P. gingivalis* protease substrate peptide covalently bound to a magnetic bead) under the effect of different concentrations of *P. gingivalis* protease solutions.

4.5 A highly specific protease-based assay for diagnosing *P. aeruginosa* in clinical samples

---

P. aeruginosa is a Gram-negative rod and is known to be the second most prevalent nosocomial bacterium. It is a life-threatening pathogen among hospitalized and immunocompromised patients [159]. It is responsible for pneumonia infection and is aggressive once it colonizes wounds or burned skin, potentially delaying the healing process [117]. Considering the importance of early detection of *P. aeruginosa*, we developed a rapid, sensitive, and specific colorimetric biosensor based on the use of MNPs for its identification in clinical samples. This biosensing platform was designed to measure the proteolytic activity of *P. aeruginosa* using a specific protease substrate.

Kaman et al. [139] designed and evaluated a fluorogenic substrate as a potential marker for the virulence proteases secreted by *P. aeruginosa*. In this study, we utilized this specific protease substrate for developing a paper-based colorimetric assay [139]. The substrate was modified by attaching hexanoic acid (Ahx)-linkers to both C- and N-terminals of the peptide sequence Gly-Gly-Gly to enhance the accessibility of the protease to the peptide substrate near the sensor surface. Then, a cysteine amino acid was linked to the C-terminal, allowing gold–thiol interactions that resulted in the formation of a SAM of *P. aeruginosa* peptide–MNPs onto the gold sensor surface. The N-terminal of the peptide was attached to the MNPs.

The fabricated sensor was studied to detect the proteolytic activity of *P. aeruginosa* protease (10^7 cfu/mL) over the functionalized gold sensor surface. This was accomplished by investigating the shift in color of the sensor from black to gold due to the cleavage of the nanomagnetic peptide complex (by the protease activity) and accumulation away from the sensor. The quantitative detection of *P. aeruginosa* was performed using different concentrations (4.5×10^7, 4.5×10^6, 4.5×10^5, 4.5×10^4, 4.5×10^3, 4.5×10^2, and 4.5×10 cfu/mL) of *P. aeruginosa*, as shown in Figure 2.6 (Figures 1 and 2 **[SAA6]**). The rise in bacterial concentration produced a gradual increase in the visible gold-colored area. The intensification of the golden area could be explained by the protease enzyme's ability to dissociate the peptide–MNP moiety; hence, the reaction was directly related to the enzymatic concentration. The developed colorimetric biosensor presented a minimum detection limit of 10^2 cfu/mL within 1 min (Figure 1 **[SAA6]**). Also, to validate the colorimetric biosensor, a negative blank (brain heart infusion [BHI] broth only) with no protease was incubated with the sensor. No cleavage was observed in this case (Figure 2 **[SAA6]**). Thus, the results confirmed the potential of the fabricated biosensor to detect *P. aeruginosa*.

The specificity of the biosensor was investigated by exposing the sensor to other pathogenic microbes, such as *L. monocytogenes* and *S. aureus.* The sensor showed no disruption of the SAM layer and no significant change in the sensor surface's golden color in the presence of *L. monocytogenes* and *S. aureus*, showing sufficient specificity. Moreover, the clinical applicability of the developed biosensor was tested using 20 *P. aeruginosa* clinical isolates. These samples were previously analyzed by traditional culture and PCR methods at the King Faisal Specialist Hospital microbiology laboratory. The samples were incubated with the invented biosensor. Positive results were observed, with a clear cleavage of the peptide–MNP moiety, resulting in the appearance of a golden color on the sensor's surface (Figure 4 **[SAA6]**). Notably, the differences in cleavage intensity of the tested samples were attributed to differences in the number of colonies of *P. aeruginosa*. A negative control provided no cleavage of the peptide–MNP moiety and no disruption of the SAM layer.

This colorimetric detection method presented a better detection limit in a shorter time than the previously reported fluorescent dye-containing lipid vesicles method reported by Thet et al. (25 **[SAA6]**). Although their approach managed to discriminate 40 clinical strains of the pathogens *P. aeruginosa* and *S. aureus* correctly, the method was used only for qualitative measurements. Another technique developed to provide quantitative detection was reported by Yong Jun et al. (26 **[SAA6]**). This method is based on magnetic enrichment and separation, and it achieved a detection limit of 10 cfu/mL.

Moreover, Tang et al. (27 **[SAA6]**) shortened the DNA extraction-to-detection time and reported a detection limit of 10 cfu/mL based on magnetic enrichment and nested PCR. However, all the methods mentioned above are complex and require centralized labs, instrumentation, and trained personnel. Besides, PCR techniques are not suitable for routine testing at physicians' clinics, unlike our colorimetric assay, which is cheap, simple, rapid, and sensitive. Furthermore, our assay does not require expensive equipment and trained personnel.

The ability of the designed colorimetric biosensor to detect *P. aeruginosa* protease in clinical samples was evaluated. The assay was simple, rapid, sensitive, specific, and feasible for on-site applications as it does not require any labeling or amplification steps.
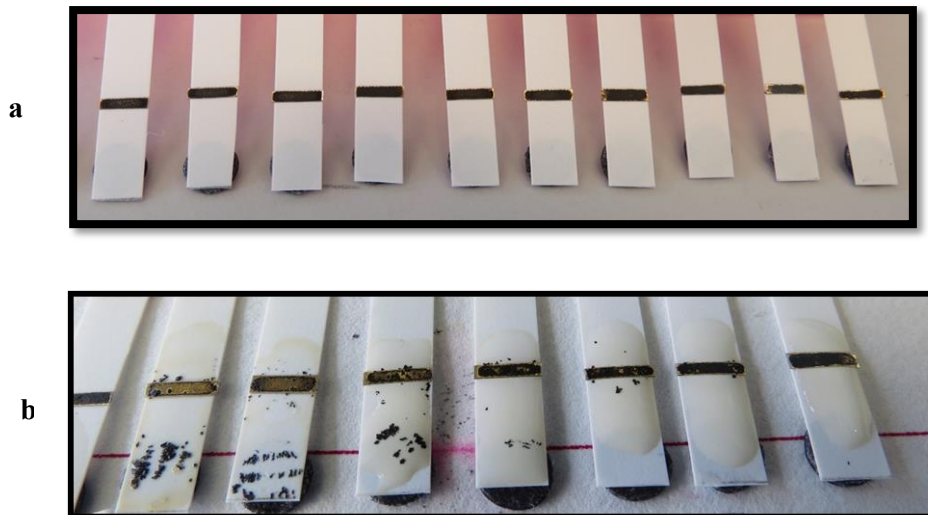
Figure 2.5: (**a**) Colorimetric *Pseudomonas aeruginosa* protease sensor probe before the addition of different concentrations of *Pseudomonas aeruginosa* (**b**) The reaction after the addition of different concentrations of *Pseudomonas aeruginosa* starting from the highest concentration of 4.5×10^7 cfu/ml to the left to the lowest concentration 4.5×10^1 cfu/ml at the rig

5. Conclusion

Infectious diseases are one of the major causes of morbidity and mortality. The timely diagnosis of such diseases is of the utmost importance, because the earlier the diagnosis, the better the outcome. A delayed diagnosis of infectious diseases, even a delay of a few hours, can cost lives or lead to severe complications. Hence, there is a dire need to develop new and efficient approaches for diagnosing infectious diseases and identifying their causative agents.

Bacterial pathogens are fundamental targets that need to be detected in medicine, food safety, and public health. The currently available bacterial identification approaches rely upon laboratory-based techniques, such as microscopic analysis, biochemical assays, and cell culture. Nevertheless, these procedures are laborious and costly and require specialized instrumentation as well as trained users. In contrast, portable stand-alone biosensors may enable rapid detection and diagnosis at the point of care. Biosensors are especially helpful when a precise diagnosis is required to guide treatment, e.g., in critical illnesses (such as meningitis). Moreover, they are also extremely important for preventing the spread of particular diseases, such as foodborne or sexually transmitted infections. The precise identification of bacteria is also crucial for anti-bioterrorism measures (e.g., anthrax detection).

Recent advances in biosensors have made it possible to precisely identify whole bacterial cells with great sensitivity within a short period of time. Additionally, bacterial detection by a biosensor does not require cumbersome sample processing. Therefore, there is a particular focus on nanoparticle-based biosensors, especially nanomagnetic biosensors, that offer ease of miniaturization, simple handling, exceptional sensitivity, and cost-effectiveness. Against this background, in the present study, sensors for the early detection of important and common pathogens causing serious human illnesses have been developed.

Protease enzymes are a crucial part of several biological processes (including cell division and cell death), and they confer important phenotypic characteristics to cells. Therefore, they are highly regulated, and any disturbance in the cascade of their regulation can be a marker of an ongoing disease. Thus, these enzymes may be used as a target for therapy as well as for diagnostic purposes. In this study, a diagnostic platform for detecting pathogens, including *Listeria monocytogenes, E. coli* O157:H11*, Staphylococcus aureus, Legionella* spp*., P. gingivalis,* and *Pseudomonas aeruginosa,* has been developed. Fluorogenic substrates were used as a potential tool for detecting the virulence of the

proteases. The identified substrates were conjugated with nanomagnetic particles to develop colorimetric, flexible, and portable platforms.

Listeria monocytogenesis protease was used to design the probe. Two designed amino acids, D-based and L-based amino acids, were prepared to compare the specificity and sensitivity of the sensor. *N*-hydroxysuccinimide (NHS), 1-(3-dimethylaminopropyl)-3-ethyl-carbodiimide (EDC) chemistry was used to connect the D-amino acid substrate to the carboxylic acid on the magnetic nanoparticles. A self-assembled monolayer (SAM), which the black magnetic nanobeads would mask, was created on the surface of the gold sensor by using the cysteine residue at the substrate's C-terminal. It is known that D-amino acids are specific and facilitate bacterial proteolytic activity. The designed D- and L-based peptide sequences were integrated with the nanomagnetic particles to develop a direct colorimetric test. To test the sensitivity of the test, *Listeria monocytogenesis* protease was diluted to determine the lowest detection limit concentration. It was observed that the size of the gold-colored surface area corresponded with the microbial concentrations. Moreover, the D-amino acid-based probe was found to be highly specific and sensitive and was quicker in detecting *L. monocytogenes* than the L-amino acid-based probe. The lowest detection limit of the biosensing platform for *Listeria* was 2.17 $\times 10^2$ cfu/mL.

Based on these results, a D-amino acid peptide sequence specific for *Staphylococcus aureus* and *E. coli* O157:H7 was fabricated. The detection setup exploited the proteolytic activity of these two bacterial species to target specific peptide substrates sandwiched between the magnetic nanobeads and the gold surface on top of the paper support. An external magnet was attached to the rear of the sensor to escalate the cleavage of the magnetic nanobead–peptide moieties away from the surface as the test sample would drop. During proteolysis, the golden color of the sensor surface gradually increased in proportion to the protease concentration. The color shift caused by the detachment of the SAM was observed with the naked eye and processed with ImageJ (an image analysis tool for quantification). The biosensors demonstrated excellent results regarding the limits of detection. The two sensors showed excellent sensitivity and were able to detect 7 cfu/mL of *Staphylococcus aureus* and 12 cfu/mL of *E. coli* O157:H7. In addition, the sensing platforms for *Listeria monocytogenes*, *Staphylococcus aureus*, and *E. coli* O157:H7 were also evaluated in food matrices contaminated with these bacteria and were found to be highly suitable for the purpose.

After successfully developing a probe for the rapid detection of foodborne pathogens, we turned our attention to the most common waterborne pathogens. Six species were targeted in this context, including *Legionella pneumophila* ATCC 33155, *Legionella pneumophila* ATCC 33152, *Legionella*

micdadei ATCC 33218, *Legionella anisa* ATCC 35292, *Fluoribacter bozemanae* ATCC 33217, and *Fluoribacter dumoffii* ATCC 33279. Fluorescence-based biosensing techniques for multiple analytes in a single detection assay were used to detect peptide sequences. *Legionella* species were able to cleave four stereopeptide sequences, namely F-F, L-L, Y-Y, and W-W, except *Fluoribacter bozemanae* ATCC 33217. The identified substrates were coupled to carboxyl-terminated nanomagnetic particles (NMPs). The Au–S linkage assimilated the C-terminal with the cysteine residue to covalently integrate it with a gold-sensing platform. Four distinct sensors from four different substrates treated with proteases from six *Legionella* species were prepared. The sensors were fabricated in the anticipation that the substrates' protease would digest the peptide sequence, causing the nanobeads to migrate off the gold surface, leading to the appearance of a golden color. The detector exhibited excellent sensitivity, and a concentration of as low as 60 cfu/mL of *Legionella micdadei*, *Legionella anisa*, and *Fluoribacter dumoffii* was detected. Other closely related bacterial species were used to evaluate the sensors' cross-reactivity, and no substantial cross-reactivity was observed. Thus, it was envisioned that the developed assays were suitable for screening targeted bacterial species. Hence, these sensors are valuable for the rapid, simple, and straightforward detection of *Legionella* protease activity and may be employed for monitoring water quality.

The next goal was to design a clinically feasible sensor for *P. gingivalis* as a point-of-care detection tool. For this purpose, a rapid sensing platform for identifying the contaminant as a salivary diagnostic biomarker of periodontitis was developed. The clinical potential of this sensor was explored by analyzing samples from patients diagnosed with periodontitis due to *P. gingivalis*. The results were not only promising but also comparable to those of conventional culture testing. Going another step further, the sensor was tested against proteases from other commonly found red-complex myriad bacteria, such as *Tannerella forsythia* and *Treponema denticola*. Moreover, the sensor was also evaluated against saliva samples of healthy controls. The results confirmed the specificity, robustness, and potential suitability of the assay for clinical use as no reaction with other periodontitis-causing bacteria was observed. The biosensor can identify *P. gingivalis* at a concentration of 49 cfu/mL within 30 s. Thus, this sensor is powerful enough for point-of-care diagnosis and can be used as a side chair test or in hospitals. Additionally, the sensor is exceptionally robust, sensitive, specific, and simple.

Furthermore, a rapid, specific, and highly sensitive colorimetric biosensor for detecting *Pseudomonas aeruginosa* in clinical samples was developed. This biosensing device used magnetic nanoparticles (MNPs) to detect *P. aeruginosa* proteolytic activity in a particular protease substrate. The N-terminal of this substrate was covalently linked to MNPs, while the C-terminal was coupled to a gold sensor surface through cystine. The golden surface of the sensor appears black to the naked eye because

the MNPs are covered. The peptide–MNP moieties are broken as a result of proteolysis, and subsequently, an external magnet attracts the proteolysis products, exposing the golden color of the sensor. This change in color can be seen with the naked eye, making this test robust and easy to use. The biosensor showed excellent results in in vitro studies as well. It specifically and quantitatively detected *P. aeruginosa*, offering a detection limit as low as 10^2 cfu/mL. Moreover, the assay's result was produced in less than one minute. Finally, the clinical applicability of the colorimetric biosensor was evaluated using patients' samples for in situ identification of the *P. aeruginosa* target pathogen. The results strongly supported the idea that this biochip may be an exceptional tool for the quick and point-of-care diagnosis of *P. aeruginosa*-linked infections.

The six different sensors developed in this study were able to detect the corresponding bacteria with high sensitivity and specificity within a short duration of time. The sensors were tested with other bacteria to investigate the cross-reactivity and assess the specificity; most of the sensors were found to be specific. Further, the lowest detection concentration for each biosensor for assessing the sensitivity was determined. In order to use the biosensors for field diagnosis, the sensors were evaluated using different food matrices and environmental samples from various sources. The sensors showed significant stability with all the samples. Likewise, the clinical applicability of the biosensors was verified by testing samples from different clinical sources. For comparison, the samples were tested by conventional culture and PCR methods beforehand.

In this study, the point of interest was to devise a sensitive and quick method for detecting pathogenic bacteria in complex samples. To that end, a colorimetric sensor employing nanomagnetic particles that targeted the proteolytic activity of protease enzymes secreted by bacteria, including *Listeria monocytogenes, E. coli* O157:H11*, Staphylococcus aureus, Legionella* spp*., P. gingivalis,* and *Pseudomonas aeruginosa*, was designed. The highly specific and semi-quantitative diagnostic device developed in the current study is portable and straightforward to operate by a nurse or a non-skilled clinician, making it a potential and highly suitable system for low-resource

6. Zusammenfassung

Infektionskrankheiten sind eine der Hauptursachen für Morbidität und Mortalität. Die rechtzeitige Diagnose solcher Erkrankungen ist von größter Bedeutung, denn je früher die Diagnose, desto besser das Ergebnis. Eine verspätete Diagnose von Infektionskrankheiten, selbst eine Verzögerung von wenigen Stunden, kann Leben kosten oder zu schweren Komplikationen führen. Daher besteht ein dringender Bedarf, neue und effiziente Ansätze zur Diagnose von Infektionskrankheiten und zur Identifizierung ihrer Erreger zu entwickeln.

Bakterielle Krankheitserreger sind grundlegende Angriffsziele, die in der Medizin, Lebensmittelsicherheit und öffentlichen Gesundheit erkannt werden müssen. Die derzeit verfügbaren Ansätze zur Identifizierung von Bakterien beruhen auf laborbasierten Techniken wie mikroskopischer Analyse, biochemischen Assays und Zellkultur. Dennoch sind diese Verfahren mühsam und kostspielig und erfordern spezialisierte Instrumentierung sowie geschulte Benutzer. Im Gegensatz dazu können tragbare eigenständige Biosensoren eine schnelle Erkennung und Diagnose am Point-of-Care ermöglichen. Biosensoren sind besonders hilfreich, wenn eine genaue Diagnose zur Therapieführung erforderlich ist, z. B. bei kritischen Erkrankungen (wie Meningitis). Darüber hinaus sind sie auch äußerst wichtig, um die Ausbreitung bestimmter Krankheiten zu verhindern, wie z. B. durch Lebensmittel übertragene oder sexuell übertragbare Infektionen. Die genaue Identifizierung von Bakterien ist auch für Maßnahmen zur Bekämpfung des Bioterrorismus (z. B. Milzbrandnachweis) entscheidend.

Neuere Fortschritte bei Biosensoren haben es ermöglicht, ganze Bakterienzellen mit hoher Sensitivität innerhalb kurzer Zeit präzise zu identifizieren. Außerdem erfordert der Bakteriennachweis durch einen Biosensor keine umständliche Probenverarbeitung. Daher liegt ein besonderer Fokus auf Nanopartikel-basierten Biosensoren, insbesondere nanomagnetischen Biosensoren, die eine leichte Miniaturisierung, einfache Handhabung, außergewöhnliche Empfindlichkeit und Kosteneffizienz bieten. Vor diesem Hintergrund wurden in der vorliegenden Studie Sensoren zur Früherkennung wichtiger und häufig vorkommender Erreger schwerer Erkrankungen des Menschen entwickelt.

Protease enzymes are a crucial part of several biological processes (including cell division and cell death), and they confer important phenotypic characteristics to cells. Therefore, they are highly regulated, and any disturbance in the cascade of their regulation can be a marker of an ongoing disease. Thus, these enzymes may be used as a target for therapy as well as for diagnostic purposes. In this study,

44

a diagnostic platform for detecting pathogens, including *Listeria monocytogenes, E. coli* O157:H11*, Staphylococcus aureus, Legionella* spp*., P. gingivalis,* and *Pseudomonas aeruginosa,* has been developed. Fluorogenic substrates were used as a potential tool for detecting the virulence of the proteases. The identified substrates were conjugated with nanomagnetic particles to develop colorimetric, flexible, and portable platforms.

Zur Entwicklung der Sonde wurde Listeria monocytogenesis-Protease verwendet. Zwei entworfene Aminosäuren, D-basierte und L-basierte Aminosäuren, wurden hergestellt, um die Spezifität und Sensitivität des Sensors zu vergleichen. Die Chemie von N-Hydroxysuccinimid (NHS), 1-(3-Dimethylaminopropyl)-3-ethyl-carbodiimid (EDC) wurde verwendet, um das D-Aminosäure-Substrat mit der Carbonsäure auf den magnetischen Nanopartikeln zu verbinden. Auf der Oberfläche des Goldsensors wurde mithilfe des Cysteinrests am C-Terminus des Substrats eine selbstorganisierte Monoschicht (SAM) erzeugt, die von den schwarzen magnetischen Nanokügelchen maskiert würde. Es ist bekannt, dass D-Aminosäuren spezifisch sind und die proteolytische Aktivität von Bakterien erleichtern. Die entworfenen D- und L-basierten Peptidsequenzen wurden mit den nanomagnetischen Partikeln integriert, um einen direkten kolorimetrischen Test zu entwickeln. Um die Sensitivität des Tests zu testen, wurde *Listeria monocytogenesis* Protease verdünnt, um die niedrigste Nachweisgrenzkonzentration zu bestimmen. Es wurde beobachtet, dass die Größe der goldfarbenen Oberfläche der mikrobiellen Konzentration entsprach. Darüber hinaus erwies sich die auf D-Aminosäure basierende Sonde als hochspezifisch und empfindlich und konnte *L. monocytogenes* schneller nachweisen als die auf L-Aminosäure basierende Sonde. Die niedrigste Nachweisgrenze der Biosensor-Plattform für *Listerien* lag bei $2,17 \times 10^2$ cfu/ml.

Basierend auf diesen Ergebnissen wurde eine D-Aminosäure-Peptidsequenz hergestellt, die für *Staphylococcus aureus* und *E. coli O157:H7* spezifisch ist. Der Detektionsaufbau nutzte die proteolytische Aktivität dieser beiden Bakterienarten, um gezielt auf spezifische Peptidsubstrate abzuzielen, die sich zwischen den magnetischen Nanokügelchen und der Goldoberfläche auf dem Papierträger befinden. Ein externer Magnet wurde an der Rückseite des Sensors angebracht, um die Abspaltung der magnetischen Nanobead-Peptid-Einheiten von der Oberfläche weg zu beschleunigen, wenn die Testprobe herunterfällt. Während der Proteolyse nahm die goldene Farbe der Sensoroberfläche proportional zur Proteasekonzentration allmählich zu. Die durch das Ablösen der SAM verursachte Farbverschiebung wurde mit bloßem Auge beobachtet und mit ImageJ (einem Bildanalysetool zur Quantifizierung) verarbeitet. Die Biosensoren zeigten hervorragende Ergebnisse bezüglich der Nachweisgrenzen. Die beiden Sensoren zeigten eine ausgezeichnete Sensitivität und konnten 7 cfu/ml *Staphylococcus aureus* und 12 cfu/ml *E. coli O157:H7* nachweisen. Darüber hinaus wurden die Sensorplattformen für *Listeria monocytogenes*, *Staphylococcus aureus und E. coli O157:H7*

auch in mit diesen Bakterien kontaminierten Lebensmittelmatrices evaluiert und für diesen Zweck als sehr geeignet befunden.

Nachdem wir erfolgreich eine Sonde für den schnellen Nachweis von lebensmittelbedingten Krankheitserregern entwickelt hatten, richteten wir unser Augenmerk auf die häufigsten wasserübertragenen Krankheitserreger. In diesem Zusammenhang wurden sechs Spezies anvisiert, darunter *Legionella pneumophila ATCC 33155, Legionella pneumophila ATCC 33152, Legionella micdadei ATCC 33218, Legionella anisa ATCC 35292, Fluoribacter bozemanae ATCC 33217* und *Fluoribacter dumoffii ATCC 33279.*Fluoreszenz-basierte Biosensortechniken für mehrere Analyten in einem einzigen Nachweisassay wurden verwendet, um Peptidsequenzen nachzuweisen. *Legionella-Spezies* waren in der Lage, vier Stereopeptidsequenzen zu spalten, nämlich F-F, L-L, Y-Y und W-W, mit Ausnahme von *Fluoribacter bozemanae ATCC 33217*. Die identifizierten Substrate wurden an carboxylterminierte nanomagnetische Partikel (NMPs) gekoppelt. Die Au-S-Verknüpfung assimiliert den C-Terminus mit dem Cysteinrest, um ihn kovalent in eine Goldsensorplattform zu integrieren. Es wurden vier verschiedene Sensoren aus vier verschiedenen Substraten hergestellt, die mit Proteasen von sechs *Legionella-Spezies* behandelt wurden. Die Sensoren wurden in der Erwartung hergestellt, dass die Protease der Substrate die Peptidsequenz verdaut, wodurch die Nanokügelchen von der Goldoberfläche wandern und eine goldene Farbe erscheinen. Der Detektor zeigte eine ausgezeichnete Empfindlichkeit, und es wurde eine Konzentration von nur 60 cfu/ml von *Legionella micdadei, Legionella anisa* und *Fluoribacter dumoffii* nachgewiesen. Andere eng verwandte Bakterienarten wurden verwendet, um die Kreuzreaktivität der Sensoren zu bewerten, und es wurde keine wesentliche Kreuzreaktivität beobachtet. Somit wurde in Betracht gezogen, dass die entwickelten Assays zum Screening gezielter Bakterienarten geeignet sind. Daher sind diese Sensoren wertvoll für den schnellen, einfachen und unkomplizierten Nachweis der Legionella-Protease-Aktivität und können zur Überwachung der Wasserqualität eingesetzt werden.

Das nächste Ziel war die Entwicklung eines klinisch praktikablen Sensors für *P. gingivalis* als Point-of-Care-Erkennungsinstrument. Zu diesem Zweck wurde eine Rapid-Sensing-Plattform zur Identifizierung der Kontaminanten als speicheldiagnostischen Biomarker der Parodontitis entwickelt. Das klinische Potenzial dieses Sensors wurde durch die Analyse von Proben von Patienten untersucht, bei denen eine Parodontitis aufgrund von *P. gingivalis* diagnostiziert wurde. Die Ergebnisse waren nicht nur vielversprechend, sondern auch mit denen konventioneller Kulturtests vergleichbar. Um noch einen Schritt weiter zu gehen, wurde der Sensor gegen Proteasen von anderen häufig vorkommenden Rot-Komplex-Bakterien wie Tannerella forsythia und Treponema denticola getestet. Darüber hinaus wurde der Sensor auch gegen Speichelproben von gesunden Kontrollen ausgewertet. Die Ergebnisse

bestätigten die Spezifität, Robustheit und potenzielle Eignung des Assays für den klinischen Einsatz, da keine Reaktion mit anderen Parodontitis verursachenden Bakterien beobachtet wurde. Der Biosensor kann *P. gingivalis* in einer Konzentration von 49 cfu/ml innerhalb von 30 s identifizieren. Damit ist dieser Sensor leistungsstark genug für die Point-of-Care-Diagnose und kann als Seitenstuhltest oder in Krankenhäusern eingesetzt werden. Darüber hinaus ist der Sensor außergewöhnlich robust, empfindlich, spezifisch und einfach.

Darüber hinaus wurde ein schneller, spezifischer und hochempfindlicher kolorimetrischer Biosensor zum Nachweis von *Pseudomonas aeruginosa* in klinischen Proben entwickelt. Dieses Biosensor-Gerät verwendet magnetische Nanopartikel (MNPs), um die proteolytische Aktivität von *P. aeruginosa* in einem bestimmten Protease-Substrat nachzuweisen. Der N-Terminus dieses Substrats war kovalent an MNPs gebunden, während der C-Terminus über Cystin an eine Goldsensoroberfläche gekoppelt war. Die goldene Oberfläche des Sensors erscheint mit bloßem Auge schwarz, da die MNPs bedeckt sind. Die Peptid-MNP-Einheiten werden als Ergebnis der Proteolyse aufgebrochen, und anschließend zieht ein externer Magnet die Proteolyseprodukte an, wodurch die goldene Farbe des Sensors freigelegt wird. Diese Farbänderung ist mit bloßem Auge erkennbar, was diesen Test robust und einfach zu handhaben macht. Auch in In-vitro-Studien zeigte der Biosensor hervorragende Ergebnisse. Es weist spezifisch und quantitativ *P. aeruginosa* nach und bietet eine Nachweisgrenze von nur 102 cfu/ml. Darüber hinaus wurde das Ergebnis des Assays in weniger als einer Minute erstellt. Schließlich wurde die klinische Anwendbarkeit des kolorimetrischen Biosensors anhand von Patientenproben zur In-situ-Identifizierung des *P. aeruginosa*-Zielpathogens bewertet. Die Ergebnisse unterstützten nachdrücklich die Idee, dass dieser Biochip ein außergewöhnliches Werkzeug für die schnelle und punktgenaue Diagnose von *P. aeruginosa*-bedingten Infektionen sein könnte.

Die in dieser Studie entwickelten sechs verschiedenen Sensoren konnten die entsprechenden Bakterien mit hoher Sensitivität und Spezifität innerhalb kurzer Zeit nachweisen. Die Sensoren wurden mit anderen Bakterien getestet, um die Kreuzreaktivität zu untersuchen und die Spezifität zu beurteilen; Die meisten Sensoren erwiesen sich als spezifisch. Weiterhin wurde die niedrigste Nachweiskonzentration für jeden Biosensor zur Beurteilung der Sensitivität bestimmt. Um die Biosensoren für die Felddiagnostik einzusetzen, wurden die Sensoren mit unterschiedlichen Lebensmittelmatrizes und Umweltproben aus unterschiedlichen Quellen evaluiert. Die Sensoren zeigten bei allen Proben eine signifikante Stabilität. Ebenso wurde die klinische Anwendbarkeit der Biosensoren durch Testen von Proben aus verschiedenen klinischen Quellen verifiziert. Zum Vergleich wurden die Proben zuvor mit konventionellen Kultur- und PCR-Methoden getestet.

In dieser Studie ging es darum, eine sensitive und schnelle Methode zum Nachweis pathogener Bakterien in komplexen Proben zu entwickeln. Zu diesem Zweck wurde ein kolorimetrischer Sensor entwickelt, der nanomagnetische Partikel verwendet, die auf die proteolytische Aktivität von

Proteaseenzymen abzielen, die von Bakterien sezerniert werden, darunter *Listeria monocytogenes, E. coli O157:H11, Staphylococcus aureus, Legionella spp., P. gingivalis* und *Pseudomonas aeruginosa* . Das in der aktuellen Studie entwickelte hochspezifische und semiquantitative Diagnosegerät ist tragbar und von einer Krankenschwester oder einem ungelernten Kliniker einfach zu bedienen, was es zu einem potentiellen und sehr geeigneten System für ressourcenarme Umgebungen macht

7. References

1. J. Wang, G. Rivas, X. Cai, et al. "DNA electrochemical biosensors for environmental monitoring. A review," Analytica Chimica Acra, vol. 347, pp. 1-8., 1997.

2. Giovanna Marrazza, Iva Chianella, Marco Mascini, "Disposable DNA electrochemical biosensors for environmental monitoring," *Analytica Chimica Acta,* vol. 387 , pp. 297-307, 1999.

3. Cohen, M. L. (1998). "Candidate bacterial conditions," *Bull World Health Organ,* vⁱol. 76 Suppl 2(Suppl 2), pp. 61-3., 1998.

4. Rasko DA, Moreira CG, Li de R, Reading NC, Ritchie JM, Waldor MK, Williams N, Taussig R, Wei S, Roth M, Hughes DT, Huntley JF, Fina MW, Falck JR, Sperandio V. "Targeting QseC signaling and virulence for antibiotic development.," *Science,* vol. 321, p. 1078 – 1, 2008.

5. Tack DM, Ray L, Griffin PM, et al. "Preliminary Incidence and Trends of Infections with Pathogens Transmitted Commonly Through Food — Foodborne Diseases Active Surveillance Network, 10 U.S. Sites, 2015–2018," vol. 68, p. 369–373. , 2019.

6. Dye BA. "Global periodontal disease epidemiology. 2000.," *Periodontol,* vol. 58(1), pp. 10-25., 2012.

7. Lazcka O, Del Campo FJ, Muñoz FX. "Pathogen detection: A perspective of traditional methods and biosensors.," *Biosensors and Bioelectronics,* vol. 22, pp. 1205-1217., 2007.

8. Essam Ahmed Mostafa "Conventional Culture Media: An Outdated Microbiological Tool but Still," *Int J Drug Disc an open access journal,* vol. 2, p. 011.

9. Jyoti Verma, Sangeeta Saxena, Sunil G. Babu. ELISA-Based Identification and Detection of Microbes, 2013.

10. Kumar S, Balakrishna K, Batra HV. "Enrichment-ELISA for detection of Salmonella typhi from food and water samples," *Biomed Environ Sci,* vol. 21(2), pp. 137-43, 2008.

11. Davey HM, Kell DB, "Flow cytometry and cell sorting of heterogeneous microbial populations: the importance of single-cell analyses.," *Microbiol Rev.,* vol. 60(4), p. 641–696, 1996 .

References

12. You M, Li Z, Feng S, Gao B, Yao C, Hu J, Xu F ."Ultrafast photonic PCR based on photothermal nanomaterials.," *Trends Biotechnol,* vol. 38 , p. 637–649, 2020.

13. Wang T, Liu Y, Sun HH, Yin BC, Ye BC. "An RNA-guided Cas9 nickase-basedmethod for universal isothermal DNA amplification, Angew," *Chem. Int. ,* vol. 58, p. 5382–5386., 2019.

14. Garibyan L, Avashia N. Polymerase chain reaction. *J Invest Dermatol.* 2013;133(3):1-4. doi:10.1038/jid.2013.

15. Kiev S Gracias, John L Mckillip "Nucleic acid sequence-based mplification (NASBA) in molecular bacteriology: a procedural guide. . Rapid Methods Autom. Microbiol. 15, 295–309.," *Microbiol. 15, 295–309.,* vol. 15, p. 295–309., 2007 .

16. Guichón A, Chiparelli H, Martínez A, et al. "Evaluation of a new NASBA assay for the qualitative detection of hepatitis C virus based on the NucliSens Basic Kit reagents". J Clin Virol. 2004 Feb;29(2):84-91.

17. Bremer J, Nowicki M, Beckner S, et al. "comparison of two amplification technology for detection and quantification of human immunodeficiency virus type 1 RNA in female genital tract," J Clin Microbiol ;, vol. 38, pp. :2665-9., 2000 .

18. Giustina A, Casanueva FF, Cavagnini F,et al. "Diagnosis and treatment of acromegaly complications," Journal of Endocrinological Investigation, pp. 1242-1247, 2014.

19. Revsbech NP. "Analysis of Microbial Communities with Electrochemical Microsensors and Microscale Biosensors," Methods in Enzymology, pp. 147-166, 2005.

20. Franke, D., Binder, S., & Gerlach, G. "Performance of Fast-Responsive, Porous Crosslinked Poly(N-Isopropylacrylamide) in a Piezoresistive Microsensor," IEEE Sensors Letters, vol. 1 (6), pp. 1-4, 2017.

21. Stephen Inbaraj B, Chen BH. "Nanomaterial-based sensors for detection of foodborne bacterial pathogens and toxins as well as pork adulteration in meat products," Journal of Food and Drug analysis, pp. 15-28, 2016.

22. Suryyani Deb, Kanjaksha Ghosh, Shrimati Dharmapal Shetty "Nanoimaging in cardiovascular diseases: Current state of the art," Indian journal of Medical Research, pp. 285-298, 2015.

23. Magdalena Swierczewska, Gang Liu, Seulki Lee, Xiaoyuan Chen "High-sensitivity nanosensors for biomarker detection," Chemical Society Reviews, pp. 2641-2655, 2012.

24. Kaittanis C, Santra S, Perez JM. "Emerging nanotechnology-based strategies for the identification of microbial pathogenesis," Advanced Drug Delivery Reviews, pp. 408-423, 2010.

25. Nath Sudip. "Dextran-coated gold nanoparticles for the assessment of antimicrobial susceptibility," Analytical chemistry, pp. 1033-1038, 2008.

26. Briza Pérez-López, Arben Merkoçi "Nanomaterials based biosensors for food analysis applications," Trends in Food Science & Technology, pp. 625-639, 2011.

27. Munawar Anam. Ong Yori, Schirhagl Romana, et al. Nanosensors for diagnosis with optical, electric and mechanical transducers. RSC Advances, The Royal Society of Chemistry, 9, 12, 6793-6803. 2019.

28. Shuyan Zhao, Bo You, Linlei Jian "Oriented Assembly of Zinc Oxide Mesocrystal in Chitosan and Applications for Glucose Biosensors," Crystal Growth Design, pp. 3359-3365, 2016.

29. Tian L, Qian K, Qi J, Liu Q, et al. "Gold nanoparticles superlattices assembly for electrochemical biosensor detection of microRNA-21," Biosens Bioelectron, pp. 564-570, 2018.

30. Jung DU, Ahmad R, Hahn YB. "Nonenzymatic flexible field-effect transistor based glucose sensor fabricated using NiO quantum dots modified ZnO nanorods," J Colloid Interface Sci., pp. 21-28, 2018.

31. Chen H, Lou R, Chen Y, Chen L, Lu J, Dong Q. "Photonic crystal materials and their application in biomedicine," Drug Delivery, pp. 775-780, 2017.

32. Lima CSA, Balogh TS, Varca JPRO, "An Updated Review of Macro, Micro, and Nanostructured Hydrogels for Biomedical and Pharmaceutical Applications," Pharmaceutics, vol. 970, p. 2020, 2020.

33. Karimi Z, Karimi L, Shokrollahi H. "Nano-magnetic particles used in biomedicine: Core and coating materials," Materials Science and Engineering: Mater Sci Eng C Mater Biol Appl. 1;33(5):2465-75. 2013.

34. G. Maduraiveeran, Wei Jin "Nanomaterials based electrochemical sensor and biosensor platforms for environmental applications," Trends Environ Anal Chem, pp. 10-23, 2017.

35. Randa Abdel-Karim,Y. Reda, Aliaa Abdelfatah "Review—Nanostructured Materials-Based Nanosensors," Journal of The Electrochemical Society, p. 167, 2020.

36. Wei Zhang, Shuyun Zhu, Rafael Luque "Recent development of carbon electrode materials and their bioanalytical and environmental applications," Chemical Society Reviews, pp. 715-752, 2016.

References

37. Tîlmaciu CM, Morris MC. "Carbon nanotube biosensors," Frontiers in Chemistry, 2015.

38. Huadong Chen, Rong Lou, Yanxiao Chen,et al "Photonic crystal materials and their application in biomedicine," Drug Delivery, pp. 775-780, 2017.

39. Fan X, White IM, Shopova SI, et al. "Sensitive optical biosensors for unlabeled targets: A review," analytica chimica acta, pp. 8-26, 2008.

40. Owais Mohammad Gatoo, Manzoor Ahmad Naseem, Sufia, et al. Physicochemical Properties of Nanomaterials: Implication in Associated Toxic Manifestations. Toxicity of Nanomaterials, 498420. 2014.

41. Yallapu, Murali Mohan et al. "Design and engineering of nanogels for cancer treatment." Drug discovery today vol. 16,9-10: 457-63. 2011

42. Li D, van Nostrum CF, Mastrobattista E, et al. "Nanogels for intracellular delivery of biotherapeutics," Journal of Controlled Release,, pp. 16-28, 2017.

43. Mahmoudi M, Sant S, Wang B "Superparamagnetic iron oxide nanoparticles (SPIONs): development, surface modification and applications in chemotherapy," Advance Drug Delivery Review, pp. 24-46, 2011.

44. Z. Karimi, L. Karimi, H. Shokrollahi "Nano-magnetic particles used in biomedicine: Core and coating materials," Materials Science and Engineering: C,, pp. 2465-2475, 2013.

45. Brian. R. Eggins, Chemical Sensors and Biosensors, John Wiley & sons, (Vol. 28) 2008.

46. Jain KK "Nanotechnology in clinical laboratory diagnostics," Clinica Chimica Acta, pp. 37-54, 2005.

47. Wang J, Katz E "Digital biosensors with built-in logic for biomedical applications—biosensors based on a biocomputing concept," Analytical and Bioanalytical Chemistry, pp. 1591-1603, 2010.

48. Tian L, Qian K, Qi J, et al. "Gold nanoparticles superlattices assembly for electrochemical biosensor detection of microRNA-21," Biosens Bioelectron, pp. 564-570, 2018.

49. Shuyan Zhao, Bo You, and Linlei Jiang "Oriented Assembly of Zinc Oxide Mesocrystal in Chitosan and Applications for Glucose Biosensors," Crystal Growth Design, pp. 3359-3365, 2016.

50. Jung DU, Ahmad R, Hahn YB. "Nonenzymatic flexible field-effect transistor based glucose sensor fabricated using NiO quantum dots modified ZnO nanorods," J Colloid Interface Sci., pp. 21-28, 2018.

51. Liang L, Lan F, Ge S, Yu J, Ren N, Yan M,et al. "Metal-Enhanced Ratiometric Fluorescence/Naked Eye Bimodal Biosensor for Lead Ions Analysis with Bifunctional Nanocomposite Probes," Anal Chem., pp. 3597-3605, 2017.

52. Qing Wang, Rongjuan Liu, Xiaohai Yang, et al. "Surface plasmon resonance biosensor for enzyme-free amplified microRNA detection based on gold nanoparticles and DNA supersandwich," Sensors and Actuators B: Chemical, pp. 613-620, 2016.

53. Tean Zaheer, Kaushik Pal, Iqra Zaheerd "Nanosensors for better diagnosis of health," in Kaushik Pal, Fernando Gomes, Elsevier, 2020, pp. 187-228.

54. Veeradasan Perumal, U. Hashim "Advances in biosensors: Principle, architecture and applications," Journal of Applied Biomedicine, vol. 12, pp. 1-15, 2014.

55. Christopher R. Lowe "Overview of biosensor and bioarray technologies," in Handbook of biosensors and biochips, 2008.

56. David W.G. Morrison, Mehmet R Dokmeci, Utkan Demirci, Ali Khademhosseini "Clinical Applications of micro- and nanoscale biosensors," in Biomedical Nanostructures, 2007, pp. 439-460.

57. Béatrice D. Leca-Bouvier, Loïc J. Blum "Enzyme for Biosensing Applications," in .Recognition receptors in biosensors, New York, NY, Springer, 2010, pp. 177-220.

58. Cass T., "Enzymology," in Handbook of biosensors and biochips, 2008.

59. Veeradasan Perumal, Uda Hashim. "Advances in biosensors: Principle, architecture and applications," Journal of Applied Biomedicine, pp. 1-15, 2014.

60. N. Bojorge Ramírez, A. M. Salgado, B. Valdman "The evolution and developments of immunosensors for health and environmental monitoring: problems and perspectives," Brazilian journal of chemical engineering, pp. 227-249, 2009.

61. S.M. Ushaa, M. Madhavilatha, G. Madhusudhan Rao "Design and analysis of nanowire sensor array for prostate cancer detection," International Journal of Nano and Biomaterials, pp. 239-255, 2011.

62. Parkinson, G., & Pejcic, B Prepared "Using Biosensors to detect emerging infectious diseases," Prepared for The Australian Biosecurity Cooperative Research Centre, 2005.

63. Chia-Hsien Yeh, Yu-Huai Chang, Hong-Ping Lin, Tsung-Chain Chang, Yu-Cheng Lin "A newly developed optical biochip for bacteria detection based on DNA hybridization," Sensors and Actuators B: Chemical, pp. 1168-1175, 2012.

64. Yantian Wang, Zhiquan Zhang, Vijay Jain, et al. "Potentiometric sensors based on surface molecular imprinting: Detection of cancer biomarkers and viruses," Sensors and Actuators B: Chemical, vol. 146, pp. 381-387, 2010.

65. Melamed S, Elad T, Belkin S. "Microbial sensor cell arrays," Current Opinion in Biotechnology, vol. 23, pp. 2-8, 2012.

66. U. Bohrna, E. Stütz, K. Fuchs, et al. Wagner "Monitoring of irritant gas using a whole-cell-based sensor system," Sensors and Actuators B: Chemical, vol. 175, pp. 208-217, 2012.

67. Jeevanandam J, Barhoum A, Chan YS, Dufresne A, Danquah MK. Review on nanoparticles and nanostructured materials: history, sources, toxicity and regulations. Beilstein J Nanotechnol. 2018;9:1050-1074. Published 2018 Apr 3. doi:10.3762/bjnano.9.98

68. Rohloff J.C., Gelinas A.D., Jarvis T.C., et al. "Nucleic Acid Ligands With Protein-like Side Chains: Modified Aptamers and Their Use as Diagnostic and Therapeutic Agents,," Moleculer therapy Nucleic Acids, vol. 3, pp. e201,ISSN 2162-2531,, 2014.

69. Wang, Y.; Xu, H.; Zhang, J.; Li, G., "Electrochemical Sensors for Clinic Analysis," Sensors, vol. 8, pp. 2043-2081, 2008.

70. Monošík R, Stred'anský M, Šturdík E. "Application of electrochemical biosensors in clinical diagnosis," Journal of clinical laboratory analysis, vol. 26, pp. 22-34, 2012.

71. Ibrahim Abdulhalim, Mohammad Zourob, Akhlesh Lakhtakia "Overview of optical biosensing techniques," in Handbook of Biosensors and Biochips, 2008.

72. Anam Munawarabc, Yori Ongb, Romana Schirhagl, et al. "Nanosensors for diagnosis with optical, electric and," Royal society of Chemistry, pp. 6793-6803, 2019.

73. Tichý, J., Erhart, J., Kittinger, E., Prívratská, J.Fundamentals of piezoelectric sensorics: mechanical, dielectric, and thermodynamical properties of piezoelectric materials, Springer Science & Business Media, 2010.

74. Bin XieKumaran RamanathanBengt Danielsson "Principles of enzyme thermistor systems: Applications to biomedical and other measurements," Thermal Biosensors, Bioactivity, Bioaffinitty, pp. 1-33, 2001.

References

75. Maskow, Thomas, Wolf, et al. "Rapid analysis of bacterial contamination of tap water using isothermal calorimetry," Thermochimica acta, pp. 273-280, 2012.

76. Draz MS, Vasan A, Muthupandian A, et al. Virus detection using nanoparticles and deep neural network-enabled smartphone system. Sci Adv. 2020;6(51):eabd5354. Published 2020 Dec 16. doi:10.1126/sciadv.abd5354

77. Ding X, Mauk MG, Yin K, Kadimisetty K, Liu C " Interfacing Pathogen Detection with Smartphones for Point-of-Care Applications.," Anal Chem. ;, vol. 91(1):, pp. 655-672. doi:10.1021/acs.analchem.8b04973, 2019.

78. David M. Cate, Jaclyn A. Adkins, Jaruwan Mettakoonpitak, and Charles S. Henry "Recent Developments in Paper-Based Microfluidic Devices," Anal. Chem. , Vols. , 87, 1, , p. 19–41, 2015.

79. Senf B, Yeo WH, Kim JH. Recent Advances in Portable Biosensors for Biomarker Detection in Body Fluids. Biosensors (Basel). 2020;10(9):127. Published 2020 Sep 18. doi:10.3390/bios10090127

80. Sharifi M, Hasan A, Haghighat S, et al. Rapid diagnostics of coronavirus disease 2019 in early stages using nanobiosensors: Challenges and opportunities. Talanta. 2021;223(Pt 1):121704. doi:10.1016/j.talanta.2020.121704

81. Gowri A, Ashwin Kumar N, Suresh Anand BS. Recent advances in nanomaterials based biosensors for point of care (PoC) diagnosis of Covid-19 - A minireview. Trends Analyt Chem. 2021;137:116205. doi:10.1016/j.trac.2021.116205

82. Hu J, Wang S, Wang L, et al. "Advances in paper-based point-of-care diagnostics," Biosensors and Bioelectronics , pp. 585-597, 2014.

83. Dincer C, Bruch R, Kling A, Dittrich PS, Urban GA. "Multiplexed Point-of-Care Testing - xPOCT.," Trends Biotechnol, vol. 35(8):, pp. 728-742. doi: 10.1016/j.tibtech.2017.03.013., . 2017 Aug;.

84. Nie Z, Nijhuis CA, Gong J, et al. "Electrochemical sensing in paper-based microfluidic devices.," Lab Chip, vol. 21;10(4):, pp. 477-83, . 2010 Feb .

85. Park TS, Li W, McCracken KE, Yoon JY "Smartphone quantifies Salmonella from paper microfluidics.," Lab Chip. , vol. 21;13(24): , pp. 4832-40., 2013 Dec .

86. Abdollahi-Aghdam A, Majidi MR, Omidi Y. Microfluidic paper-based analytical devices (μPADs) for fast and ultrasensitive sensing of biomarkers and monitoring of diseases. Bioimpacts. 2018;8(4):237-240. doi:10.15171/bi.2018.

87. F. Li ,Xu Wang ,Jiachang Liu ,Yuting Hu ,Jian-Bo He "Double-layered microfluidic paper-based device with multiple colorimetric indicators for multiplexed detection of biomolecules,," Sensors and Actuators B-chemicaL,, vol. 288, pp. 266-273, 2019.

88. Koczula KM, Gallotta A. " Lateral flow assays.," Essays Biochem. ;, vol. 60(1):, pp. 111-120. doi:10.1042/EBC20150012, 2016.

89. Mahapatra S, Chandra P. Clinically practiced and commercially viable nanobio engineered analytical methods for COVID-19 diagnosis. Biosens Bioelectron. 2020;165:112361. doi:10.1016/j.bios.2020.112361 "

90. K. Nielsen, W. L. Yu, M. Lin,et al. Prototype single step lateral flow technology for detection of avian influenza virus and chicken antibody to avian influenza virus.," J Immunoay Immunochem. , 2007;28(4):307-18.

91. Miroslav Pohanka "Point-of-Care Diagnoses and Assays Based on Lateral Flow Test," International Journal of Analytical Chemistry., pp. 1-9, 2021.

92. St John A, Price CP "Existing and Emerging Technologies for Point-of-Care Testing.," Clin Biochem Rev., pp. ;35(3):155-167., 2014.

93. Hua Xua, Dayong Gua, Jian'an Hea, et al." Multiplex biomarker analysis biosensor for detection of hepatitis B virus.," Bio-Medical Materials and Engineering , vol. 26, pp. S2091-S2100, 2015.

94. Henderson WA . Henderson WA, " Simple lateral flow assays for microbial detection in stool.," Anal Methods., pp. 7;10(45):5358-5363. doi:, 2018 Dec.

95. Blažková, M., Koets, M., Rauch, P. et al. "Development of a nucleic acid lateral flow immunoassay for simultaneous detection of Listeria spp. and Listeria monocytogenes in food.," Eur Food Res Technol , pp. 229, 867, 2009.

96. Bahadır EB, Sezgintürk MK. " Applications of commercial biosensors in clinical, food, environmental, and biothreat/biowarfare analyses.," Anal Biochem, pp. 1;478:107-20, 2015 .

97. Sharifi M, Hasan A, Haghighat S, Taghizadeh A, Attar F, Bloukh SH, Edis Z, Xue M, Khan S, Falahati M. Rapid diagnostics of coronavirus disease 2019 in early stages using nanobiosensors: Challenges and opportunities. Talanta. 2021 Feb 1;223(Pt 1):121704. doi: 10.1016/j.talanta.2020.121704. Epub 2020 Sep 28. PMID: 33303154; PMCID: PMC7521920.

98. A. Gessesse, " The use of nug meal as a low-cost substrate for the production of alkaline protease by the alkaliphilic Bacillus sp. AR-009 and some properties of the enzyme.," Bioresour. Technol. , vol. 62, pp. , 59–61doi: 10.1016/S0960-8524(97)00059-, 1997.

99. Panda MK, Sahu MK, Tayung K "Isolation and characterization of a thermophilic Bacillus sp. with protease activity isolated from hot spring of Tarabalo, Odisha, India. Iran," . J. Microbiol., p. 5:159, 2013.

100. Jose L. Adrio, Arnold L. Demain, "Microbial enzymes: tools for biotechnological processes.," Biomolecules, vol. 4, p. 117–139. doi: 10.3390/biom4010117., 2014.

101. B. Johnvesly and G. R. Naik. "Studies on production of thermostable alkaline protease from thermophilic and alkaliphilic Bacillus sp. JB-99 in a chemically defined medium.," Process Biochem., Vols. 37, , pp. 139–144. doi: 10.1016/S0032-95, 2001.

102. Barrett AJ, McDonald JK. Nomenclature: protease, proteinase and peptidase. Biochem J. 1986;237(3):935. doi:10.1042/bj2370935.

103. Mayuri Sharma,Yogesh Gat, Shalini Arya, et al."A Review on Microbial Alkaline Protease: An Essential Tool for Various Industrial Approaches," Industrial Biotechnology, vol. 15, pp. 69-78./doi.org/10.1089/ind.2018.0032, 2019.

104. Dramsi S, Magnet S, Davison S, Arthur M "Covalent attachment of proteins to peptidoglycan," FEMS Microbiology Reviews, vol. 32, pp. 307–320,, 2008.

105. F. C. B. J. Neuhaus, " A Continuum of Anionic Charge: Structures and Functions of D-Alanyl-Teichoic Acids in Gram-Positive Bacteria.," Microbiol. Mol. Biol. Rev., vol. 67, pp. 686-723, 2003.

106. J. P. a. T. Uehara, " How Bacteria Consume Their Own Exoskeletons (Turnover and Recycling of Cell Wall Peptidoglycan.," Microbiology and Molecular Biology Reviews, vol. 72, p. 211 – 227, 2008.

107. Schmidt R, Bukau B, Mogk A, ".Principles of general and regulatory proteolysis by AAAþ proteases in Escherichia coli.," Research in Microbiology, vol. 160, pp. 629-636, 2009.

108. Zeinert RD, Baniasadi H, Tu BP, Chien P, "The Protease Links Nucleotide Metabolism with Proteotoxic Stress,," Molecular Cell, vol. 79, no. 5, pp. 758-767, 2020.

109. Blackman SA, Smith TJ, Foster SJ, "The role of autolysins during vegetative growth of Bacillus subtilis 168 .," Microbiology , vol. 144, no. 1, p. 1998.

110. Smith TJ, Blackman SA, Foster SJ, "Autolysins of Bacillus subtilis: multiple enzymes with multiple functions," Microbiology , vol. 146, p. 249–262, 2000.

111. Kaminishi H, Hamatake H, Cho T, et al. "Activation of blood clotting factors by microbial proteinases.," FEMS Microbiology Letters, , vol. 121, no. 3, p. 327–332, 1994.

112. Bowler PG, Duerden BI, Armstrong DG, "Wound Microbiology and Associated Approaches to Wound Management," Clin Microbiol Rev. , vol. 14, no. 2, p. 244–269, 2001.

113. Frees D, Brøndsted L, Ingmer H, Bacterial Proteases and Virulence. In: Dougan D. (eds), vol. 66, 2013, pp. 161-192.

114. M.A.F. Anéas, F.C.V. Portaro, I. Lebrun, et al. " a possible virulence factor from Proteus mirabilis exhibits broad protease substrate specificity," . Braz. J. Med.Biol. Res., vol. 34 (11), p. 1397403., 2001.

115. Grady PG, Davis AT, Shapira E, "The Effect of Some Protease Substrates and Inhibitors on Chemotaxis and Protease Activity of Human Polymorphonuclear Leukocytes," The Journal of Infectious Diseases, vol. 140, no. 6, pp. 999-1003, 1979.

116. Ghoreishi FS, Roghanian R, Emtiazi G, "Inhibition of quorum sensing-controlled virulence factors with naturalsubstances and novel protease, obtained from Halobacillus karajensis," Microbial Pathogenesis, vol. 149, p. 104555, 2020.

117. McCarty SM, Cochrane CA, Clegg PD, Percival SL, " The role of endogenous and exogenous enzymes in chronic wounds: a focus on the implications of aberrant levels of both host and bacterial proteases in wound healing," Wound Repair Regen, vol. 20, no. 2, pp. 125-3, 2012.

118. Jusko M, Potempa J, Kantyka T, Bielecka E, et al. "Staphylococcal Proteases Aid in Evasion of the Human Complement System," J Innate Immun , vol. 6, pp. 31-46, 2014.

119. Lebrun I, Marques-Porto R, Pereira AS, et al. "Bacterial Toxins: An Overview on Bacterial Proteases and their Action as Virulence Factors.," Mini-Reviews in Medicinal Chemistry , vol. 9, no. 7, pp. 820-828, 2009.

120. Jennifer Bromberg-White, Chih-Shia Lee, Nicholas Duesbery, "Consequences and Utility of the Zinc-Dependent Metalloprotease Activity of Anthrax Lethal Toxin," Toxins , vol. 2, no. 5, pp. 1038-1053;, 2010.

121. L-Ruth Montes 1, Félix M Goñi, Norah C Johnston, et al. "Membrane Fusion Induced by the Catalytic Activity of a Phospholipase C/Sphingomyelinase from Listeria monocytogenes," Biochemistry , vol. 43, no. 12, p. 3688–3695, 2004.

122. Y Sakata , T Akaike, M Suga, S Ijiri, et al. "Bradykinin Generation Triggered by Pseudomonas Proteases Facilitates Invasion of the Systemic Circulation by

Pseudomonas aerugino," Microbiology and Immunology, vol. 40, no. 6, pp. 415-423, 1996 .

123. Robert Thänert, Oliver Goldmann, Andreas Beineke, Eva Medinaa, "Host-inherent variability influences the transcriptional response of Staphylococcus aureus during in vivo infection," Nature Communications, vol. 8, p. 14268. , 2017.

124. David Ribet , Pascale Cossart, " How bacterial pathogens colonize their hosts and invade deeper tissues," Microbes Infect , vol. 17, no. 3, pp. 173-83. , 2015 .

125. Koki Matsumoto, "Role of bacterial proteases in pseudomonal and serratial keratitis.," Biol Chem. , vol. 385, no. 11, pp. 1007-16, 2004 .

126. M. T. Pöllänen, M. A. Laine, R. Ihalin, V.-J. Uitto, " Proteases and their inhibitors in chronic inflammatory periodontal disease. .," J Clin Periodontol, vol. 13, no. 1, pp. 19-26, 1986.

127. K Maruo 1, T Akaike, Y Matsumura, et al. ". Triggering of the vascular permeability reaction by activation of the Hageman factor-prekallikrein system by house dust mite proteinase.," Biochimica et Biophysica Acta (, Vols. 1074, Issue 1,, pp. 62-68,, 1991.

128. T Akaike , A Molla, M Ando, et al. "Molecular mechanism of complex infection by bacteria and virus analyzed by a model using serratial protease and influenza virus in mice.," J Virol., vol. 63, no. 5, pp. 2252-9, 1989 .

129. Ian Alan Holder, " Pseudomonas elastase acts as a virulence factor in burned hosts by Hageman factor-dependent activation of the host kinin cascade.," Infect Immun, vol. 57, no. 11, pp. 3345-3348., 1989.

130. H Maeda, T Akaike, J Wu, et al. " Bradykinin and nitric oxide in infectious disease and cancer.," Immunopharmacology, Vols. 33(1-3):, pp. 222-30, 1996 .

131. M B Wikström, "Detection of microbial proteolytic activity by a cultivation plate assay in which different proteins adsorbed to a hydrophobic surface are used as substrates.," Appl Environ Microbiol, vol. 45(2): , p. 393–400., 1983 .

132. Suaifan GARY, Al Nobani SWA, Shehadeh MB, Darwish RM. "Engineered colorimetric detection of Staphylococcus aureus extracellular proteases,," Talanta, vol. 198, pp. 30-38, 2019.

133. Vermelho AB, Meirelles MN, Lopes A, e. al, "Detection of extracellular proteases from microorganisms on agar plates," BIOCHEMISTRY , vol. 91, no. 6, pp. 755-760, 1996.

134. Yager P, Domingo GJ, Gerdes J. "Point-of-care diagnostics for global health,," Annu. Rev. Biomed. Eng, vol. 10, p. 107–144., 2008 .

135. Kaman WE, Galassi F, de Soet JJ, et al. "Highly specific protease-based approach for detection of porphyromonas gingivalis in diagnosis of periodontitis". J Clin Microbiol. 2012 Jan;50(1):104-12. doi: 10.1128/JCM.05313-11. Epub 2011 Nov 9. PMID: 22075590; PMCID: PMC3256702 .

136. Kaman, Wendy E; Nora El Arkoubi-El Arkoubi; Roffel, Sanne; E, et al. "Evaluation of a FRET-Peptide Substrate to Predict Virulence in Pseudomonas aeruginosa," PLOS one, vol. 8, no. 11, p. e81428 , 2013 .

137. Kaman WE, Hulst AG, van Alphen PT, et al. "Peptide-based fluorescence resonance energy transfer protease substrates for the detection and diagnosis of Bacillus species," Anal Chem. Apr , vol. 1;83(7), pp. 2511-7, 2011 .

138. Galassi F, Kaman WE, Anssari Moin D, et al. "Comparing culture, real-time PCR and fluorescence resonion of Porphyromonas gingivalis in of Porphyromonas gingivalis in patients with or without peri-implant infections," J Periodontal Res. , vol. 47(5):, pp. 616-25, 2012 .

139. Dickenson NE, Picking WD. Förster resonance energy transfer (FRET) as a tool for dissecting the molecular mechanisms for maturation of the Shigella type III secretion needle tip complex. Int J Mol Sci. 2012;13(11):15137-15161. Published 2012 Nov 16. doi:10.3390/ijms131115137

140. Zindel S, Kaman WE, Fröls S, et al. The papain inhibitor (SPI) of Streptomyces mobaraensis inhibits bacterial cysteine proteases and is an antagonist of bacterial growth. Antimicrob Agents Chemother. 2013;57(7):3388-3391. doi:10.1128/AAC.00129-13

141. . Nath-Chowdhury M, Sangaralingam M, Bastien P, et al. Real-time PCR using FRET technology for Old World cutaneous leishmaniasis species differentiation. Parasit Vectors. 2016;9:255. Published 2016 May 3. doi:10.1186/s13071-016-1531-4.

142. Xue Qiu &Niko Hildebrandt "A clinical role for Förster resonance energy transfer in molecular diagnostics ofdisease," EXPERT REVIEW OF MOLECULAR DIAGNOSTICS , Vols. 19, NO. 9, , p. 767–771, 2019.

143. Van Dorst B, Mehta J, Bekaert K, " Recent advance in recognition element of food and environmental at biosensor.," Biosensor Bioelectronics, vol. 28, pp. 1178-1194, 2010.

144. J Wang, G Rivas, X Cai, E Palecek, P Nielsen, et al. "DNA electrochemical biosensors for environmental monitoring," .A review 'Analytica Chimica Acra ,., vol. 347 , pp. 1-8, 1997.

145. Giovanna Marrazza, Iva Chianella, Marco Mascini, "Disposable DNA electrochemical biosensors for environmental monitoring „" Analytica Chimica Acta vol. 387 , pp. 297-307, 1999.

146. Su H, Li S, Jin Y, Xian ZY, et al. "Nanomaterial-based biosensors for biological detections.," Advanced Health Care Technologies., vol. 3, pp. 19-29, 2017.

147. Niemz A, Ferguson TM, Boyle DS. " Point-of-care nucleic acid testing for infectious diseases.," Trends Biotechnol, vol. 29(5):, pp. 240-50., 2011 .

148. Quentin Palomar, XingXing Xu, Robert Selegård. "Peptide decorated gold nanoparticle/carbon nanotube electrochemical sensor for ultrasensitive detection of matrix metalloproteinase-7.," Sensors and Actuators B: Chemical, vol. 325, p. 128789, 2020.

149. Seonhwa Park, a Yu Mi Shin,b Jeongwook Seo,a et al . "A highly sensitive and simply operated protease sensor toward point-of-care testing," Analyst, vol. 141, pp. 2481-2486, 2016.

150. Ghadeer Suaifan, M Zourob "Rapid Detection of Prostate Specific Antigen Biomarker Using Magnetic-Nanoparticles," Procedia Technology, vol. 27, pp. 122-125, 2017.

151. Kaman WE, Voskamp-Visser I, de Jongh DM "Evaluation of a D-amino-acid-containing fluorescence resonance energy transfer peptide library for profili," Analytical Biochemistry, , Vols. 441,1,, pp. 38-43., 2013.

152. AL Välimaa, A Tilsala-Timisjärvi, E Virtanen "*Listeria monocytogenes*; Food; Detection; Rapid; Alternative; Methods," Food Control, vol. 55, pp. 103-114, 2015.

153. Fu Z, Zhou X, Xing D. "Sensitive colorimetric detection of *Listeria monocytogenes* based on isothermal gene amplification and unmodified gold nanoparticles" Methods, vol. 64, p. 260—266., 2013.

154. Law JW, Ab Mutalib NS, Chan KG, Lee LH. " An insight into the isolation, enumeration, and molecular detection of Listeria monocytogenes in food.," Front Microbiol. , p. ;6:1227. , 2015.

155. Data, WHO Library Cataloguing-in-Publication "WHO estimates of the global burden of foodborne diseases: foodborne disease burden," World Health Organization., p. ISBN 978 92 4 156516 5 , 2007-2015.

156. H. Tronel, P. Hartemann "Overview of diagnostic and detection methods for legionellosis and Legionella spp.," Letters in Applied Microbiology, vol. 48 , p. 653–656, 2009.

157. Wayne Conlan, Baskerville A. "Separation of Legionella pneumophila Proteases and Purification of a Protease Which Produces Lesions Like Those of Legionnaires"

Disease in Guinea Pig Lung.," Journal of general microbiology.vol. 132, pp. 1565-1574, 1986.

158. J.S. Rosenfeld, F. Kueppers, T. Newkirk, et al. " A protease from Legionella pneumophila with cytotoxic and dermal ulcerative activity,," FEMS Microbiology Letters,, vol. 37, no. 1, pp. 51–58,, 1986.

159. Anuj SN, Whiley DM, Kidd TJ,et al.. "Identification of Pseudomonas aeruginosa by a duplex real-time polymerase chain reaction assay targeting the ecfX and the gyrB genes.," Diagn Microbiol Infect Dis, vol. 63(2):, pp. 12-16, 2009 .

160. Carol W. Price,a   Daniel C. Lesliea, James P. Landers "Nucleic acid extraction techniques and application to microchip.," lab chip;, vol. 9, pp. 2484-2494., 2009.

8. Publications

[SAA 1]

Rapid colorimetric sensing platform for the detection of *Listeria monocytogenes* foodborne pathogen.

Sahar Alhogail , Ghadeer A R Y Suaifan , Mohammed Zourob Biosensor Bioelectronics'. 15;86, 2016, 1061-1066 . doi: 10.1016/j.bios.2016.07.043. Epub 2016 Jul14.

	Sahar Alhogail	Ghadeer A R Y Suaifan
Konzeption des Forschungsansatzes	X	X
Planung der Untersuchungen	X	X
Datenerhebung	X	
Datenanalyse und – interpretation	X	
Schreiben des Manuskripts	X	
Vorschlag Anrechnung Publikationsäquivalente	1,0	

Contents lists available at ScienceDirect

Biosensors and Bioelectronics

journal homepage: www.elsevier.com/locate/bios

Rapid colorimetric sensing platform for the detection of *Listeria monocytogenes* foodborne pathogen

Sahar Alhogail [a], Ghadeer A.R.Y. Suaifan [b], Mohammed Zourob [a,c,*]

[a] Department of Chemistry, Alfaisal University, Al Zahrawi Street, Al Maather, Al Takhassusi Road, Riyadh 11533, Saudi Arabia
[b] Department of Pharmaceutical Sciences, Faculty of Pharmacy, The University of Jordan, Amman 11942, Jordan
[c] King Faisal Specialist Hospital and Research Center, Zahrawi Street, Al Maather, Riyadh 12713, Saudi Arabia

ARTICLE INFO

ABSTRACT

Listeria monocytogenes is a serious cause of human foodborne infections worldwide, which needs spending billions of dollars for inspection of bacterial contamination in food every year. Therefore, there is an urgent need for rapid, in-field and cost effective detection techniques. In this study, rapid, low-cost and simple colorimetric assay was developed using magnetic nanoparticles for the detection of listeria bacteria. The protease from the listeria bacteria was detected using D-amino acid substrate. D-amino acid substrate was linked to the carboxylic acid on the magnetic nanoparticles using EDC/NHS chemistry. The cysteine residue at the C-terminal of the substrate was used for the self-assembled monolayer formation on the gold sensor surface, which in turn the black magnetic nanobeads will mask the golden color. The color will change from black to golden color upon the cleavage of the specific peptide sequence by the Listeria protease. The sensor was tested with serial dilutions of *Listeria* bacteria. It was found that the appearance of the gold surface area is proportional to the bacterial concentrations in CFU/ml. The lowest detection limit of the developed sensor for Listeria was found to be 2.17×10^2 colony forming unit/ml (CFU/ml). The specificity of the biosensor was tested against four different foodborne associated bacteria (*Escherichia coli*, *Salmonella*, *Shigella flexnerii* and *Staphylococcus aureus*). Finally, the sensor was tested with artificially spiked whole milk and ground meat spiked with *listeria*.

© 2016 Elsevier B.V. All rights reserved.

1. Introduction

Ingestion of foods contaminated with pathogens such as bacteria, viruses, and parasites leads to the Foodborne diseases (FBD). Foodborne disease pose a significant health problem in the world, with significant rate of morbidity and mortality, in both developed and developing countries. The most common known bacterial foodborne pathogens are *Escherichia coli* O157: H7, *Salmonella enterica*, *Staphylococcus aureus*, *Listeria monocytogenes*, *Campylobacter jejuni* and *Bacillus cereus* (Zhao et al., 2014). *Listeria monocytogenes* considered as one of the pathogens causing gastroenteritis, and more likely to lead to death (Robert et al., 2009; Vazquez-Boland et al., 2001; GarridO, et al. 2008). *L. monocytogenes* has been associated with listeriosis, which has fatality rates up to 30% (Roberts et al., 2009; Auvolat and Gnanou Besse, 2016). Listeriosis affect human's health by either an invasive or non-invasive way. The non-invasive gastrointestinal form is characterized by symptoms like fever, muscles ache, nausea and diarrhea. The invasive form symptoms are much more serious, as upon spreading to the central nervous system, it could lead to meningitis, stiff neck, confusion, loss of balance, convulsion and ocular listeriosis (Mead et al., 2006; Shoughy and Tabbar, 2014). Invasive listeriosis is dominant among immunocompromised populations such as pregnant women, elderly people above 65, new born babies and acquired immune deficiency syndrome (AIDS) patients (Zhao et al., 2014; Centers for Disease Control and Prevention, 2013; Swaminathan and Smidt, 2007).

In pregnant women disease manifestations include miscarriage, stillbirth, perinatal septicemia and meningitis in new born (Mokta et al., 2010; Bobade et al., 2016).

L. monocytogenes contaminates water, soil, silage, fruits, vegetables and food samples such as dairy product (unpasteurized milk and soft cheese), meat and either raw or cooked sea-food. Animals can also be infected by eating contaminated vegetation or poorly prepared animal feed. In general, *L. monocytogenes* grows best at neutral to slightly alkaline pH, tolerate high stress environment form and wide range of temperature (from -18 to $37\,°C$). Thus contamination of ready to eat food by *L. monocytogenes* increases

64

the risk of foodborne disease (O'Connor et al., 2010; Junttila et al., 1988). Food contamination could occur during food processing, packaging and distribution. In food industry, the time between food packaging, inspection and consumption is very crucial. Therefore, *L. monocytogenes* is considered a serious cause of human foodborne infections worldwide (Roberts et al., 2009; Vazquez-Boland et al., 2001; GarridO, et al. 2008; Liu, 2006).

L. monocytogenes detection is commonly achieved by culture methods, which typically requires few days to confirm the results. Moreover, this method is laborious and require trained-personnel (Jadhav et al., 2012; Alessandria et al., 2010; Kabuki et al., 2004; Frece et al., 2010; Gasanov et al., 2005; Brehm-Stecher and Johnson, 2007). Immunoassays based techniques are also used, where it involve specific antigen–antibody reaction. However, the immunoassays suffer from poor sensitivity in comparison with culture based method with detection limit between 10^5 cells/ml and 10^4 cells/ml (Gasanov et al., 2005). Other more-sensitive real-time detection kits were developed, which require sample pre-enrichment procedures and very expensive for the routine lab analysis (Chen et al., 2012). Based on the fact that *L. monocytogenes* foodborne disease represents major concern to public health worldwide. Developing a rapid, specific and sensitive *L. monocytogenes* detection method is urgently needed.

L. monocytogenes has several virulence factors which contributes to its pathogenicity. During infection, *L. monocytogenes* invade the host cell by lysing the phagocytic vacuoles and proliferate in the cytosol with the help of Listeriolysin O (LLO) and two secreted phospholipases C (PLC): a broad-range phospholipase C (PC-PLC) and a phosphatidylinositol specific PLC (PI-PLC) (Portnoy et al., 1992; Smith et al., 1995). Broad-range phospholipase C is released as an inactive propeptide and is activated by the cleavage of the propeptide by a metalloprotease (MMP) at low pH (Marquis and Hager, 2000). Therefore, higher level of MMP would be observed in the host infected with *L. monocytogenes*. This virulence protease could be used as a biomarker for the detection of food contamination. In addition, protease are known to break the peptide bonds in a protein substrate, and some protease are known, to be very specific with regard to the type of peptide bond they are able to cleave (Mitchell, 2003; Kasana et al., 2011). Protease enzyme cleave a selective peptide bond at specific site in protein and polypeptide and contribute in the pathogenicity and feasibility of the disease (Kasana, 2010). Therefore, proteases has been used as biomarkers for the detection of microbial infection due to the specificity and the stability of the enzyme under diverse conditions (Suaifan and Shehadeh, 2013).

Biosensors are a powerful substitute to conventional analytical techniques, due to their high specificity and sensitivity, as well as their small size and cost-effectiveness. Nanoparticles were found to be an excellent tool to be applied for microbe's detection and drug therapy (Suaifan et al., 2013). Our group has developed a number of colorimetric assay based nanoparticles and peptide sequence for prostate specific antigen (PSA), HIV and periodontitis. The assay employing a monolayer of specific substrate peptide conjugated with magnetic nano-particles which has black color. The color will change upon the protease cleavage of the peptide-magnetic nanobeads conjugate (Suaifan and Shehadeh, 2013; Suaifan et al., 2013; Wignarajah et al., 2015).

Overall, simple, cost effective screening assays are needed for the detection of *L. monocytogenes* food contamination from the time it is produced to the time it is purchased. Accordingly, this study aimed towards the development of novel rapid and low-cost colorimetric paper-based detection tool with high sensitivity and specificity. Magnetic nanoparticles conjugated with *L. monocytogenes* protease specific substrate was employed which will be selectively cleaved by the *L. monocytogenes* proteases.

2. Materials and method

Carboxylic acid terminated magnetic nanoparticles (MNPs) with less than 50 nm dispersed as 10 mg/ml in water was purchased form Turbobeads (Zurich, Switzerland). N-Hydroxysuccinimide (NHS) and 1-(3-Dimethylaminopropyl)-3-Ethyl-Carbodiimide (EDC) and pH stripes, Potassium Phosphate, Sodium Chloride, Bovine Serum Albumin (BSA), Ethylenediaminetetraacetic acid (EDTA), Sodium Azide, Tris buffer were purchased from sigma-Aldrich (Dorest, UK). *Listeria monocytogenes* ATCC 19115 *E. coli* ATCC 25922, *Salmonella* ATCC13312, *Shigella flexnerii* ATCC 12022 and *Staphylococcus aureus* ATCC 25923 were purchased from LGC Standards (Middlesex, UK).

Peptide sequences with specific cleavage sites for *L. monocytogenes* (Gasanov et al., 2005) were synthesized by Pepmic Co., Ltd (Suzhou, China) with a purity of about 90%. Two different peptides substrates with D- and L-amino acids have been synthesized for *L. monocytogenes* . Peptides were provided as lyophilized powder and was then dissolved in Dimethyl sulfoxide (DMSO).

2.1. Bacteria growing

Bacteria were grown in 5 ml of Brain heart infusion (BHI) broth, incubated at 37 °C for 18 h. Subsequently, 8 serial dilutions in Phosphate buffer saline (PBS) buffer were prepared to determine the bacterial colony forming unit (CFU) value of the original stocks, using viable count spread dilution method. Subsequently, the bacteria were pelted by centrifugation at $3000 \times g$ for 10 min. The supernatant was then filtered with sterile syringe filter 0.22 μm purchased from Millipore (Middlesex, UK) to obtain the protease which is directly proportional to each bacterial concentration.

2.2. Conjugation of the MNPs with L. monocytogenes peptide substrates

Peptide substrates (1 mg/ml) dissolved in DMSO mixed with freshly prepared coupling agent EDC (0.57 mg/ ml) and NHS (12 mg/ml) in water and previously washed MNPs. The mixture was gently mixed by end over end at room temperature for 4 h. After which, uncoupled peptides were removed by washing the beads 3 times with washing buffer. The unreacted carboxylic acids in the beads were blocked by the Tris base in the washing buffer. Finally, the functionalized MNPs were stored at 4° C in storage buffer.

2.3. Preparation of the sensing platform

Self-adhesive sheet was purchased from Whatman (London, U. K.) and was then gold plated using sputtering machine at the School of Engineering at Canfield University. The sheet was cut into narrow pieces (1–2 mm width) and then stacked over plastic strip at standardized distance as shown in Schematic 1A. A specific amount of the MNPs-peptides solution was placed over the gold sensing platform and allowed to dry at room temperature. Then, a permanent magnet (12.5 × 12.5 × 5 cm), strength (3360 gauss and 573 gauss) was passed over the sensor surface to remove unreacted MNPs-peptide. A change in the gold sensor surface into black will be observed by the naked eye upon completion of the immobilization step as shown in Schematic 1B.

Self-adhesive magnetic sheets were provided from Polarity Magnetic Company was cut into 1 mm diameter circle and was stacked at the back of the strip at a standardized distance of 5 mm from the immobilized sensing surface. This magnet would assist collection of the cleaved MNPs-peptide sequence as shown in Scheme 1C.
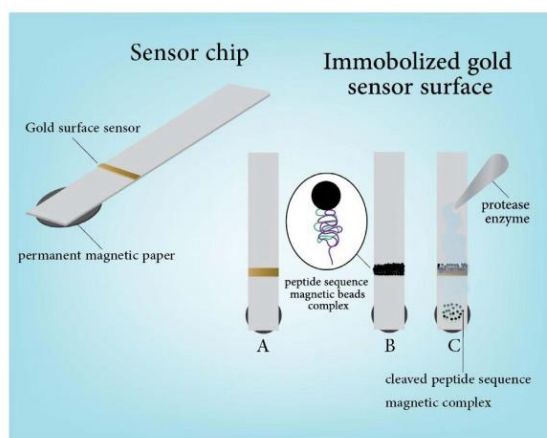
Scheme 1. Schematic image of fabricated sensor assay. The sensor designed specifically for *Listeria monocytogenes* detection. (A) The sensor with gold surface, (B) Immobilized peptide sequence magnetic beads complex over the gold sensor surface masking its gold color, (C) In the presence of protease enzyme of *L. monocytogenes* the proteolytic activity of the enzyme will observed by the dissociation of the magnetic beads complex exposes the gold color background.

2.4. Biosensing of the L. monocytogenes protease

The current colorimetric detection assay is based on the detection of *L. monocytogenes* proteases proteolytic activity using a specific MNPs-peptide-gold sensing probe. Accordingly, *L. monocytogenes protease (bacterial extract containing proteases)* solution (20 μl) was added over the black color sensing probe, which in turn cleave MNPs-peptide complex rendering peptide moiety-gold sensor probe golden color visible to the naked eye. The percentage of the cleaved area was proportional to the protease concentration. Cleaved MNPs-peptide moiety was attracted by the permanent magnetic endorsing a visual colorimetric detection for qualitative evaluation of the tested sample as shown in Schematic 1C.

2.5. Food spiking and testing

5 ml of fresh full-fat milk provided from diary company UK and 2 g of minced ready to eat meat were mixed with 5 ml sterile water, inoculated with a colony of the *L. monocytogenes* and incubated at 35 C° for 15–18 h. The samples were centrifuged at 10,000 × g and the supernatants containing protease were filtrated with 0.22 μm filter (Sigma-Aldrich, UK) and then added onto the sensor surface. Negative blank sample containing no bacteria was also prepared in a similar way and tested to check the matrices effect of the milk and meat content on the sensor.

2.6. Quantification measurements

The developed biosensor was intended to be used by visual observation, the color change (black to golden), as a result of the proteolytic activity of *bacterial* proteases was easily viewed by the naked eye. The appearance of yellow color was quantified by a simple method using the ImageJ program (a public-domain, Java-based image processing program developed at the National Institute of Health). The images taken from smart mobile phone camera before and after the addition of the bacterial samples were processed using the ImageJ software. The results presented as percentage of the amount of the cleaved magnetic beads (appearance of yellow color) to the total immobilized black magnetic nanobeads (black area).

3. Results and discussion

Today, *L. monocytogenes* is considered to be one of the most important pathogenic agents causing foodborne diseases. Small undetectable number of microbes can multiply and become life threatening, especially among the immune compromised populations. Ready to eat foods are considered as a vehicle for the transmission of listeria. As ready to eat food are subjected to different processes and thus are more susceptible to bacterial contamination especially by listeria. Moreover, Listeria has the ability to grow and survive in a wide unfavorable conditions. Thus gives the attentions to assess *Listeria monocytogenes* in the food during manufacturing and distribution.

Proteases are enzymes involved in the bacterial growth, multiplication, and pathogenicity. Therefore, the focus of this study is to develop novel portable low-cost colorimetric screening assay for the detection of *Listeria monocytogenes* proteases using nano-magnetic particles.

3.1. Detection using D-peptide sequences

The proteases extracted from each *Listeria monocytogenes* bacterial concentration was applied to the D-peptide sequence. Figs. 1a and b show the typical results before and after the addition of various bacterial protease concentrations respectively. It shows that there is clear visible correlation between the proteases concentration and the appearance of the yellow area as a result of the cleavage of the black magnetic nanobeads. Second confirmation spot was formed by the accumulation of the black cleaved magnetic nanoparticles at the paper magnetic area. The gradual increase in the appearance of the golden background, reflect the increase in the concentration of the protease. Fig. 2 shows that there is a liner relationship between the amount of cleaved magnetic nanobeads (appearance of the yellow color) and the proteases concentration from various bacterial concentration in CFU/ml.

It is known that the peptide substrate containing D-amino acids are specific and facilitate the prokaryotic cleavages (Kaman and Voskamp-Visser, 2013). In this study, two peptide sequences using D- and L-amino acids were synthesized to compare the proteolytic activity for *Listeria monocytogenes*. Then the selected peptide sequence can be integrated with magnetic nanoparticles for the construction of highly specific peptide sequence which can be cleaved specifically by *Listeria monocytogenes* proteases. Serial dilution of the *Listeria monocytogenes* was prepared to compare the detection limit as colony forming unit (CFU/ml) for both D and L-peptide sequences peptides. The protease extracted from each bacterial concentration was applied to the peptide sequences containing D-and L-aminoacids. Fig. 2 shows the comparison of the percentage of the cleaved nanobeads area for the D- and L-amino acid sequences as a function of various bacteria concentrations. The results show that the peptide sequence containing D-amino acid, is highly specific with lower detection concentration 2.17×10^2 CFU/ml within 30 s, than the sequence containing L-amino acids which gave higher detection limit 2.1×10^3 CFU/ml in 2 h. The detection limit of the D-aminoacids probe sensor in this study, without any pre-concentration of the sample is comparable to the other reported methods. For example, Moreno et al. (2012) was able to detect the *L. monocytogenes* using PCR with D.L 7.4×10^2 after 7 h culturing (Välimaa et al., 2015). Fu et al. (2013) proposed colorimetric method using gold nanomagnetic particles combined with hyper branching rolling circle amplification (HRCA). The method gave detection limit as low as 100 aM synthetic hly gene targets and about 75 copies of *L. monocytogenes* (Fu et al., 2013). Law et al. (2015) used DNA microarray assay and Sabat et al. (2013) used NGS molecular method for the detection and identification of *L. monocytogenes*. Both methods were highly sensitive and specific but laborious, costly and unsuitable for field applications (Law et al., 2015). Table 1 summarizes the detection

Fig. 1. a) Colorimetric *Listeria monocytogenes* protease sensor probe using D-amino acid covalently bound to a magnetic nanobead; a) before adding the sample to the specific *Listeria monocytogenes* protease substrate; b) after adding different concentrations of *Listeria monocytogenes* protease solutions. (For interpretation of the references to color in this figure legend, the reader is referred to the web version of this article.)

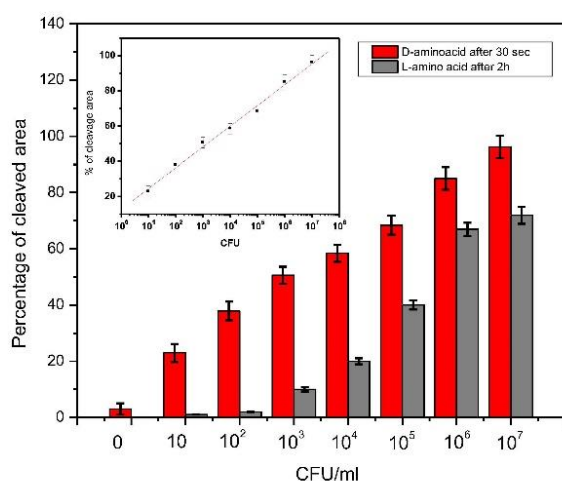limits for the most recent developed assays. Indeed the detection limit

Fig. 2. Shows the comparison of using D- and L-aminoacids in the *Listeria* peptide sequence probe with various bacteria concentrations. The Calibration curve is inserted in the figure to show the potential for quantitative analysis. (For interpretation of the references to color in this figure legend, the reader is referred to the web version of this article.)

from the developed sensor is comparable with the other reported methods but it has alot shorter response time.

3.2. Specificity of the sensor

The sensor was tested for the specificity by using proteases extracted from other commonly associated foodborne bacteria. In this study, proteases extracted from *Staphylococcus aureus*, *Escherichia coli*, *Shigella* and *Salmonella* were used to check the cross-reactivity with the Listeria specific substrate. The results in Fig. 3 show the cleavage only occur with the *Listeria* unlike other bacteria where no cleavage was observed. It can be concluded that the Listeria peptide probe is highly specific to the *Listeria* bacteria detection.

3.3. Testing the sensor with food samples

The sensor was tested with the whole milk and the supernatant of the ready to eat meat to check if the food has any proteolytic activity due to Listeria. Fig. 4A (before adding the sample) and Fig. 4B (B1, meat sample without inoculation) shows that the food supernatant has no effect on the sensor performance. Fresh whole milk and ready to eat meat were spiked with the colony of *Listeria monocytogenes* and incubated at 35 °C for 15–18 h. The concentrations of the bacteria stock after 18 h for the meat was 13.8×10^7 CFU/g and the fresh whole milk count was 11.7×10^7 CFU/ml. The stock concentration was used to make 8 serial dilutions and viable count of spread dilution method was

Table 1
Detection limits of the standard and some alternative, rapid *L. monocytogenes* (LM) detection methods.

| Method detection	Detection limit	Matrix	Refs.
Amperometric	10^2 CFU/g	Blueberries (A)	Davis et al., 2013
Impedance spectroscopy	4 CFU/ml	Tomato extract (A)	Radhakrishnan et al., 2013
Piezoelectric	10^2–10^3 CFU/ml	Milk	Sharma and Mutharasan, 2013
Fe$_3$O$_4$ NPC	5.4×10^3 CFU/ml		Zhang et al., 2016
ELISA based on VHH clone L5-79 and monoclonal Ab	1×10^4 CFU/Ml	Milk	Tu Zhui et al., 2016
Platinum interdigitated array microelectrode	$5.39 +_- 0.21$ CFU/ml		Sidhu et al., 2016
Metagenomics	$< 2 \times 10^2$ CFU/ml	Soft cheese	Wang, 2016

67

1065
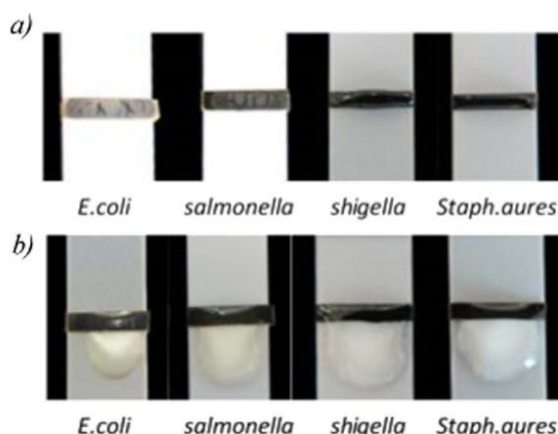
Fig. 3. a) Colorimetric *Listeria monocytogenes* protease sensor probe before the application of different bacterial protease. b) sensor probe under the effect of other bacterial protease.
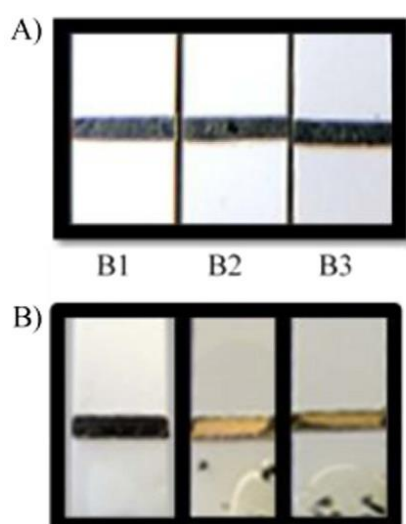

Fig. 4. Colorimetric *Listeria monocytogenes* sensor probe with D- amino acid peptide substrate application on spiked meat; A) Sensor chip functionalized with magnetic beads-specific *Listeria monocytogenes* probe before adding the samples; B) Functionalized biosensor tested with B1) meat supernatant without inoculation. B2) meat supernatant after 18 h of inoculation. B3) meat supernatant after 18 h of inoculation centrifuged.
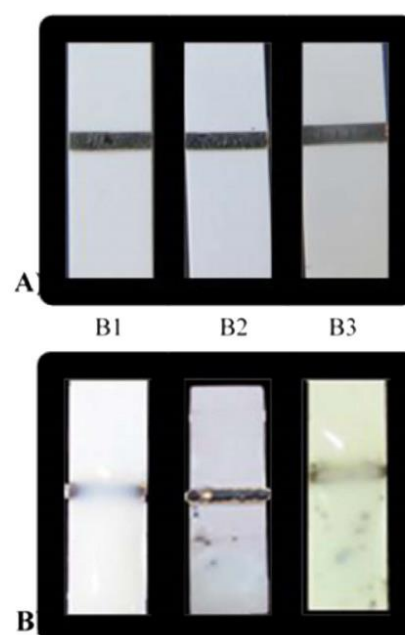

Fig. 5. Colorimetric *Listeria monocytogenes* sensor probe with D- amino acid peptide substrate application on spiked milk. A) Biosensor chip functionalized with magnetic nanobeads-specific *Listeria monocytogenes* probe before adding the sample. B) Functionalized biosensor tested with B1) fresh milk without inoculation. B2) Milk after 18 h of inoculation. B3) Milk supernatant after 18 h of inoculation.

4. Conclusion

In this study, the protease produced from *Listeria monocytogenes* was used as biomarker for the detection of pathogenic *Listeria monocytogenes,* using D- amino acid substrate specific to Listeria. The change of the black color to the golden color, was due to the cleaved magnetic nanobeads, which was proportional to the concentration of the *Listeria*. The detection limit for the *Listeria* was found to be 2.1×10^2 CFU/ml in 30 s. The specificity of the sensor has been tested using the protease extract from other bacteria associated with foodborne diseases. The developed diagnostic tool is low-cost, rapid, sensitive and simple where does not require instrumentation for the read-out. The reported rapid screening assay can be applied as a point of care detecting the contamination of food by pathogenic bacteria and other sectors such as biomedical, environmental and security.

Acknowledgments

References

Alessandria, V., Rantsiou, K., Dolci, P., Cocolin, L., 2010. Int. J. Food Microbiol. 141, 156–162.
Auvolat, A., Gnanou Besse, N., 2016. Food Microbiol. 53, 135–149.
Bobade, S., Warke, S., Kalorey, D., 2016. Int. J. Health Sci. Res. 6 (1), 440–449.

used to confirm the correct bacteria number. The negative control sensor (B1 in Figs. 4 and 5) shows no proteolytic activity with the meat and milk ingredient (before spiking). The sensor (B2 in Figs. 4 and 5) was tested with the spiked samples directly (without centrifugation) and also the samples were tested after centrifugation (B3 in Figs. 4 and 5). It is clear from the amount of the cleaved magnetic nanobeads by the protease on the sensor surface that both give similar detection limit whether the sample is centrifuged or not. The detection limit of the sensor in the spiked milk was 11.7×10^2 CFU/ml and in the spiked meat was 13.8×10 CFU/g. The results obtained within 15 min and without any pre-enrichment steps.

S. Alhogail et al. / Biosensors and Bioelectronics 86 (2016) 1061–1066

Brehm-Stecher, B.F., Johnson, E.A., 2007. Listeria, Listeriosis and Food Safety. Crc Press, Taylor And Francis Group, Boca Raton.

Centers for Disease Control and Prevention, 2013. Vital Signs: Listeria Illnesses, Deaths, and Outbreaks - United States, 2009–2011. MMWR Morbidity and mortality weekly report, 62 (22), pp. 448–52.

Chen, J., Tang, J., Liu, J., Cai, Z., Bai, X., 2012. J. Appl Microbiol. 112 (4), 823–830.

Davis, D., Guo, X., Musavi, L., Lin, C.S., Chen, S.H., Wu, V.C.H., 2013. Ind. Biotechnol. 9 (1), 31–36.

Frece, J., Markov, K., Čvek, D., Kolarec, K., Delaš, F., 2010. J. Dairy Res. 77, 112–116.

Fu, Z., Zhou, X., Xing, D., 2013. Methods 64 (3), 260–266.

GarridO, V., Torroba, L., García-jalón, I., Vitas, A.I., 2008. Eur. Surveill. 13 (49), 1–6.

Gasanov, U., Hughes, D., Hansbro, P.M., 2005. FEMS Microbiol. Rev. 29, 851–875.

Jadhav, S., Bhave, M., Palombo, E.A., 2012. J. Microbiol. Methods 88 (3), 327–341.

Junttila, J.R., Niemala, S.I., Hirn, J., 1988. J. Appl. Bacteriol. 65, 321–327.

Kabuki, D.Y., Kuaye, A.Y., Wiedmann, M., Boor, K.J., 2004. J. Dairy Sci. 87, 2803–2812.

Kaman, W.E., Voskamp-Visser, 2013. Anal. Biochem. 441, 38–43.

Kasana, R.C., 2010. Crit. Rev. Microbiol. 36 (2), 134–145.

Kasana, R.C., Salwana, R., Yadava, S.K., 2011. Crit. Rev. Microbiol. 37, 262–276.

Law, J., Ab Mutalib, N.S., Chan, K.G., Lee, L.H., 2015. Front. Microbiol. 6 (1227), 1–15.

Liu, D., 2006. J. Med. Microbiol. 55, 645–659.

Marquis, H., Hager, E.J., 2000. Mol. Microbiol. 35, 289–298.

Mead, P.S., Dunne, E.F., Graves, L., Wiedmann, M., Patrick, M., Hunter, S., Salehi, E., Mostashari, F., Craig, A., Mshar, P., Bannerman, T., Sauders, B.D., Hayes, P., De-witt, W., Sparling, P., Griffin, P., Morse, D., Slutsker, L., Swaminathan, B., 2006. Epidemiol. Infect. 134, 744–751.

Mitchell C. Sanders, 2003. Pub. N0.: US 2003/0096315 A1 (19) United States San-ders (43) PUB, Date: May 22.

Mokta, K.K., Kange, A.K., Kaushal, R.K., 2010. J. Med. Microbiol. 28 (4), 385–387.

O'Connor, L., O'Leary, M., Leonard, N., Godinho, M., O'Reilly, C., Coffey, L., Egan, J., O'Mahony, R., 2010. Lett. Appl Microbiol. 51 (5), 490–498.

Portnoy, D.A., Chakraborty, T., Goebel, W., Cossart, P., 1992. Infect. Immun. 60, 1263–1267.

Radhakrishnan, R., Jahne, M., Rogers, S., Suni, I.I., 2013. Electroanalysis 25 (9), 2231–2237.

Roberts, T., Kowalcyk, B., Buck, P., Blaser, M.J., J.K., Frenke, B., Lorber, J., Smith Tarr, P. I., 2009. Available at: ⟨http://www.foodborneillness.org/images/stories/cfi_⟩ (accessed on 31.08.10).

Sharma, H., Mutharasan, R., 2013. Biosens. Bioelectron. 45, 158–162.

Shoughy, S., Tabbar, K.F., 2014. Clin. Ophthalmol. 8, 301–304.

Sidhu, R., Rong, Y., Vanegas, D.C., Claussen, J., McLamore, E.S., Gomes, C., 2016. SPIE. Published in SPIE Proceedings. Vol. 9863.

Smith, G.A., Marquis, S., Jones, H., Johnston, N.C., Portnoy, D.A., Goldfine, H.S., 1995. Infect. Immun. 63, 4231–4237.

Suaifan, G.A., Shehadeh, M., 2013a. Expert Rev. Mol. Diagn. 3 (7), 707–718.

Suaifan, G.A., Esseghaier, C., Ng, A., Zourob, M., 2013b. Analyst 138, 3735–3739.

Swaminathan, B., Smidt, P.G., 2007. Microbes Infect. 9 (10), 1236–1243.

Välimaa, A.L., Timisjärvi, A.T., Virtanen, E., 2015. Food Control 55, 103–114, A review.

Vazquez-Boland, J.A., Kuhn, M., Berche, P., Chakraborty, T., Dominguez-Bernal, G., Goebel, W., Gonzalez-Zorn, B., Wehland, J., Kreft, J., 2001. Clin. Microbiol. Rev. 14, 584–640.

Wang, W., 2016. IAFP Food Control 64, 54–59.

Wignarajah, S., Suaifan, G., Bizzarro, S., Bikker, F., Kaman, W., Zourob, M., 2015. Anal. Chem. 87 (24), 12161–12168.

Zhao, X., Lin, C., Wang, J., Hwan, D., 2014. J. Microbiol. Biotechnol. 24 (3), 297–312.

Zhang, L., Huang, R., Liu, W., Liu, H., Zhou, X., Xing, D., 2016. Biosens. Bioelectron. (Available online)

69

[SAA2]

Rapid and low-cost biosensor for the detection of *Staphylococcus aureus*

Ghadeer A R Y Suaifan , Sahar Alhogail , Mohammed Zourob

	Sahar Alhogail	Ghadeer A R Y Suaifan
Konzeption des Forschungsansatzes	**X**	**X**
Planung der Untersuchungen	**X**	
Datenerhebung	**X**	
Datenanalyse und – interpretation	**X**	
Schreiben des Manuskripts	**X**	**X**
Vorschlag Anrechnung Publikationsäquivalente	**1,0**	

Rapid and low-cost biosensor for the detection of Staphylococcus aureus

CrossMark

Ghadeer A.R.Y. Suaifan[a], Sahar Alhogail[b], Mohammed Zourob[b,c,*]

[a] Department of Pharmaceutical Sciences, Faculty of Pharmacy, The University of Jordan, Amman 11942, Jordan
[b] Department of Chemistry, Alfaisal University, Al Zahrawi Street, Al Maather, AlTakhassusi Rd, Riyadh 11533, Saudi Arabia
[c] King Faisal Specialist Hospital and Research Center, Zahrawi Street, Al Maather, Riyadh 12713, Saudi Arabia

ARTICLE INFO

ABSTRACT

Staphylococcus aureus (S. aureus) is one of the most common etiological agents in hospital-acquired infections and food-borne illness. S. aureus toxins and virulence proteases often circulate in host blood vessels leading to life-threatening diseases. Standard identification approaches include bacterial culturing method, which takes several days. Other nucleic acid-based methods were expensive and required trained personnel. To surmount these limitations, a paper-based biosensor was developed. The sensing mechanism was based on the proteolytic activity of S. aureus proteases on a specific peptide substrate, sandwiched between magnetic nanobeads and gold surface on top of a paper support. An external magnet was fixed on the back of the sensor to accelerate the cleavage of the magnetic nanobeads-peptide moieties away from the sensor surface upon test sample dropping. The colour change resulting from the dissociation of the magnetic nanobeads moieties was detected by the naked eye and analysed using ImageJ analysis software for the purpose of quantitative measurement. Experimental results showed detection limits as low as 7, 40 and 100 CFU/mL for S. aureus in pure broth culture, and inoculated in food produces and environmental samples, respectively upon visual observation. The specificity of the sensor was examined by blind testing a panel of food-contaminating pathogens (Listeria monocytogenesis 19115 and E. coli O157:H7), clinical isolates (methicillin-resistant S. aureus (MRSA) and Candida albicans) and standard (Pseudomonas aeruginosa 15692) pathogens. Negative read-out was observed by the naked eye for all tested isolates except for MRSA. Moreover, this sensing tool requires minute's time to obtain the results. In conclusion, this sensing platform is a powerful tool for the detection of S. aureus as a potential point-of-care diagnostic platform in hospitals and for use by regulatory agencies for better control of health-risks associated with contaminated food consumption.

1. Introduction

Staphylococcus aureus (S. aureus) is a facultative anaerobic, gram-positive bacterium discovered by Dr. Alexander Ogston (Ogston, 1984). After which, S. aureus bacterium received a lot of attention, being allied with health care-associated infections (HAIs) (http://www.cdc.gov/HAI/organisms/staph.html). These infections were correlated with a number of risk factors, including long-time hospitalization, hospital-costs and mortality. On the other hand, S. aureus bacterium was among the top five pathogens associated with food-borne illnesses (http://www.cdc.gov/foodborneburden/2011-foodborne-estimates.html; Wang et al., 2011).

S aureus pathogens usually grow in open wounds and urinary tracts, leading to numerous ailments, from minor skin infections to life-threatening diseases such as abscesses (Kapral et al., 1980), pneumonia (Robertson et al., 1958), meningitis (Gordon et al., 1985), endocarditis (Fowler et al., 2007) and septicaemia (Cross et al., 1983). The National Institute of Health and Center for Disease Control and Prevention reported 94,000 life-threatening antibiotic-resistant infection cases out of which 500,000 people were infected with S. aureus pathogen in the United States of America annually (Klein et al., 2007).

Methicillin-resistant Staphylococcus aureus (MRSA) is one of the most common S aureus resistant strains in hospitals (Wang et al., 2011). MRSA infections always cause serious antibiotic resistant illnesses and high mortality (Cosgrove et al., 2003). Thus, to combat the spread of MRSA infections and to minimize the waste of public resources, new strategies for the development of a specific and feasible diagnostic biosensor for the detection of S. aureus is urgently needed.

It is worth mentioning that the Staphylococcus species is usually present in the nostrils and on the skin of warm-blooded animals, and thus can contaminate food products derived from animals such as meat, milk and eggs (Yang et al., 2011). Also, poor hygienic conditions by food handlers during manufacturing processes can contaminate

foods (Goto et al., 2007). *S. aureus* bacterium can also live in harsh environments, and so, under temperature-abused conditions, it grows and produces virulence proteases in addition to other endotoxins, leading to staphylococcal food poisoning (SFP), which is marked by severe gastrointestinal symptoms such as emesis, diarrhea, and/or abdominal pain (Doyle MP et al., 2007). Recently, the Center for Disease Control and Prevention (CDC) estimated 240,000 illnesses with 1,000 hospitalizations and 6 deaths associated with SFP annually (Scallan et al., 2011).

Clearly, in case of food poisoning, specific *S. aureus* detection is important for proper treatment, but it is more important to prevent the occurrence of the disease. One way of doing so is to spot contaminated products and sites. For example, it is preferred to detect contaminated food products before reaching consumers. Conspicuously, this could be achieved through the development of cheap, stripe formate biosensors applicable at the retail level in order to protect the consumer.

Conventionally, *S. aureus* detection was based on bacterial culture methodology (Bocher et al., 2008). However, this process is time-consuming, labor-intensive and takes several days. This delays bacterium identification, which is unacceptable in emergency and critical illnesses such as sepsis, thus limiting its practical application for rapid diagnosis (Gilbert, 2002). Other ultra-sensitive detection methods were reported based on nucleic acid amplification, such as ligase chain reaction (LCR) (Moore and Curry, 1998), strand displacement amplification (SDA) (Edman et al., 2000) and polymerase chain reaction (PCR) (Cheng et al., 2006). Fortunately, these technologies were capable of detecting low numbers of bacterial cells, but took several hours. Moreover, these technologies were expensive and required prior bacterial DNA isolation, preparation of enzyme reaction mixtures and expensive instruments for nucleic acid amplification. Alternative methods such as antibody-based immunoassays and immuno-PCR assays were well-established and used extensively (Huang and Chang, 2004; Zhu et al., 2014). However, antibody-DNA conjugation and purification processes are tedious, in addition to the high costs of the instruments, which prevents them from being procured quickly. Chang et al. (2013) reported the development of a non-PCR–based method, which combines aptamer-conjugated gold nanoparticles and a resonance light-scattering detection system. This method successfully detects a single *S. aureus* cell within 1.5 h. However, this method needs sophisticated instruments. At present, nanotechnology's application in the development of biosensors-in particular, those capable of identifying protease activity as a disease biomarker, were very attractive due to their high specificity and sensitivity (Esseghaier et al., 2014; Suaifan et al., 2013a, 2013b; Suaifan et al., 2016a, 2016b; Wignarajah et al., 2015; Alhogail et al., 2016; Suaifan, 2016). However, expensive instruments are still required for these real-time detection methods. Therefore, there is a need for a "sample-to-answer", "hand-held", specific and sensitive diagnostic biosensor capable of detecting *S. aureus* proteases, as a biomarker for the presence/contamination of *S. aureus* in a short time.

Accordingly, this study aimed at the development of a magnetic nanobeads-peptide probe, which would be cleaved specifically by *S. aureus* virulence proteases. This probe would then be integrated with a gold sensing platform via Au-S linkage to provide specific and cost-effective strip-format diagnostic biosensor for the qualitative and quantitative detection of *S. aureus*. This biosensor would be label-free, cost-effective, quick, simple and can be read by the naked eye.

2. Experimental section

2.1. Materials and method

Carboxyl-terminated magnetic nanobeads (50 nm in diameter) were supplied by Turbo beads (Switzerland). *N*-Hydroxysuccinimide (NHS), 1-(3-Dimethylaminopropyl)-3-Ethyl-Carbodiimide (EDC), pH indicator strips were purchased from Sigma Aldrich (Dorset, UK). Self-

adhesive Magnet sheets were purchased from Polarity Magnets Company (UK). The peptide sequence NH$_2$-Ahx-ETKVEENEAIQK-Ahx-Cys was synthesised by Pepmic Co., Ltd. (Suzhou, China). Self-adhesive tape was purchased from Whatman (London, UK). Brain Heart Infusion broth and agar were purchased from SDA Oxoid, Ltd. (Basingstoke, UK). Sterile filter 0.22 μm was from Millipore (UK). The wash/storage buffer (10 mM Tris base, 0.15 M sodium chloride, 0.1% (w/v) bovine serum albumin, 1 mM ethylenediaminetetraacetic acid, 0.1% sodium azide, pH 7.5) and the coupling buffer (10 mM potassium phosphate, 0.15 M sodium chloride, pH 5.5) were prepared from chemicals of analytical grade.

2.2. Bacterial strain culturing and protease preparation

S aureus (ATCC 25923), *Listeria* monocytogenes (ATCC 19115) and *Pseudomonas* aeruginosa (*P. aeruginosa*, ATCC 15692), purchased from Sigma Aldrich (UK) were streaked on BHI agar plate and incubated at 37.0 °C for 24 h. One colony was then isolated, inoculated into BHI broth and incubated overnight at 37 °C. The primary bacterial culture (PBC) was serially diluted to get the bacterial colony forming unit (CFU/mL) value of the original stocks by using viable count spread dilution method. Then, the bacteria were pelted by centrifugation at 3000Xg for 10 min. The supernatant was then filtered to obtain the crude protease solution of each bacterial concentration. The protease's proteolytic activity was measured by the universal, non-specific casien assay and was determined as the amount in micromoles of tyrosine equivalents released from casien per minute (Cupp-Enyard, 2008). An increase in *S. aureus* protease's proteolytic activity strength was correlated to bacterial culture concentration (colony forming unit (CFU/mL)).

2.3. Conjugation of S. aureus peptide substrates with magnetic-nanobeads

Magnetic-nanobeads suspension (1 mL) was mixed with the peptide substrate NH$_2$-Ahx-ETKVEENEAIQK-Ahx-Cys (1.0 mg/mL), coupling agent EDC (0.57 mg/mL) and NHS (12 μg/mL). The mixture was tremor gently at room temperature for 24 h. The uncoupled peptides were removed by washing the magnetic-nanobeads three times with a wash buffer. Finally, the beads were stored at 4 °C in a storage buffer. (Esseghaier et al., 2014; Suaifan et al., 2012; 2013a; 2013b).

2.4. Fabrication of the gold sensing platform

Schematic 1 shows the detailed steps for the preparation of the sensing platform. Self-adhesive tape was coated with a thin layer (30 nm) of gold which was sputtered using RF magnetron sputtering (Nordiko Ltd). Conditions 5mT pressure Argon gas. Power 100 W, 5 min at School of Engineering at Cranfield University. Following this, a rectangular piece (~1.5–2×3 mm) was stacked over the front face of the plastic physical support (Scheme 1A).

2.5. Immobilization of the sensing monolayer (SAM)

Magnetic nanobeads-peptide solution was placed over the gold sensing platform and allowed to dry at room temperature (Scheme 1B). Upon completion of the immobilization step, the sensor platform golden colour turns into black as observed by the naked eye. Following this, an external magnet (12.5×12.5×5 mm) with field strength of 573 gauss at a distance of 10 mm was passed over the sensor platform to remove any unattached magnetic nanobeads as shown in (Scheme 1C). Then, a round paper magnet was fixed on the back of the strip at around 5 mm distance beneath the gold sensor platform as shown in (Scheme 1D).
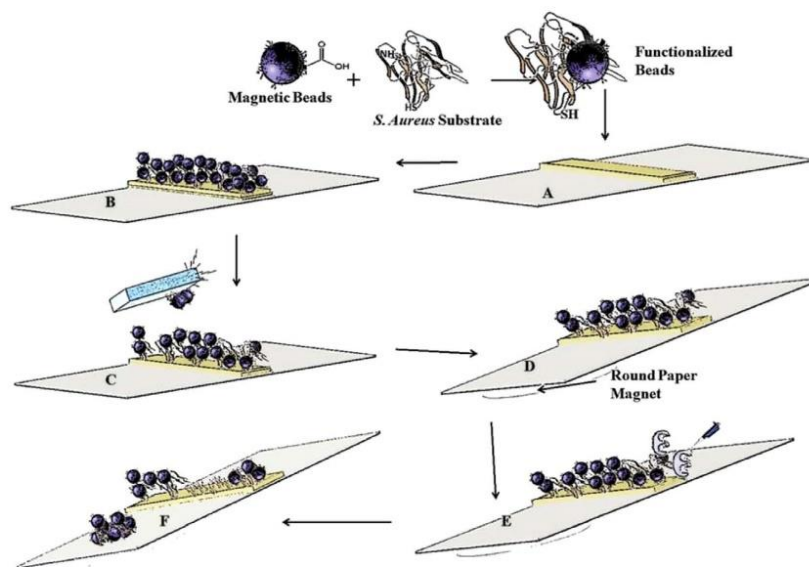
Scheme 1. . Fabrication and mechanism of *S aureus* protease detection using colorimetric paper-based biosensor. (A) Preparation of gold sensor platform; (B) Gold biosensor covered with *S aureus* protease specific substrate peptide-magnetic nanobeads; (C) External magnet to attract unattached nanobeads; (D) Round paper magnet stacked at the back of the strip; (E) Sensing process upon application of *S aureus* proteases; (F) Dissociation of the peptide-magnetic nanobeads complex from the sensor surface upon dripping *S aureus* protease solution. (For interpretation of the references to color in this Scheme, the reader is referred to the web version of this article.)

2.6. Biosensing of S. aureus proteases

The current diagnostic sensing platform is based on the measurement of *S. aureus proteases* proteolytic activity using a specific magnetic nanobeads-peptide gold sensing probe. Accordingly, *S. aureus* proteases solution (30 μL) was dropped over the black colour functionalized sensing platform. During the enzymatic cleavage reaction, the round permanent magnets stacked at the back of the strip will attract the cleaved magnetic nanobeads-peptide moiety, which in turn prompting a visual observation of the sensor golden colour for a qualitative evaluation of the tested sample (Scheme 1).

2.7. Quantitative measurements of biosensor colour change

The designed biosensor was intended to be used by visual observation of the colour change (black to golden) via naked eye. Additionally, the area of the golden colour increased with increasing the concentration of *S. aureus* protease prepared from different PBC (7.5×10^6 CFU/mL, 7.5×10^5 CFU/mL, 5×10^4 CFU/mL, 5×10^3 CFU/mL, 5×10^2 CFU/mL, 75 CFU/mL, 7.5 CFU/mL) as shown in Fig. 2A. The black colour magnetic nanobeads quantity was quantified by using the ImageJ program developed at National Institute of Health (Collins, 2007; Rajwa et al., 2004). Images were obtained by direct photography of the biosensor after protease application by a smartphone and were saved in JPEG format. Then, images were split into red, green and blue channels using the RGB stack command. Next, the images were performed through red channel following the discard of the blue and green channels since this channel showed less background level. Threshold was adjusted manually until only the black beads were highlighted in red and then Set Measurements dialogue was checked for "Area". Afterwhich, the area of the magnetic nanobeads on the sensor surface after protease application and the area of the cleaved magnetic nanobeads-peptide moieties were selected and measured separately as shown in Fig. 2BII.

Total magnetic nanobeads-peptide SAM area = Black magnetic nanobeads area on the sensor surface after protease application + Cleaved magnetic nanobeads moieties area.

The percentage of cleavage = Cleaved magnetic nanobeads moieties area / Total magnetic nanobeads SAM area.

However, as the threshold adjustment process is subjective, the analysis was performed by two experimenters who followed the proposed protocol. The two experimenters measured the highlighted red-colored area. Different *S. aureus* protease concentration obtained from different *S. aureus* pure culture (CFU/mL) were plotted against the percent cleavage of the magnetic nanobeads-peptide moieties as shown in Fig. 2B I and II.

2.8. Bacterial spiking and proteases preparation

2.8.1. Environmental samples

Dust samples (Wiped from different places, including Jordan University Hospital Intensive Care Unit, Jordan University Hospital stairs and The University of Jordan courtyard corners) were suspended in sterile water. Afterward, different *S. aureus* PBC dilution was spiked into the dust samples and incubated at room temperature for about 2 h. The samples were then clarified by centrifugation at $3000\times g$ for 10 min and the supernatant was filtered through a 0.22 μm sterile syringe filter. The filtrates were either used immediately or stored at −20 °C for later use. Unspiked dust samples were used as a negative control.

2.8.2. Food products

Food products (ground beef, turkey sausage, lettuce and milk) were purchased from local markets. Ground beef and turkey sausages were homogenized with sterile water at 1:5 (w: v) ratio in a blender for 1 min, and then were rocked at room temperature for 2 h. Lettuce leaves were rinsed with vegetable detergent and phosphate buffered saline (PBS, pH 7.4), and then cut into 4-cm^2 pieces using sterile scissors, to remove any potential adulterates which may exist on the leafy surface.

Afterward, the PBC stock of *S. aureus* was added to food products to create 10-fold dilution samples. The spiked matrices were allowed to incubate at room temperature for 2 h and were then clarified by centrifugation (5 min, 2000 rpm) (Medina, 2003). The supernatant was then collected, centrifuged (10 min, 3000 X g) to pellet bacteria

and then filtered through a 0.22 μm sterile filter. The filtrate containing crude bacterial proteases was used immediately. Positive control was prepared by creating 10-fold serial dilution from the *S aureus* PBC stock. Different *S aureus* concentrations in CFU/mL were determined by placing 10-fold serial dilutions of the positive control (PBC) on the BHI agar plates. The plates were then incubated overnight at 37 °C and then enumerated. Negative blank samples containing no bacteria were also prepared in a similar way and tested to check the effect of food matrices content on the sensor.

2.8.3. Clinical isolates

Clinical isolates (methicillin-resistant *S. aureus*, *P. aeruginosa* brown and green), *E. coli* and *Candida albicans* were obtained from The University of Jordan Hospital. These isolates were identified and characterized by the Mycological investigation laboratory at the hospital and provided as an *inocula* in the proper broth with 5% glycerol and then was stored at −20 °C for later use.

3. Results and discussion

Dramatic progress has been made in the field of nanomaterials-based biosensors specifically in biomedical and bioanalytical themes (Guo et al., 2013). Of particular interest, magnetic nanobeads which has a large surface/volume ratio (Citartan et al., 2012), easily separate or enrich specific analyte from complex matrices, under the effect of an external magnetic field and provide a direct readout by naked eye (Huang et al., 2010). Based on these unique magnetic nanobeads properties, a novel diagnostic sensing probe for the specific detection of *S. aureus* by naked eye has been constructed.

3.1. Sensor fabrication and sensing mechanism

The biosensor peptide probe was prepared by using *S. aureus* specific substrate (ETKVEENEAIQK) to detect the proteolytic activity of *S. aureus* proteases (Sanders et al., 2005) This substrate was elongated with Ahx-residue linker on both ends of the peptide (NH_2-Ahx-ETKVEENEAIQK-Ahx-Cys). The Ahx-residue spacer endorses protease's accessibility to their specific peptide cleavage site. The N-terminal of the peptide was coupled with carboxyl-terminated magnetic nanobeads. The cysteine residue at the C-terminal allows gold-sulfur interaction to construct the magnetic nanobeads-peptide complex SAM on the surface of the gold sensor (Scheme 1A, B and C). The amount of
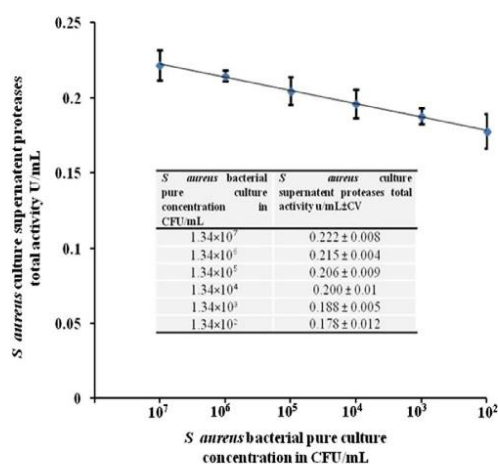
the peptide substrate required for MNPs functionalization was optimized in a previous work to get the optimal monolayer performance (Esseghaier et al., 2014; Suaifan et al., 2013a, 2013b). The detailed protocol steps in sensor preparation are shown in Scheme 1A-D. The sensing mechanism is based on the proteolytic activity of *S. aureus* proteases on a specific peptide substrate, sandwiched between magnetic nanobeads and gold surface on top of a paper substrate. An external magnet fixed at the back of the sensor accelerates the cleavage of the peptide-magnetic nanobeads moieties. This dissociation process reveals the golden colour of the sensor surface visible to the naked eyes as shown in (Scheme 1E and F).

3.2. Sensor testing

The proteolytic activity of the *S. aureus* proteases was detected by placing 30 μL of the protease solution (7.5×10^6 CFU/mL) over the functionalized gold sensor surface. The optimum read out time was chosen to be after one minute of protease application as it provides about 85% of the sensor response. To gain insight into the applicability of the sensor for quantitative detection of *S. aureus*, a number of biosensors were prepared and exposed to different *S aureus* proteases solutions prepared from different bacterial pure broth culture concentrations (7.5×10^6 CFU/mL, 7.5×10^5 CFU/mL, 5×10^4 CFU/mL, 5×10^3 CFU/mL, 5×10^2 CFU/mL, 75 CFU/mL, 7.5 CFU/mL). Fig. 2 clearly showed a proportional increase in the visible sensor golden colored area with the protease solution concentrations. This is due to the proteolytic activity of the protease, which resulted in the dissociation of the peptide-magnetic nanobeads complex. Blank samples showed no reaction since the sensor demonstrated no disruption of the SAM layer. A comparable proteolytic activity for *S. aureus* protease was estab-
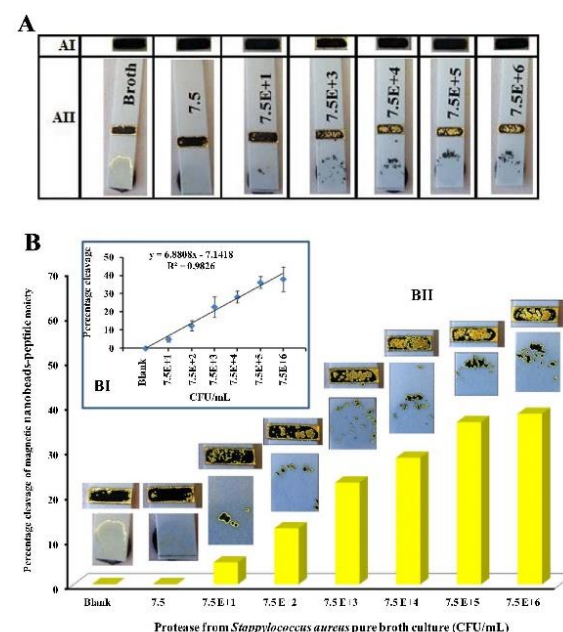

Fig. 2. (A) Colorimetric*S aureus*sensor probe (*S aureus*-specific peptide substrate covalently bound to magnetic nanobeads). (AI) Biosensor chip immobilized with magnetic nanobeads–specific *S aureus* peptide substrate. (AII) Immobilized biosensor under the effect of different *S aureus* protease concentrations.(B) Quantitative measurement of biosensor colour changes using ImageJ software. (BI) The response curve with the respective standard deviation. (BII) The intensity colour of the magnetic nanobeads on the sensor surface after protease application and the cleaved magnetic nanobeads moieties attracted by the backwards magnet as processed by imageJ software. (For interpretation of the references to color in this figure legend, the reader is referred to the web version of this article.)

Fig. 1. Proteolytic activity of different *S aureus* culture supernatent measured by Sigma's Non-specific Protease Activity Assay. Proteases activity is determined in terms of Units, which is the amount in micromoles of tyrosine equivalents released from casein per minute.

G.A.R.Y. Suaifan et al.

lished upon the measurement of the proteolytic activity by the universal, non-specific casien assay (Fig. 1) and the developed biosensor (Fig. 2I and II). The results approved the powerful use of *S aureus* proteases as a biomarker. As a ten-fold decrease in bacterial concentration showed an effect on *S. aureus* proteases proteolytic activity and the consequent biosensor cleavage. As it has been observed, ten fold dilution in bacterial proteases concentration resulted in a drop in the proteolytic activity by approximately 6–10% of magnetic nanobeads cleavage. For example, 10^5 resulted of 36% of magnetic nanobeads cleavage, whereas 10^4 resulted in 28% and 10^3 resulted in 22%. This difference can explains the adequate sensitivity of the developed biosensor.

Additionally, a quantitative approach was developed for *S. aureus*-specific detection using ImageJ software. The image software measures the amount of cleaved area (appearance of golden colour) to the total black area (before cleavage). Thus, we have adjusted the colour threshold function, as shown in Fig. 2BII. Photos analysis was performed three times. The correlation between the percentage cleavage of magnetic nanobeads-peptide moieties and different *S. aureus* protease prepared from different PBC showed a consistent correlation (Fig. 2B).

Detection limit determination was either based on visual evaluation of the lowest protease concentration incapable of cleaving peptide-magnetic beads, covalently attached to the golden sensor surface i.e. the sensor golden surface area is invisible to the naked eye due to intact SAM layer (Fig. 2A), or based on the standard deviation of the response
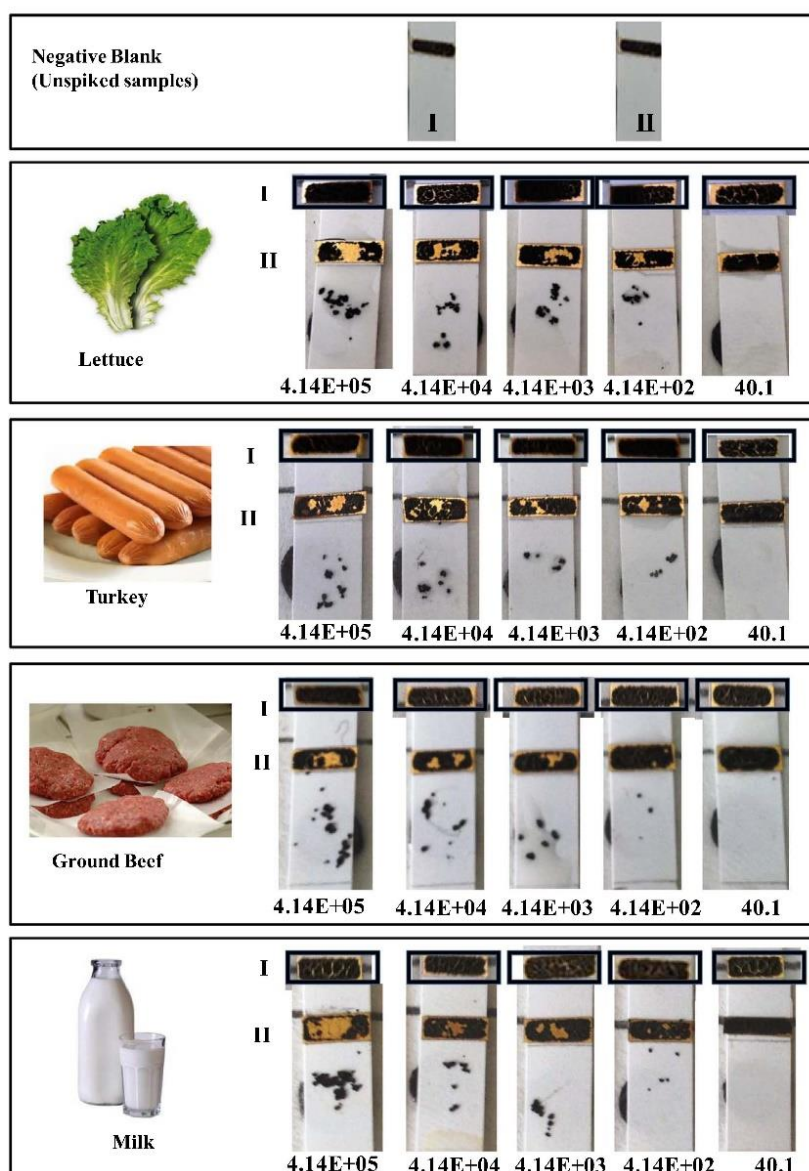

Fig. 3. Colorimetric *S. aureus* sensor probe application on spiked food produces (specific *S. aureus* substrate peptide covalently bound to a magnetic nanobeads). (I), Biosensor chip functionalized with magnetic nanobeads–specific *S. aureus* peptide substrate. (II) Functionalized biosensor under the effect of different *S. aureus* protease concentrations spiked in food produces.

and the slope: LOD =3.3 standard deviation of low concentration(σ) / slope of the calibration line (Fig. 2BI). Interestingly, the developed sensor revealed low limits of detection without the use of any instrumentation and with one minute of incubation time.

3.3. Biosensor detection of S. aureus in spiked food matrices, environmental samples and clinical isolates

The developed biosensor proved its potential ability to detect *S. aureus* in PBS. The next step was to evaluate its feasibility to detect *S. aureus* in contaminated food products and environmental samples. To contaminate food produces, 1.0 mL of different *S. aureus* concentrations (range from 4.14×10^5 CFU/mL to 4.14 CFU/mL) was spiked into 9 mL of ground beef, turkey sausage, lettuce and milk. The results are shown in Fig. 2. A negative control was prepared by spiking 1 mL of BHI broth with 9 mL of food samples. On the other hand, to contaminate environmental samples, dust samples collected from different sites were suspended in sterile water, and spiked with six different concentrations ranging from 1.12×10^7 CFU/mL to 11.2 CFU/mL. The results are shown in Fig. 3. Positive and negative controls were also prepared. Both controls, spiked food products and environmental

samples were allowed to incubate at room temperature for 2 h prior to testing. The samples were then centrifuged, filtered and exposed to the developed biosensor. It is clearly observed by the naked eye that there is a directly proportional relationship between the sensor golden area and bacteria concentrations. The results in Fig. 3 and Fig. 4 clearly demonstrate the ability to detect *S. aureus* contamination. The detection limits were as low as 40 CFU/mL and 100 CFU/mL, respectively, in one minute.

3.4. Sensor stability

To evaluate the stability of the biosensor over time, the ready-to-use immobilized strip sensors were stored in empty petri dishes at 4 °C. Every week, three sensors were used to detect the proteolytic activity of known *S. aureus* protease solution. In every experiment, a negative control (no *S. aureus* protease) was tested to ensure that the magnetic nanobeads-peptide moieties dissociation was attributed to *S. aureus* proteolytic activity. The designed biosensor showed adequate long-term stability for up to six months at room temperature. Fig. 5A shows the comparion of the sneosr response for less than 6 months and more than six months. It can be observed that the application of similar *S.*
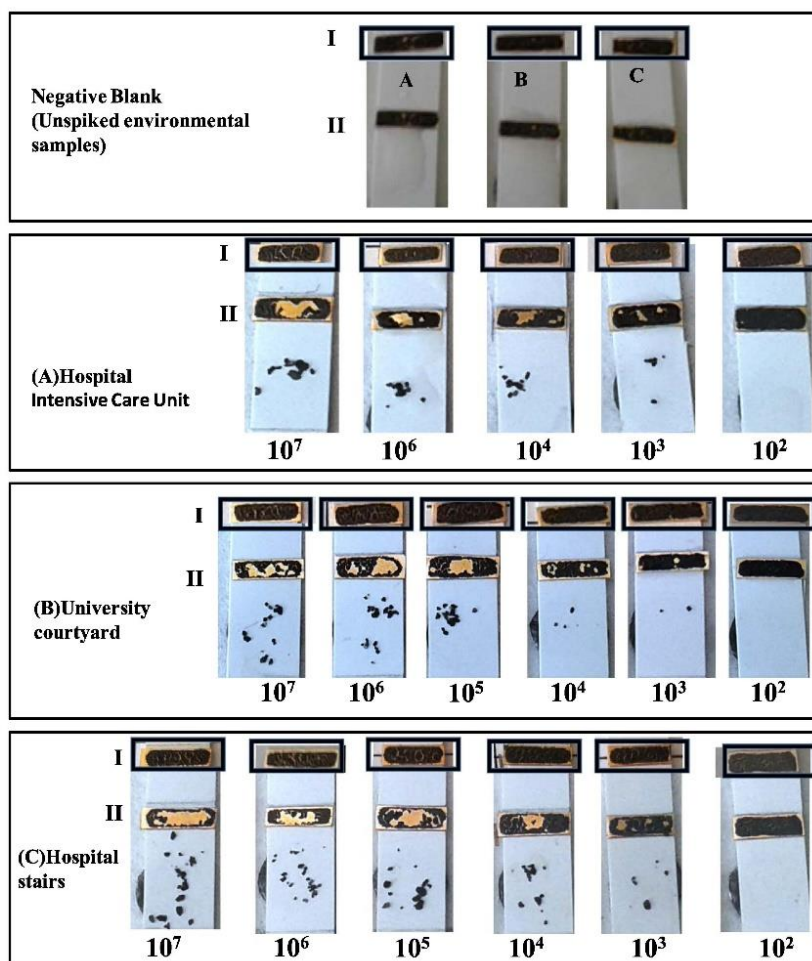
Fig. 4. Testing the colorimetric *S. aureus* sensor probe on spiked environmental samples (specific *S. aureus* substrate peptide covalently bound to a magnetic bead). (I) Biosensor chip functionalized with magnetic nanobeads–specific *S. aureus* peptide substrate (before exposing to the contaminated samples); (II) Functionalized biosensor exposed to different concentrations of *S. aureus* proteases spiked in environmental samples.
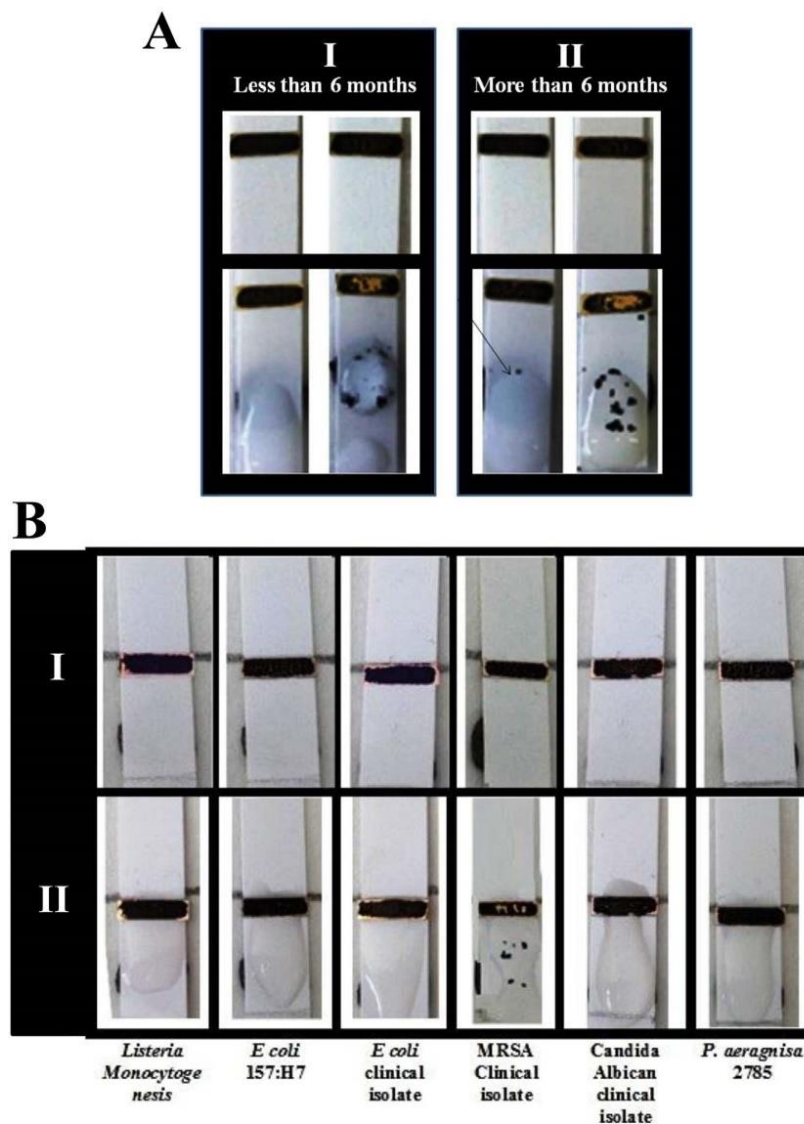
235

Fig. 5. (A) Stability study of *S. aureus* sensor probe. (AI) Application of negative control (broth only) and known protease concentration over biosensor probe stored for less than 6 months. (AII) Application of negative control (broth only) and the same protease concentration over biosensor probe stored for more than 6 months. (B) Specificty of the colorimetric *S. aureus* sensor. (BI) Biosensor chip functionalized with magnetic nanobeads-specific *S. aureus* peptide substrate. (BII) Sensor exposed to various food-borne pathogens (*L. Monocytogenesis, E. coli* 157:H7), clinical isolates (*E. coli, MRSA* and *C. albican*) and standard pathogens (*P. aeruginosa* 2785).

aureus protease concentrations revealed higher percentage of cleavage on sensor probes stored for more than 6 months in comparison with those stored for less than six months.

3.5. Sensor specificity

A significant improvement in disease control could be made if the target pathogen, in the clinical bio-samples, and contaminated food produces were specifically and directly detected by a low-cost and sensitive method. The developed biosensor was exposed to 30 µL of a panel of blinded clinical isolates samples (MRSA, *P. aeraginosa* brown and green and *Candida albicans*) and standard pathogen (*P. aeraginosa* ATCC2785). The results are shown in Fig. 5B. Positive read-out by the naked eye was only observed for MRSA clinical isolate. Furthermore, the biosensor was exposed to a panel of food contaminating pathogens such as *Listeria monocytogenesis and E. coli* 157 as shown in Fig. 5B. It was clearly observed that there was no disruption in the SAM layer of the tested pathogens and no significant change in the sensor surface golden colour, except for *S. aureus*, showing again a high specificity for the *S. aureus*.

3.6. Comparison with literature

The developed biosensor is simple and highly sensitive, which is comparable with PCR techniques without the need for bacteria preconcentration. It needs only the supernatant of the sample, which

can be easily prepared by untrained personnel. On the other hand, PCR and culture conventional methods require trained personnel and/or expensive instrumentation use. The ease of on-site use of this colorimetric biosensor by untrained personal and food makers stands behind its simplicity. Currently, a number of colorimetric detection methods were developed (dos Santos Pires et al., 2011; Sung et al., 2013; Tote et al., 2008). However, these methods do not fully satisfy the optimal detection performance criteria for field applications. For comparison purposes, Sung et al. (2013) reported a detection limit as low as $1.5×10^3$ and $1.5×10^5$ CFU for *S. aureus* in PBS and milk samples, respectively, in 40 min using antibody/gold, nanoparticle/magnetic nanoparticles. Pires et al. (2011) reported the use of 10,12-pentacosadiynoic acid (PCDA) -N-[(2-tetradecanamide)-ethyl]- ribonamide (TDER) vesicles, to determine the colorimetric response induced by *S. aureus* in a culture medium and in apple juice. Other methods used antibody-labeled gold nanoparticles (AuNPs) as an immunological reporter for an easy visual sensing of the biomolecules (Jian and Huang, 2011; Kim et al., 2012; Li et al., 2009). However, tested samples had to be purified and concentrated prior to the immunological reaction to achieve a specific and sensitive response with low noise (Li et al., 2009).

4. Conclusions

This study has demonstrated the ability of the developed biosensor to detect *S. aureus* pathogen qualitatively by naked eye and quantitatively by using imaging software. Additionally, the biosensor detected *S. aureus* specifically among different clinical isolates, contaminated food matrices and environmental samples. The limits of detection were as low as 7, 40 and 100 CFU/mL for *S. aureus* in pure broth culture, and *S. aureus* inoculated in food produces and environmental samples respectively, in very short time. This assay is simple to perform, cheap, can be performed at the retail to prevent the consumer from being susceptible to food-borne diseases, or at the hospital to protect patients from hospital-acquired infections. The detection mechanism does not require any amplification steps.

References

Alhogail, S., Suaifan, G.A., Zourob, M., 2016. Biosens. Bioelectron. 86, 1061–1066.
Bocher, S., Smyth, R., Kahlmeter, G., Kerremans, J., Vos, M.C., Skov, R., 2008. J. Clin. Microbiol. 46, 3136–3138.
Chang, Y.C., Yang, C.Y., Sun, R.L., Cheng, Y.F., Kao, W.C., Yang, P.C., 2013. Sci. Rep., 3.
Cheng, J.C., Huang, C.L., Lin, C.C., Chen, C.C., Chang, Y.C., Chang, S.S., Tseng, C.P., 2006. Clin. Chem. 52, 1997–2004.
Citartan, M., Gopinath, S.C.B., Tominaga, J., Tan, S.C., Tang, T.H., 2012. Biosens. Bioelectron 34. 1–11.
Collins, T.J., 2007. Biotechniques 43, 25–30.
Cosgrove, S.E., Sakoulas, G., Perencevich, E.N., Schwaber, M.J., Karchmer, A.W.,
Carmeli, Y., 2003. Clin. Infect. Dis. 36, 53–59.
Cross, A.S., Zierdt, C.H., Roup, B., Almazan, R., Swan, J.C., 1983. Am. J. Clin. Pathol. 79, 598–603.
Cupp-Enyard, C., 2008. J. Vis. Exp. 899, 1–2. http://dx.doi.org/10.3791/899de.
dos Santos Pires, A.C., Ferreira Soares, Nd.F., Mendes da Silva, L.H., Hespanhol da Silva, Md.C., De Almeida, M.V., Le Hyaric, M., de Andrade, N.J., Soares, R.F., Mageste, A.B., Reis, S.G., 2011. Sens. Act. B-Chem. 153, 17–23.
Doyle, M.P., Beuchat, L.R., TJ, M., 2007. Food Microbiology: Fundamentals and Frontiers third ed. ASM Press, Washington, DC.
Edman, C.F., Mehta, P., Press, R., Spargo, C.A., Walker, G.T., Nerenberg, M., 2000. J. Investig. Med. 48, 93–101.
Esseghaier, C., Suaifan, G.A., Ng, A., Zourob, M., 2014. J. Biomed. Nanotechnol. 10, 1123–1129.
Fowler, V.G., Boucher, G.W., Corey, G.R., 2007. Ann. Intern. Med. 147, 415–416.
Gilbert, G.L., 2002. Trends Mol. Med. 8, 280–287.
Gordon, J.J., Harter, D.H., Phair, J.P., 1985. Am. J. Med. 78, 965–970.
Goto, M., Hayashidani, H., Takatori, K., Hara-Kudo, Y., 2007. Lett. Appl. Microbiol. 45, 100–107.
Guo, J., Yang, W., Wang, C., 2013. Adv. Mater. 25, 5196–5214.
Huang, S.H., Chang, T.C., 2004. Clin. Chem. 50, 1673–1674.
Huang, Y.F., Wang, Y.F., Yan, X.P., 2010. Environ. Sci. Technol. 44, 7908–7913.
Jian, J.W., Huang, C.C., 2011. Chem. Eur. J. 17, 2374–2380.
Kapral, F.A., Godwin, J.R., Dye, E.S., 1980. Infect. Immun. 30, 204–211.
Kim, Y.T., Chen, Y., Choi, J.Y., Kim, W.-J., Dae, H.-M., Jung, J., Seo, T.S., 2012. Biosens. Bioelectron. 33, 88–94.
Klein, E., Smith, D.L., Laxminarayan, R., 2007. Emerg. Infect. Dis. 13, 1840–1846.
Li, X.X., Cao, C., Han, S.J., Sim, S.J., 2009. Water Res. 43, 1425–1431.
Medina, M.B., 2003. J. Rapid Meth. Aut. Microbiol. 11, 225–243.
Moore, D.F., Curry, J.I., 1998. J. Clin. Microbiol 36, 1028–1031.
Ogston, A., 1984. Rev. Infect. Dis. 6, 122–128.
Rajwa, B., McNally, H.A., Varadharajan, P., Sturgis, J., Robinson, J.P., 2004. Microsc. Res. Tech. 64, 176–184.
Robertson, L., Caley, J.P., Moore, J., 1958. Lancet 2, 233–236.
Sanders, M.C., Colpas, G.J., Ellis-Busby, D.L., Havard, J.M., 2005. Google Patents.
Scallan, E., Hoekstra, R.M., Angulo, F.J., Tauxe, R.V., Widdowson, M.-A., Roy, S.L., Jones, J.L., Griffin, P.M., 2011. Emerg. Infect. Dis. 17, 7–15.
Suaifan, G.A., Alhogail, S., Zourob, M., 2016a. Biosens. Bioelectron., (In press).
Suaifan, G.A., Jaber, D., Shchadch, M.B., Zourob, M., 2016b. Mini Rev Med Chem., (In press).
Suaifan, G.A., Esseghaier, C., Ng, A., Zourob, M., 2012. Analyst 137, 5614–5619.
Suaifan, G.A., Esseghaier, C., Ng, A., Zourob, M., 2013a. Analyst 138, 3735–3739.
Suaifan, G.A., Shchadch, M., Al-Ijel, H., Ng, A., Zourob, M., 2013b. Expert Rev. Mol. Diagn. 13, 707–718.
Suaifan, G.A., 2016. Colorimetric biosensors for bacterial detection. In: Minhaz, U.A., Mohammed, Z., Eiichi, T. (Eds.), Food Biosensors. E-. Royal Society of Chemistry Inc, United Kingdom, 182–202.
Sung, Y.J., Suk, H.J., Sung, H.Y., Li, T., Poo, H., Kim, M.G., 2013. Biosens. Bioelectron. 43, 432–439.
Tote, K., Vanden Berghe, D., Maes, L., Cos, P., 2008. Lett. Appl. Microbiol. 46, 249–254.
Wang, C.H., Lien, K.Y., Wu, J.J., Lee, G.B., 2011. Lab Chip 11, 1521–1531.
Wignarajah, S., Suaifan, G.A., Bizzarro, S., Bikker, F.J., Kaman, W.E., Zourob, M., 2015. Anal. Chem. 24, 12161–12168.
Yang, H., Ma, X., Zhang, X., Wang, Y., Zhang, W., 2011. Eur. Food Res. Technol. 232, 769–776.
Zhu, K., Dietrich, R., Didier, A., Doyscher, D., 2014. Märtlbauer. Toxins 4, 1325–1348.

Further readingWeb References:

(http://www.cdc.gov/foodborneburden/2011-foodborne-estimates.html).
(http://www.cdc.gov/HAI/organisms/staph.html).

[SAA 3]

Paper-based magnetic nanoparticle-peptide probe for rapid and quantitative colorimetric detection of *Escherichia coli O157:H7.*

Suaifan GARY, Alhogail S, Zourob M.

	Sahar Alhogail	Ghadeer A R Y Suaifan
Konzeption des Forschungsansatzes	**X**	**X**
Planung der Untersuchungen	**X**	
Datenerhebung	**X**	
Datenanalyse und – interpretation	**X**	
Schreiben des Manuskripts	**X**	**X**
Vorschlag Anrechnung Publikationsäquivalente	**1,0**	

CrossMark

Paper-based magnetic nanoparticle-peptide probe for rapid and quantitative colorimetric detection of *Escherichia coli* O157:H7

Ghadeer A.R.Y. Suaifan[a], Sahar Alhogail[b], Mohammed Zourob[b,c,*]

[a] *Department of Pharmaceutical Sciences, Faculty of Pharmacy, The University of Jordan, Amman 11942, Jordan*
[b] *Department of Chemistry, Alfaisal University, Al Zahrawi Street, Al Maather, Al Takhassusi Rd, Riyadh 11533, Saudi Arabia*
[c] *King Faisal Specialist Hospital and Research Center, Zahrawi Street, Al Maather, Riyadh 12713, Saudi Arabia*

ARTICLE INFO

ABSTRACT

There is a critical and urgent demand for a simple, rapid and specific qualitative and quantitative colorimetric biosensor for the detection of the food contaminant *Escherichia coli* O157:H7 (*E. coli* O157:H7) in complex food products due to the recent outbreaks of food-borne diseases. Traditional detection techniques are time-consuming, require expensive instrumentation and are labour-intensive. To overcome these limitations, a novel, ultra-rapid visual biosensor was developed based on the ability of *E. coli* O157:H7 proteases to change the optical response of a surface-modified, magnetic nanoparticle-specific (MNP-specific) peptide probe. Upon proteolysis, a gradual increase in the golden color of the sensor surface was visually observed. The intensification of color was correlated with the *E. coli* O157:H7 concentration. The color change resulting from the dissociation of the self-assembled monolayer (SAM) was detected by the naked eye and analysed using an image analysis software (ImageJ) for the purpose of quantitative detection. This biosensor demonstrated high sensitivity and applicability, with lower limits of detection of 12 CFU mL^{-1} in broth samples and 30–300 CFU mL^{-1} in spiked complex food matrices. In conclusion, this approach permits the use of a disposable biosensor chip that can be mass-produced at low cost and can be used not only by food manufacturers but also by regulatory agencies for better control of potential health risks associated with the consumption of contaminated foods.

1. Introduction

Food-borne illnesses linked to the consumption of freshly and minimally processed food cause wide discomfort and economic loss for many people each year (Beuchat, 2002; Shriver-Lake et al., 2007; Tauxe et al., 1997). In general, washing fresh fruits and vegetables with cold water removes dirt lingering on the surface but does not remove pathogens that may exist inside. Fresh products might be contaminated with microbial pathogens upon contact with contaminated water or manure from the soil (Ingham et al., 2004; Song et al., 2006). A current report shows that the United States Department of Food Safety and Inspection Services (FSIS) spent over half a billion dollars annually on food inspection for bacterial contaminants. Approximately 73,000 cases of food-borne infections occur every year, of which 2–7% result in a severe complication called hemolytic uremic syndrome (HUS), as reported by the Center for Disease Control and Prevention (CDC, *Escherichia coli*, O157:H7, 2006, www.cdc.gov/ncidod/dbmd/diseaseinfo/*Escherichia coli* g.htm).

It is imperative to develop techniques for the identification of food-borne pathogens after food ingestion in order to ensure proper disease treatment. However, it is more important to prevent the occurrence of infections. One way of doing this is to identify contaminated food products prior to ingestion, preferably before they are distributed to grocery stores, restaurants and manufacturing facilities. This could be achieved through the development of rapid detection devices applicable at the retail level in order to protect the consumer.

There are several techniques that are conventionally used to detect pathogenic microbes: the culturing method is commonly used but remains problematic due to the lack of phenotypic characteristics to distinguish between generic pathogens (Gould et al., 2009); other techniques such as DNA-based assays are currently the most specific and sensitive tests available as confirmatory assays (Call, 2005; Deisingh and Thompson, 2004; Simpson and Lim, 2005; Uttamchandani et al., 2009). However, these assays require a long time (up to 48 h) to yield results due to the extensive list of steps required for sample pretreatment, including enrichment and extraction. Additionally, highly trained staff is required to perform these assays and to analyse the assay results. Further, polymerase chain

---

reaction (PCR) inhibitors such as humics are commonly present in complex food matrices and must be removed prior to analysis (Shriver-Lake et al., 2007) to avoid faulty results. Other immunoassay-based methods have been employed recently to achieve high sensitivity while avoiding many of the disadvantages of DNA-based assays. However, these methods are less specific than DNA-based assays (Shriver-Lake et al., 2007). Presently, researchers are attempting to improve the specificity of these assays through the employment of antibodies and by exploiting changes in optical properties, such as transmitted light, surface plasmon or acoustic waves resulting from antibody–antigen binding (Berkenpas et al., 2006; Deisingh and Thompson, 2004; Subramanian et al., 2006). Additionally, some of these assays use fluorescent labels to provide an optical signal (DeCory et al., 2005; Ho and Hsu, 2003; Nyquist-Battie et al., 2004). However, the application of these assays is limited by the inconsistency and high variability of the target DNA labelling. In addition, these assays require expensive and non-portable scanners for data acquisition and analysis (Call, 2005; Kuck and Taylor, 2008; Vora et al., 2008). Other alternative detection methods such as enzyme-linked immunosorbent assays (Abuknesha and Darwish, 2005), spectrometric techniques (Siripatrawan and Harte, 2007) and electrochemical techniques (Gehring and Tu, 2005) have also been employed for the detection of food-borne pathogens. With these methods, a detection range of 10^3–10^5 cells mL^{-1} was achieved without enrichment and was as low as 1 CFU mL^{-1} with enrichment. Nevertheless, this low limit of detection is valid only for the detection of microorganisms that can be grown on specific media. Kuck and Taylor (2008) used a particular colorimetric assay for the detection of *E. coli*. This assay involves unstable reagents that require a temperature-controlled environment with variable development times, leading to an increase in the nonspecific background. Notably, none of the above-mentioned detection methods fully satisfy the detection performance criteria because they are sophisticated, costly in terms of both time and money and require cumbersome preparation steps.

This study aimed at the development of simple, sensitive, specific and cost-effective strip-format colorimetric biosensor for the qualitative and quantitative detection of *E. coli* O157:H7 in food products at the retail level or even at home. This biosensor is based on the use of the proteolytic activity of *E. coli* proteases as a biomarker. Specific *E. coli* O157:H7 proteases peptide substrate was labelled with magnetic nanoparticles (MNPs) and then immobilized on a gold sensing platform to provide a hand-held peptide probe in strip format. Upon application of *E. coli* O157:H7 proteases, the MNP-peptide moiety leaves the gold sensing platform, resulting in a color change. This method is simple, and the signal change can be detected by the naked eye. Therefore, the sensor holds potential for the specific detection of *E. coli* O157:H7 (Scheme 1).

2. Experimental

2.1. Materials and reagents

Carboxyl-terminated beads (50 nm in diameter), *N*-hydroxysuccinimide (NHS), 1-(3-dimethylaminopropyl)-3-ethyl-carbodiimide (EDC) and plastic pH indicator strips were purchased from Sigma Aldrich (Dorset, UK). Self-adhesive magnet sheets were purchased from Polarity Magnets Company (UK). The peptide for *E. coli* O157:H7, NH_2-Ahx- KVSRRRRRGGDKVDRRRRRGGD-Ahx-Cys, was synthesized by Pepmic Co., Ltd (Suzhou, China). The self-adhesive tape was purchased from Whatman (London, U.K). Nutrient agar and nutrient broth were purchased from Oxoid (Amman, Jordan). Sterile filters (0.22 µm) were purchased from Millipore (Amman, Jordan). The wash/storage buffer (10 mM Tris base, 0.15 M sodium chloride, 0.1% (w/v) bovine serum albumin, 1 mM ethylenediaminetetraacetic acid, 0.1% sodium azide, pH 7.5) and the coupling buffer (10 mM potassium phosphate, 0.15 M sodium chloride, pH 5.5) were prepared from

chemicals of analytical grade.

2.2. E. coli O157:H7-specific peptide substrate labelled with MNPs

The MNP suspension (1 mL) was mixed with the peptide (1.0 mg/mL), the coupling agent EDC (0.57 mg/mL) and NHS (12 µg/mL). The mixture was shaken gently at room temperature for 24 h. The uncoupled peptides were removed by washing the beads three times with a wash buffer. Finally, the beads were stored at 4 °C in a storage buffer, as shown in Scheme 1A.

2.3. Preparation of the gold sensor platform

Self-adhesive tape was coated with a thin layer of gold at Canfield University Engineering Department. Following this, a narrow piece (~1.5 to 2×3 mm) was cut and stacked over a plastic strip providing physical support, as shown in Scheme 1B.

2.4. Immobilization of the sensing monolayer (SAM)

The gold sensing surface was mounted with the MNPs-peptide solution and allowed to stand at room temperature for 1 h. Following this, an external magnet was passed over the immobilized sensor to remove any unattached MNPs-peptide moieties (Scheme 1D). Then, a round paper magnet was fixed on the back of the strip at a distance of 2–3 mm below the gold sensing platform, as shown in Scheme 1E (side view).

2.5. Bacterial strain culturing and protease preparation

E. coli O157:H7, *Listeria monocytogenes* ATCC 19115, *Staphylococcus aureus* (*S. aureus*) ATCC 25923 and *Pseudomonas. aeruginosa* (ATCC 15692), purchased from Sigma Aldrich UK, were grown in 5 mL of nutrient broth and incubated at 37 °C for 18 h. The primary bacterial culture (PBC) was then enumerated using the serial dilution and plate counting method. Consequently, each bacterial culture was pelted by centrifugation at 3000×g for 10 min and the supernatant was filtered to obtain *E. coli* O157:H7 crude protease solution of specific proteolytic activity strength. Proteases proteolytic activity was measured by the universal non-specific casien assay and was determined as the amount in micromoles of tyrosine equivalents released from casien per minute. However, an increase in proteases proteolytic activity strength was correlated to bacterial culture concentration (colony forming unit (CFU/mL)).

2.6. Food matrix spiking

Food samples (ground beef, turkey sausage, lettuce and milk) were obtained from a local grocery market. Ground beef and turkey sausage were homogenized with sterile water at a 1:5 (w:v) ratio in a blender for 1 min and then rocked at room temperature for 2 h. Lettuce leaves were rinsed with vegetable detergent, phosphate-buffered saline (PBS pH 7.4) and then cut into 4 cm^2 pieces using sterile scissors to remove any potential adulterates on the leafy surface.

Next, *E. coli* O157:H7 bacterial culture was added to food matrices to create 10-fold dilution samples. The spiked matrices were allowed to incubate at room temperature for 2 h and were then clarified by centrifugation (5 min, 2000 rpm) (Medina, 2003). The supernatant was then collected, centrifuged (10 min, 10.000×g) to sediment bacteria, filtered through a 0.22 µm sterile filter and tested directly. Blank samples spiked with culture broth (no *E coli* O157:H7) was prepared in a similar way and tested using the biosensor. Different *E. coli* O157:H7 concentrations in CFU/mL were determined by placing 10-fold serial dilutions of the bacterial culture on the agar plates. The experiments were conducted in triplicate.
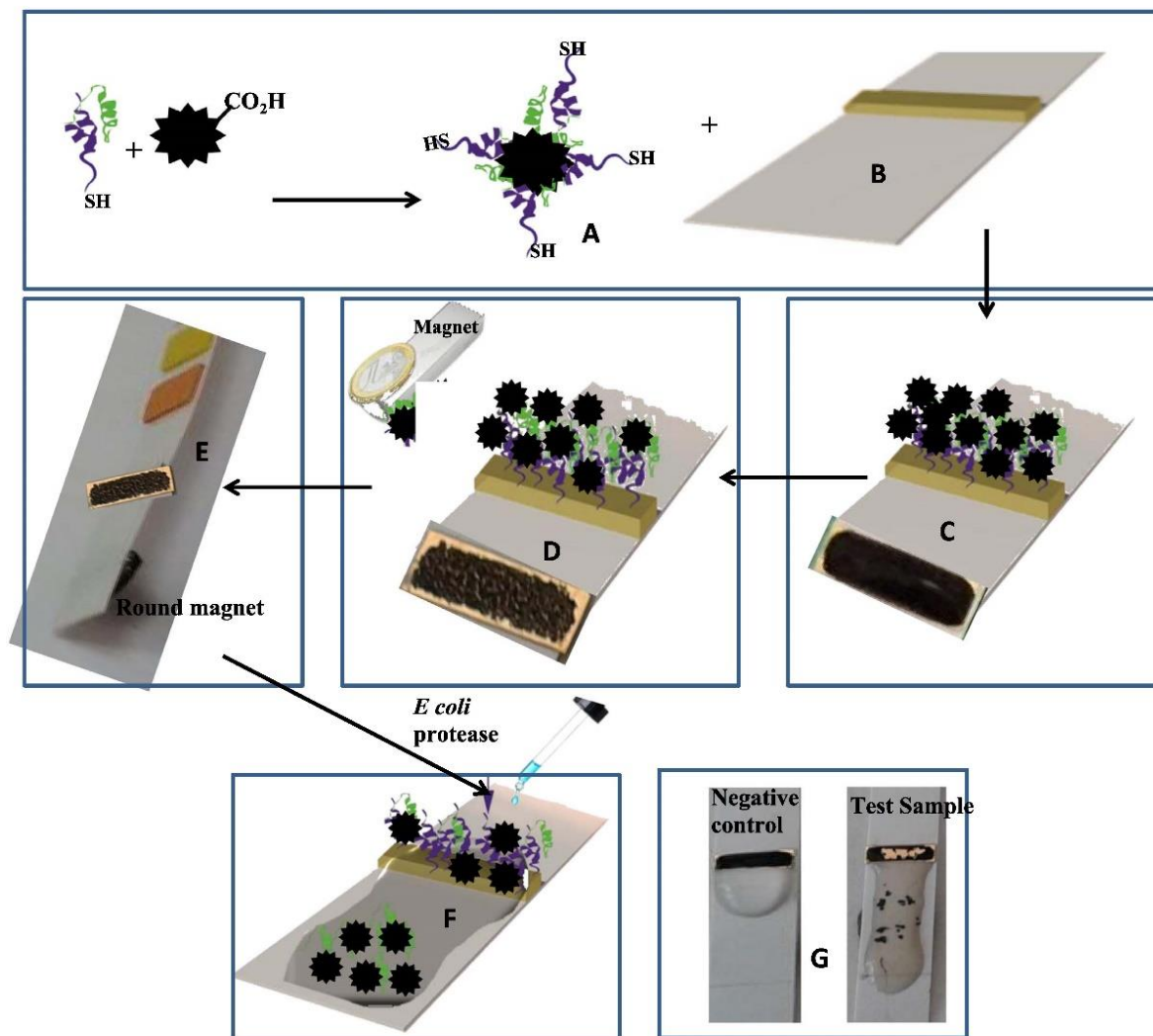
Scheme 1. Schematic and actual image of the colorimetric biosensor designed to specifically detect *E. coli* O157:H7. (A) *E. coli* O157:H7-specific peptide substrate labelled with magnetic-nanoparticles (MNPs). (B) Gold biosensing platform. (C) Immobilization of the sensing monolayer (SAM). (D) Sensor platform under the effect of an external magnet to remove unattached MNPs. (E) Side view of the sensing platform showing the round magnet fixed on the strip back. (F) Schematic view of the *E. coli* O157:H7 biosensing step. (G) Actual application of the test *E. coli* O157:H7 proteases and a negative blank control (no *E. coli* O157:H7 proteases) on the paper-based biosensor.

2.7. Biosensing of E. coli O157:H7 proteases

The solution of *E. coli* O157:H7 crude protease was down-streamed over the immobilized sensing platform. During the enzymatic cleavage reaction, the permanent round magnet stacked at the back of the sensor stripe (Scheme 1E) attracts the cleaved MNP-peptide moieties, prompting a visual observation for qualitative evaluation of the tested sample (Scheme 1F and G). The experiments were conducted in triplicate.

2.8. Quantitative measurement of the color change

Because the developed biosensor was intended to be used by visual observation, the color change (black to golden) as a result of *E. coli* O157:H7 proteases proteolytic activity was easily viewed by the naked eye. Additionally, intensification of the sensor golden color raised with

increasing the concentration of *E. coli* O157:H7 culture (121 CFU/mL, 1.21×10^2 CFU/mL, 1.21×10^3 CFU/mL, 1.21×10^4 CFU/mL, 1.21×10^5 CFU/mL, 1.21×10^6 CFU/mL), as shown in Fig. 1A and B. The color change was quantified by a simple method using the ImageJ program (a public-domain, Java-based image processing program developed at the National Institute of Health) (Collins, 2007). ImageJ is a simple, practical and freely downloadable program that can be used on any computer with Java 5 or a virtual machine (Rajwa et al., 2004). Images were obtained by direct photography of the biosensor using smart phone camera after protease application and were saved in JPEG format. These images were processed through the red channel, which shows lower background levels. The intensity color of the black MNPs-peptide SAM area was highlighted by the color threshold function with a red color and then the area was measured (Fig. 1C-II). Next, the cleaved MNPs attracted by the backwards magnet were also highlighted and measured (Fig. 1C-III).
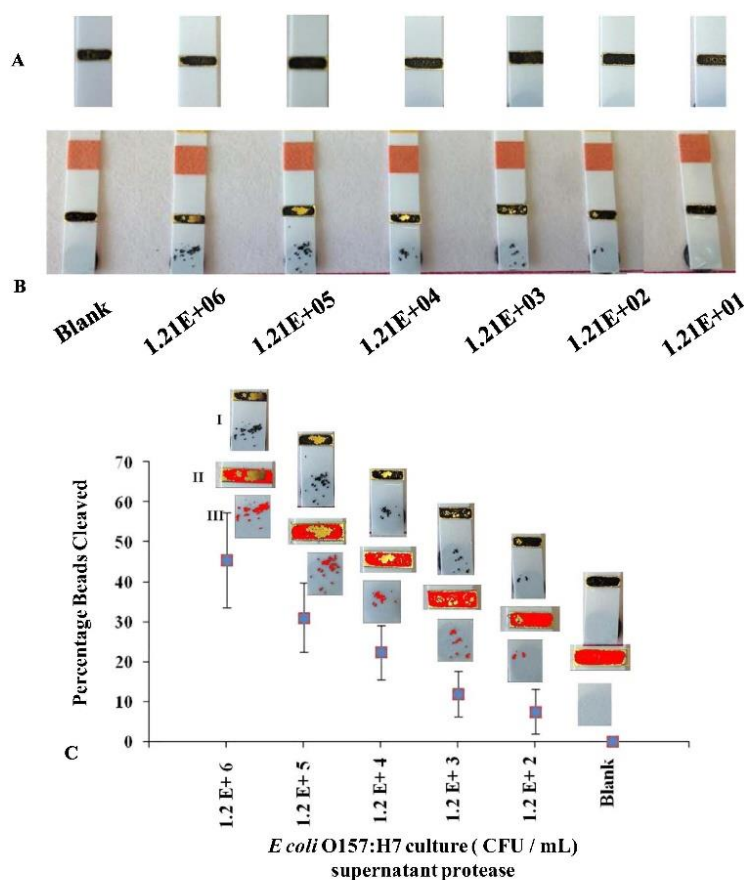
Fig. 1. Colorimetric *E. coli* sensor probe (*E. coli*-specific peptide substrate covalently bound to magnetic nanobeads). (A) Biosensor chip immobilized with magnetic bead–specific *E. coli* O157:H7 peptide substrate. (B) Immobilized biosensor under the effect of different *E. coli* O157:H7 protease concentrations. (C) Correlation of different concentration of *E. coli* O157:H7 supernatant protease concentration obtained from *E. coli* O157:H7 culture of different concentrations (CFU/mL) and the percentage of peptide-magnetic beads moieties cleaved ± RSD. I Biosensor JPG photo. II The intensity color of the black peptide-MNPs area on the sensor surface as processed by imageJ software. III Cleaved MNPs attracted by the backwards magnet as processed by imageJ software. (For interpretation of the references to color in this figure, the reader is referred to the web version of this article.)

Total MNP-peptide SAM area=MNP-peptide moieties area on the sensor surface after protease application+Cleaved MNP-peptide moieties area.

The percentage of MNP-peptide moieties cleaved=Cleaved MNP-peptide moieties area/Total MNP-peptide SAM area.

However, as the threshold adjustment process is subjective, the analysis was performed by two experimenters who followed the proposed protocol. The two experimenters measured the highlighted red-colored area. The correlation between different *E. coli* O157:H7 protease concentration obtained from *E. coli* O157:H7 culture of different concentrations (CFU/mL.) was plotted against the percentage MNP-peptide moieties cleaved as shown in Fig. 1C. All experiments were conducted in triplicate.

3. Results and discussion

The detection and identification of the food-borne pathogen *E. coli* O157:H7 relies on the culturing methodology, evaluation of colony morphology, identification of characteristic nucleic acid sequences, biochemical markers and antigenic signatures associated with the microbe (Ivnitski et al., 1999; Marusov et al., 2012). However, these assays are complex, tedious, labour-intensive and time-consuming (Siripatrawan et al., 2006).

Recently, colorimetric assays have gained importance for clinical and environmental diagnosis because of their simplicity and low cost. These assays are convenient because of the ease of qualitative detection using the naked eye without the need for a specific apparatus. In comparison, quantitative detection of the color change is usually accomplished by using instruments such as spectrophotometers, epifluorescence microscopes and luminescence counters. Thus far, a number of colorimetric methods have been reported for the detection of *E. coli* O157:H7. However, these assays require several preparative steps as well as sophisticated instrumentation and trained personnel.

Today, nanotechnology plays a crucial role in the implementation of nanostructured materials in the development nanobiosensors. Of particular interest, MNPs which combine high surface area and high affinity, can be implemented in biological samples labelling and provide a direct readout by naked eye (Huang et al., 2010). Based on this, a novel colorimetric MNPs based biosensors, which identify specific *E. coli* O157:H7 proteins, such as proteases, as a biomarkers (Hanumegowda et al., 2005; Zhou et al., 2006), would provide a detection tool for use in retail stores or at home to detect contamination by the food-borne pathogen *E. coli* O157:H7. Therefore, this work reports the development of a rapid, strip-format biosensor for the specific detection of *E. coli* O157:H7.
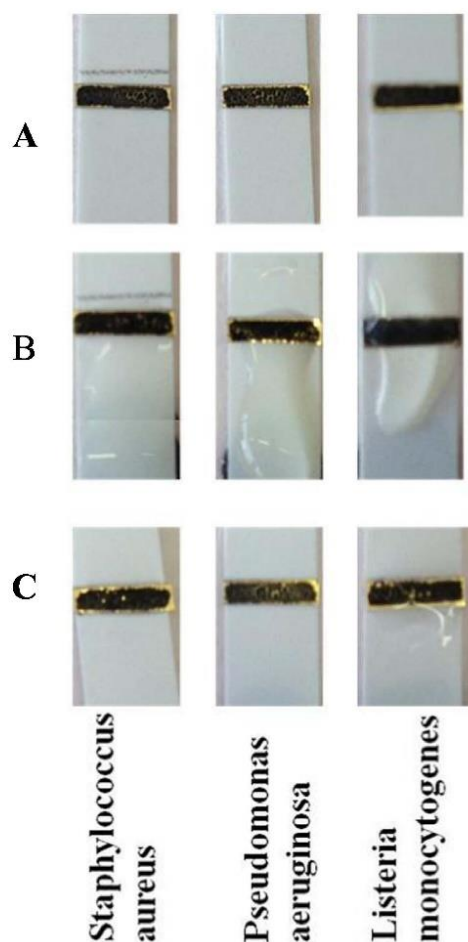
Fig. 2. Colorimetric *E. coli* protease sensor probe under the effect of other food-borne pathogens proteases. (A) Biosensor chip functionalized with MNPs–specific *E. coli* peptide substrate. (B) Functionalized biosensor incubated with different proteases. (C) Functionalized biosensor after incubation with different proteases. (For interpretation of the references to color in this figure, the reader is referred to the web version of this article.)

3.1. Sensor fabrication

The designed sensing platform is based on the detection of the proteolytic activity of *E. coli* O157:H7 proteases on a specific peptide substrate. This substrate is covalently attached at one end to carboxyl-terminated MNPs, while the other end possesses an S-S linkage joining it to the gold sensor surface (Scheme 1A). A color change occurs upon proteolysis of the MNP-peptide moieties, indicating the presence of the contaminating *E. coli* O157:H7, as described in Scheme 1.

The biosensor peptide probe was prepared using a specific *E. coli* O157:H7 peptide substrate sequence (NH$_2$-Ahx-KVSRRRRRGGDKVDRRRRRGGD-Ahx-Cys) (Bayliff et al., 2012), with an Ahx-residue linker on either terminus of the peptide. The N-terminus of the peptide was attached to the MNP. The cysteine residue at the C-terminus allows gold-sulfur interaction for the formation of the MNP-peptide complex SAM on the gold sensing platform, as shown in Scheme 1A, B and C (Esseghaier et al., 2014; Suaifan et al., 2012, 2013). The amount of the peptide substrate required for MNPs functionalization was optimized in previous work to achieve optimal

monolayer performance and stability (Alhogail et al., 2016; Wignarajah et al., 2015; Esseghaier et al., 2014; Suaifan et al., 2012, 2013).

The MNPs-peptide solution was mounted over the gold sensing platform and left intact at room temperature until dry to ensure proper immobilization of the SAM. Following this, the golden color of the biosensor turned black as shown in Scheme 1C. Next, an external magnetic field was applied over the SAM to remove any unattached peptide-MNPs moieties (Scheme 1D). After which, a round paper magnet was stacked at the back of the strip (Scheme 1E). The sensor probe was then ready for *E. coli* O157:H7 detection using the *E. coli* O157:H7 proteases as a biomarker (Scheme 1E).

3.2. Sensor testing

The proteolytic activity of the *E. coli* O157:H7 proteases was analysed by dropping protease solution prepared from *E. coli* O157:H7 culture (1.21×10^6 CFU/mL) over the functionalized gold sensor (Scheme 1F and G). The cleavage of the MNP-peptide moieties from the sensor surface was accelerated by the round paper magnet stacked at the back of the plastic physical support and beneath the sensing surface revealing the golden color visible to the naked eye, as shown in Fig. 1F and G.

To gain insight into the applicability of the sensor for quantitative detection of *E. coli* O157:H7, different *E. coli* O157:H7 protease solutions obtained from different *E. coli* O157:H7 culture concentrations (1.21×10^6 CFU/mL, 1.21×10^5 CFU/mL, 1.21×10^4 CFU/mL, 1.21×10^3 CFU/mL, 1.21×10^2 CFU/mL and 12 CFU/mL) were dripped over the black-colored sensing platform. A gradual visible increase in the golden area was observed, correlated with the concentrations of the *E. coli* O157:H7 protease solution. This is due to the proteolytic activity of *E. coli* O157:H7 proteases, which results in the dissociation of the MNP-peptide moieties. Additionally, a quantitative analytical approach was developed for the *E. coli* O157:H7-specific detection using ImageJ software (NIH, Bethesda, Maryland, USA; http://rsb.info.nih.gov/ij). Sensor reproducibility was examined by performing tests under the same experimental conditions in triplicate and the relative standard deviation (RSD) of the percentage MNP-peptide cleaved was calculate (Fig. 1C).

3.2.1. Response time
The test response time (using a digital stopwatch with naked eye inspection) was defined as the time needed for the *E. coli* O157:H7 protease solution to dissociate the MNP-peptide SAM, followed by attraction of these moieties to the magnet stacked at the back of the biosensor. The response time was found to be 30 s, which is quite a rapid response.

3.2.2. Sensor stability
To evaluate the stability of the biosensor under storage, the ready-to-use immobilized sensing strips were stored in empty petri dishes at 4 °C. Every week, three strips were used to detect *E. coli* O157:H7 protease solution prepared from known *E. coli* O157:H7 stock culture. In every experiment, a blank sample (no *E. coli* O157:H7 protease) was tested to ensure that SAM dissociation was attributed to *E. coli* O157:H7 proteolytic activity and that food matrix has no effect on the sensor. The designed biosensor showed adequate long-term stability for up to six months.

3.3. Specificity testing

To assess the specificity of the biosensor, proteases of different food-contaminating pathogens, including *Listeria monocytogenes*, *Pseudomonas aeruginosa* and *Staphylococcus aureus*, were tested over the designed *E. coli* O157:H7 biosensor. No disruption of the SAM layer and no read-out for the color change were observed by the naked eye, showing sufficient detection specificity, as shown in Fig. 2. The
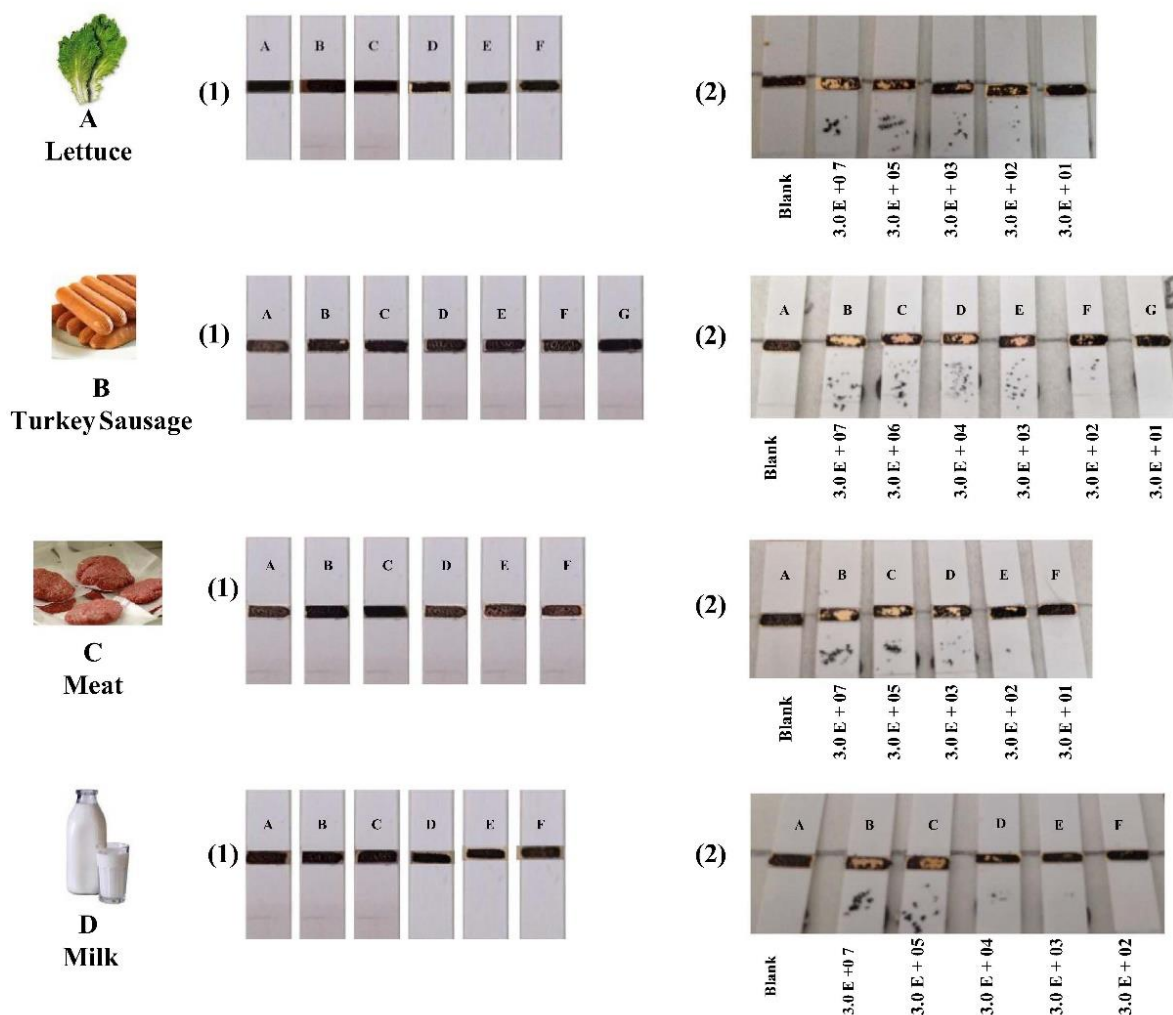
G.A.R.Y. Suaifan et al.

Fig. 3. Application of the colorimetric *E coli* O157:H7 sensor probe (specific *E coli* substrate peptide covalently bound to MNPs) for the detection of food contaminated samples; (A) Lettuce, (B) Sausage, (C) Meat and (D) Milk. (1) Biosensor chip functionalized with MNP–specific *E coli* O157:H7 peptide substrate. (2) Immobilized biosensor under the effect of blank sample (spiked with broth, no *E coli* O157:H7) and test samples (food produce spiked with different concentrations of *E coli* O157:H7 culture (CFU/mL).

experiments were conducted in triplicate.

3.4. Biosensor detection of E. coli O157:H7 spiked in food matrices

Because our developed colorimetric biosensor was able to detect *E. coli* O157:H7, we then determined its applicability for the detection of *E. coli* O157:H7 in contaminated food products. Thus, fresh PBC of *E. coli* O157:H7 was spiked into different food matrices, including ground beef, turkey sausage, lettuce and milk. First, 9 mL of different food products samples was spiked with 1.0 mL of fresh PBC of *E. coli* O157:H7 at eight bacterial culture concentrations ranging from 2.9×10^{8} CFU/mL to 2.9×10^{1} CFU/mL. A negative (blank) control was prepared by spiking food products with broth only, containing no bacteria. A positive control was also prepared by spiking 9 mL of water with 1.0 mL of fresh PBC of different concentrations ranging from 2.9×10^{8} CFU/mL to 2.9×10^{1} CFU/mL. After which, the spiked test, negative (blank) and positive control samples were allowed to incubate at room temperature for 2 h. Then, positive control samples were enumerated. The negative (blank) and spiked test samples were

then centrifuged, and the supernatant was examined on the developed biosensor. A clear and steady increase in the gold-colored area of the sensing platform was observed in relation to bacterial culture concentration for the contaminated samples. Whereas, a negative read out was observed for the uncontaminated food products (Blank samples), as shown in Fig. 3A–D. The developed biosensor displayed the ability to detect *E. coli* O157:H7 contamination in different food matrices, with a lower detection limit of 30 CFU/mL in ground beef, turkey sausage and lettuce and a lower detection limit of 300 CFU/mL in milk, as shown in Fig. 3A–D.

In view of the above results, the developed sensor would act as a quality control and hygiene monitoring tool in food industry due to its high sensitivity to detect low *E. coli* O157:H7 concentrations in 30 s without the use of any instrumentation. In addition, it is low-cost and ease to use by non-skilled personnel. It is worth mentioning is that although different colorimetric sensors have been developed previously, no single approach satisfies all or even most of these criterions. For example, Quinones et al. (2011) designed a colorimetric detection method for *E. coli* O157:H7 based on the use of DNA microarrays in

combination with photopolymerization. The detection limit range was 100–1000 CFU/mL. Additionally, Patricio et al. (Villalobos et al., 2012) reported the use of polymerized lipid vesicles as a colorimetric biosensor for detecting the presence of *E. coli* O157:H7 in water, with a detection limit of over 10^8 CFU. The detection sensitivity was improved by the use of a cytochrome C peroxidase-encoding bacteriophage (limit 10^7 CFU/mL) (Hoang et al., 2014) or by the application of an aptamer-based technique (aptasensor) (limit 10^4–10^8 CFU/mL) (Wu et al., 2012). However, to the best of our knowledge and accessibility to literature resources, the lowest limit of detection for *E. coli* O157:H7 is 7 CFU/mL in a method that involves the measurement of absorbance at 652 nm. This low sensitivity was achieved using functionalized Au@ Pt nanoparticles with a detection time of approximately 40 min (Su et al., 2013). In comparison, the sensor reported in this work was able to specifically detect *E. coli* O157:H7 with a lower limit of detection of 12 CFU/mL without the use of any instrument and in 30 s.

4. Conclusions

This work demonstrated the ability of the developed biosensor to specifically and simultaneously detect *E. coli* O157:H7 proteases in complex food matrices. The limits of detection were 12 CFU/mL in broth and 30–300 CFU/mL in food matrices. The assay was simple to perform, was rapid, required no sample pretreatment or pre-concentration and could be performed at the retail level to protect the consumer and at home. The detection mechanism does not require any labelling or amplification schemes and can be applied without requirement for any sophisticated and/or expensive instrumentation. This novel, low-cost colorimetric method used covalently attached specific MNP-substrate complexes. This biosensing configuration is amenable to the qualitative and quantitative detection of *E. coli* O157:H7. The main advantage of the developed biosensor over existing technology is its ability to detect *E. coli* O157:H7 food contamination in less than 30 s and with a very low limit of detection. This study provides the first step towards establishing a *proof-of-concept* biosensor for the detection of other microbial pathogens in contaminated food. Thus, this biosensor presents a valuable tool not only for the produce industry but also for agencies to better control potential risks associated with the consumption of contaminated foods.

Acknowledgements

References

Abuknesha, R.A., Darwish, F., 2005. Talanta 65, 343–348.
Alhogail, S., Suaifan, G.A., Zourob, M., 2016. Biosens. Bioelectron. 86, 1061–1066.
Bayliff, S.W., Del, B.M., Biott, M.C., Lindsay-Watt, S., 2012. Diagnostic Swab and Biopsy Punch Systems, Google Patents.
Berkenpas, E., Millard, P., da Cunha, M.P., 2006. Biosens. Bioelectron. 21, 2255–2262.
Beuchat, L.R., 2002. Microbes Infect. 4, 413–423.
Call, D.R., 2005. Crit. Rev. Microbiol. 31, 91–99.
CDC, 2006. Escherichia coli O157:H7. ⟨www.cdc.gov/ncidod/dbmd/diseaseinfo/escherichiacoli g.htm⟩
Collins, T.J., 2007. Biotechniques 43, 25–30.
DeCory, T.R., Durst, R.A., Zimmerman, S.J., Garringer, L.A., Paluca, G., DeCory, H.H., Montagna, R.A., 2005. Appl. Environ. Microbiol. 71, 1856–1864.
Deisingh, A.K., Thompson, M., 2004. J. Appl. Microbiol. 96, 419–429.
Esseghaier, C., Suaifan, G.A., Ng, A., Zourob, M., 2014. J. Biomed. Nanotechnol. 10, 1123–1129.
Gehring, A.G., Tu, S.I., 2005. J. Food Prot. 68, 146–149.
Gould, L.H., Bopp, C., Strockbine, N., Atkinson, R., Baselski, V., Body, B., Carey, R., Crandall, C., Hurd, S., Kaplan, R., Neill, M., Shea, S., Somsel, P., Tobin-D'Angelo, M., Griffin, P.M., Gerner-Smidt, P., 2009. Centers for Disease Control and Prevention (CDC), MMWR Recommendations and Reports, 16, pp. 1–14.
Hanumegowda, N.M., White, I.M., Oveys, H., Fan, X.D., 2005. Sens. Lett. 3, 315–319.
Ho, J.A.A., Hsu, H.W., 2003. Anal. Chem. 75, 4330–4334.
Hoang, H.A., Abe, M., Nakasaki, K., 2014. FEMS Microbiol. Lett. 352, 97–103.
Huang, Y.F., Wang, Y.F., Yan, X.P., 2010. Environ. Sci. Technol. 44, 7908–7913.
Ingham, S.C., Losinski, J.A., Andrews, M.P., Breuer, J.E., Breuer, J.R., Wood, T.M., Wright, T.H., 2004. Appl. Environ. Microbiol. 70, 6420–6427.
Ivnitski, D., Abdel-Hamid, I., Atanasov, P., Wilkins, E., 1999. Biosens. Bioelectron. 14, 599–624.
Kuck, L.R., Taylor, A.W., 2008. Biotechniques 45, 179–182.
Marusov, G., Sweatt, A., Pietrosimone, K., Benson, D., Geary, S.J., Silbart, L.K., Challa, S., Lagoy, J., Lawrence, D.A., Lynes, M.A., 2012. Environ. Sci. Technol. 46, 348–359.
Medina, M.B., 2003. J. Rapid Methods Autom. Microbiol. 11, 225–243.
Nyquist-Battie, C., Frank, L.E., Lund, D., Lim, D.V., 2004. J. Food Prot. 67, 2756–2759.
Quinones, B., Swimley, M.S., Taylor, A.W., Dawson, E.D., 2011. Foodborne Pathog. Dis. 8, 705–711.
Rajwa, B., McNally, H.A., Varadharajan, P., Sturgis, J., Robinson, J.P., 2004. Microsc. Res. Tech. 64, 176–184.
Shriver-Lake, L.C., Turner, S., Taitt, C.R., 2007. Anal. Chim. Acta 584, 66–71.
Simpson, J.M., Lim, D.V., 2005. Biosens. Bioelectron. 21, 881–887.
Siripatrawan, U., Harte, B.R., 2007. Anal. Chim. Acta 581, 63–70.
Siripatrawan, U., Linz, J.E., Harte, B.R., 2006. Sens. Actuators B: Chem. 119, 64–69.
Song, I., Stine, S., Choi, C., Gerba, C., 2006. J. Environ. Eng. 132, 1243–1248.
Su, H., Zhao, H., Qiao, F., Chen, L., Duan, R., Ai, S., 2013. Analyst 138, 3026–3031.
Suaifan, G.A., Esseghaier, C., Ng, A., Zourob, M., 2012. Analyst 137, 5614–5619.
Suaifan, G.A., Esseghaier, C., Ng, A., Zourob, M., 2013. Analyst 138, 3735–3739.
Subramanian, A., Irudayaraj, J., Ryan, T., 2006. Biosens. Bioelectron. 21, 998–1006.
Tauxe, R., Kruse, H., Hedberg, C., Potter, M., Madden, J., Wachsmuth, K., 1997. J. Food Prot. 60, 1400–1408.
Uttamchandani, M., Neo, J.L., Ong, B.N.Z., Moochhala, S., 2009. Trends Biotechnol. 27, 53–61.
Villalobos, P., Isabel Chavez, M., Olguin, Y., Sanchez, E., Valdes, E., Galindo, R., Young, M.E., 2012. Electron. J. Biotechnol., 15.
Vora, G.J., Meador, C.E., Anderson, G.P., Taitt, C.R., 2008. Mol. Cell. Probes 22, 294–300.
Wignarajah, S., Suaifan, G.A., Bizzarro, S., Bikker, F.J., Kaman, W.E., Zourob, M., 2015. Anal. Chem. 87, 12161–12168.
Wu, W., Zhang, J., Zheng, M., Zhong, Y., Yang, J., Zhao, Y., Ye, W., Wen, J., Wang, Q., Lu, J., 2012. PLoS One 7, e48999.
Zhou, Y., Krause, S., Chazalviel, J.-N., McNeil, C.J., IEEE, 2006. Biosensor arrays based on the degradation of thin polymer films interrogated by scanning photo-induced impedance microscopy. In: Proceedings of the 2006 IEEE Sensors, vols. 1–3, pp. 259–262.

[SAA 4]

Simple and rapid peptide nanoprobe biosensor for the detection of *Legionellaceae*

Sahar Alhogail, Raja Chinnappan, Majeda Alrifai, Ghadeer A. R. Y. Suaifan, Floris J. Bikker, Wendy E. Kaman, Karina Weber, Dana Cialla-May,Jürgen Popp, Mohamed B. Alfageeh, K. Al-Kattan and Mohammed M. Zourob

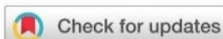|	Sahar Alhogail	Raja Chinnappan
Konzeption des Forschungsansatzes	**X**	**X**
Planung der Untersuchungen	**X**	**X**
Datenerhebung	**X**	
Datenanalyse und – interpretation	**X**	
Schreiben des Manuskripts	**X**	
Vorschlag Anrechnung Publikationsäquivalente	**1,0**	

Analyst

PAPER

Check for updates

Simple and rapid peptide nanoprobe biosensor for the detection of *Legionellaceae*

Sahar Alhogail,[a,b] Raja Chinnappan,[b] Majeda Alrifai,[b] Ghadeer A. R. Y. Suaifan, [ID][c] Floris J. Bikker,[d] Wendy E. Kaman,[d,e] Karina Weber,[f,g,h] Dana Cialla-May,[f,g,h] Jürgen Popp,[f,g,h] Mohamed B. Alfageeh,[i] K. Al-Kattan [ID][b] and Mohammed M. Zourob [ID] *[b,j]

This study demonstrates the development of a sensitive, specific, and quantitative peptide-based nanoprobe prototype assay for the detection of *Legionellaceae* in a simple way and in a short time. In this work, proteases present in the culture supernatants of *Legionella* spp. were used as a biomarker. Fluorogenic peptide substrates, specific to *Legionella* strains culture supernatant proteases, were identified. Peptidases produced a significant increase in the fluorescence intensity following the cleavage of the dipeptide fluorogenic substrates. The specific substrates were identified and coupled with carboxyl-terminated nano-magnetic particles (NMPs). On the other hand, the C-terminal was conjugated with the cysteine residue to covalently integrate with a gold sensing platform *via* the Au—S linkage. Four different sensors were fabricated from the four specific substrates, which were treated with the protesase of six different species of *Legionella*. In the presence of specific protease, the peptide sequence is digested and the magnetic nanobeads moved out of the gold surface, resulting in the apparence of gold color. One of the nanoprobes sensitivity detects as low as 60 CFU mL^{-1} of *Legionella anisa*, *Legionella micdadei*, and *Fluoribacter dumoffii*. The cross-reactivity of the sensors was tested using other closely associated bacterial species and no significant cross-reactivity of the sensors was found. It is envisaged that this assay could be useful for screening purposes or might be supportive for the fast and easy detection of *Legionella* protease activity for water monitoring purposes.

[a]Department of Clinical Laboratory Science, King Saud University, Ad Diriyah district 11433, Kingdom of Saudi Arabia
[b]Alfaisal University, Al Zahrawi Street, Al Maather, Al Takhassusi Rd, Riyadh 11533, Saudi Arabia. E-mail: mzourob@alfaisal.edu
[c]Department of Pharmaceutical Sciences, Faculty of Pharmacy, The University of Jordan, Amman 11942, Jordan
[d]Department of Oral Biochemistry, Academic Centre for Dentistry Amsterdam, University of Amsterdam and VU University Amsterdam, Gustav Mahlerlaan 3004, 1081 LA Amsterdam, The Netherlands
[e]Department of Medical Microbiology and Infectious Diseases, Erasmus Medical Center, Wytemaweg 80, 3015 CE Rotterdam, The Netherlands
[f]Institute of Physical Chemistry and Abbe Center of Photonics, Friedrich Schiller University Jena, Helmholtzweg 4, 07743 Jena, Germany
[g]InfectoGnostics Research Campus Jena, Center for Applied Research, Philosophenweg 7, 07743 Jena, Germany
[h]Leibniz Institute of Photonic Technology, Member of the Leibniz research alliance "Leibniz Health Technologies", Albert-Einstein-Straße 9, 07745 Jena, Germany
[i]King Abdulaziz City for Science and Technology, King Abdullah Rd, Al Raed, Riyadh 12354, Saudi Arabia
[j]King Faisal Specialist Hospital and Research Center, Zahrawi Street, Al Maather, Riyadh 12713, Saudi Arabia

1. Introduction

Legionella pneumophila is a pleomorphic Gram-negative facultative intracellular bacterial parasite co-evolved within freshwater protozoa (amoeba).[1,2] In July 1976, *L. pneumophila* was recognized to be pathogenic to humans, following an outbreak of acute pneumonia at the American Legion convention in Philadelphia, USA.[3] This pathogen was reported to contaminate warm engineered water systems[4,5] and to be associated with the occurrence of Legionnaires' disease (LD), which is a pneumonic devastating[6,7] life-threatening infection with a fatality rate of more than 50%, particularly in individuals with compromised health conditions.[2] *L. pneumophila* was found to proliferate and persist within biofilms. Thus, it possesses the ability to resist various purification systems in aquatic media. Accordingly, the inhalation of *L. pneumophila*-contaminated aerosols occurring in, for example, showers, hot tubs, spas, faucets, dental lines, air conditioning systems, and cooling towers, may cause human infections by attacking the alveolar mucosa.[8]

In 1978, Winn *et al.* proposed the contribution of *L. pneumophila* products to the pathogenesis of LD.[9,10] Then,

Dreyfus *et al.* purified and characterized an extracellular metalloprotease, also called tissue-destructive protease or major secretory protein.[11] This extracellular protease exhibited hemolytic, cytotoxic, and dermal ulcerative activities,[12-14] which is considered as one of the virulent factors of this organism.

In practice, LD diagnosis is based on the culture methodology, which can detect all *Legionella* spp. and serogroups specifically. However, this assay is time-consuming, as it takes more than three days to obtain the results and fails to detect viable but non-culturable (VBND) *Legionella* cells in freshwater.[15-17] Another medically approved test is based on the detection of *Legionella* antigen in urine using ELISA.[15] This test possesses moderate sensitivity and specificity in comparison with the culture and PCR methods, but the *Legionella* antigen is typically detectable in urine in the initial 2 to 3 days after the onset of clinical symptoms.[15] In addition, test results may remain positive for a year upon treatment and the ELISA test is unable to detect pathogenic *Legionella* species other than the *L. pneumophilia* serogroup 1.[6,17] In clinical practice, real-time polymerase chain reaction (rtPCR) is an ultra-sensitive assay for LD diagnosis. This method is quantitative, rapid with a short turnaround time, and sensitive in comparison with to the culturing technique. The PCR method is based on the amplification of conserved regions of rRNA sequences; however, these regions are not specific and, hence, can be applied for the detection of any *Legionella* subspecies.[17] Moreover, this technique is unable to differentiate between viable and dead cells (except with PMA or EMA). Also, this method requires trained personnel.[15,17] Alternative methods such as direct fluorescent antibody staining and immunohistochemistry are highly specific, but with procedural difficulties.[18] Other valuable tools for *Legionella* detection include matrix-assisted laser desorption/ionization time-of-flight mass spectrometry. This method is simple, reproducible, and inexpensive but cannot identify *Legionella* strains at the serogroup level.[19]

In accordance, the development of an easy and fast, in-field, colorimetric, rapid, sensitive, and highly specific test would be an excellent tool for screening purposes to support laborious detection methodologies. In this work, we present a fluorescence-based, portable, and low-cost colorimetric assay for the detection of *L. pneumophila* extracellular proteases as a biomarker.

At first, various fluorescence resonance energy transfer (FRET) peptides were selected from a FRET peptide library.[20] Subsequently positive substrates were conjugated to nano-magnetic particles (NMPs) terminated with a thiol group to covalently integrate with a gold sensing platform *via* the Au–S linkage, offering a colorimetric sensor. Ideally, this could be useful for application in water monitoring purposes.

2. Materials and methods

2.1. Chemicals and reagents

Turbobeads™ carboxyl-terminated nanomagnetic particles (NMPs) (50 nm diameter) were purchased from Turbobeads (Zurich, Switzerland). *N*-Hydroxysuccinimide (NHS), 1-(3-di-methylaminopropyl)-3-ethyl-carbodiimide (EDC), pH stripes, potassium phosphate, sodium chloride, bovine serum albumin (BSA), ethylenediaminetetraactic acid (EDTA), sodium azide, and Tris buffer were purchased from Sigma-Aldrich (Dorset, UK). Self-adhesive magnetic sheets A4 were purchased from a polarity magnets company (Wickford, UK). Brain heart infusion broth (BHI), blood agar, and buffered charcoal yeast extract (BCYE) agar were purchased from SDA Oxoid, Ltd (Basingstoke, UK). Sterile filters 0.22 μm were purchased from Millipore (UK). The wash/storage buffer (10 mM Tris base, 0.15 M sodium chloride, 0.1% (w/v) bovine serum albumin, 1 mM ethylenediaminetetraacetic acid, 0.1% sodium azide, pH 7.5), and the coupling buffer (10 mM potassium phosphate, 0.15 M sodium chloride, pH 5.5) were prepared from chemicals of analytical grade. FRET-based dipeptide library was purchased from PepScan Presto B.V. (Lelystad, The Netherlands).

The peptide library consists of 115 protease substrates with two amino acids. The substrates were designed using (a) L-amino acid; (b) C-terminal L-amino acid and N-terminal D-amino acid; (c) a combination of L- and D-amino acids. L-Amino acids are denoted in uppercase letters, whereas D-amino acids are denoted in lowercase letters.[20] Fluorogenic substrates were synthesized with a purity of approximately >90%. Substrate identity was confirmed by mass spectrometry. All substrates were C-terminally flanked with fluorescein isothiocyanate (FITC); fluorescent probe and N-terminally flanked with Dabcyl (KDbc), a lysin-coupled quencher. The peptides sequences used for the paper based sensing platfrom was purchased from Pepmic Co. (Suzhou, China). The peptide sequence was conjugated with cystein residue-aminohexanoic acid (Ahx) at the C-terminus of the substrate to covalently attached to the gold sensing platform, and elongated with the aminohexanoic acid (Ahx) spacer at the N-terminal.

2.2. Bacterial culture

Legionella pneumophila (*L. pneumophila*) ATCC 33155, *L. pneumophila* ATCC 33152, *Legionella micdadei* (*L. micdadei*) ATCC 33218, *Legionella anisa* (*L. anisa*) ATCC 35292 and *Fluoribacter dumoffii* (*F. dumoffii*), ATCC 33279 were purchased from ATCC (Manassas, VA, USA). These organisms were cultured in buffered charcoal yeast extract agar at 37 °C, 5% CO$_2$ for 48–72 h. Other pathogens such as *Campylobacter* ATCC 33560, *Escherichia coli* (*E. coli*) O157:H7, and *Salmonella enterica* (*S. enterica*) ATCC 13312 were purchased from ATCC (Manassas, VA, USA) and cultured in BHI. *Campylobacter* was cultured at 45 °C for 24 h under microaerophilic conditions, whereas *E. coli* and *S. enterica* were incubated at 37 °C for 18–24 h.

2.3. Preparation of *Legionella* spp. culture supernatant proteases

Legionella pneumophila (*L. pneumophila*) ATCC 33155, *L. pneumophila* ATCC 33152, *Legionella Tatlockia micdadei* (*T.L. micdadei*) ATCC 33218, *Legionella anisa* (*L. anisa*) ATCC 35292, and *Fluoribacter dumoffii* (*F. dumoffii*) ATCC 33279 were purchased in the lyophilized form from ATCC (Manassas, VA, USA). All the strains were resuspended with BHI broth, then cul-

89

tured on buffered activated charcoal and yeast extract agar incubated at 37 °C, 5% CO_2, and humidity for 48 –72 h. Afterwards, the strains were harvested from the plate in liquid BHI tubes. Following appropriate bacterial culture, bacterial cell count was estimated by McFarland standards and the used cell concentration was diluted to 6×10^8 CFU mL^{-1} for all bacterial strains. Subsequently, each bacterial culture was pelleted by centrifugation at 3000g for 10 min and the suspension was filtered using a 0.5 micrometer filter to obtain the crude protease solution with specific proteolytic activity proportional to the bacterial concentration in the range of 6×10^1 to 6×10^8 CFU mL^{-1}. All the bacterial growth media were pushed from Saudi Prepared Media Laboratory Company Limited (Riyadh, Saudi Arabia).

2.4. Substrate detection using the FRET assay

A high throughput screening method for the selection of a specific peptide substrate was performed in a clear bottom black 96-well-plates (Corning, Lowell, USA) using a FRET-peptide library,[20,21] as shown in Fig. 1A. All the peptide substrates were labeled with FITC fluorophore at the C-terminal and KDbc quencher at the N-terminal. The proteolytic activity of the different organisms was monitored using 0.5 µL of each substrate (800 µM) in a 1 : 1 filtered PBC supernatant and PBS buffer (100 µL). Culture media was used as the negative

control. The change in the fluorescence intensity was monitored every minute for 2 h at 37 °C using an excitation wavelength of 485 and an emission wavelength of 535 nm. The relative fluorescence unit (RFU) of each sample was calculated by subtracting the negative control values of the culture media. Proteolytic activity was defined in RFU per minute. The test was performed in triplicate.

2.5. Preparation of peptide–NMPs

Carboxylated NMPs suspension (15 mg mL^{-1}) was dispersed by sonication and activated by washing three times with the coupling buffer (10 mM potassium phosphate, 0.15 M sodium chloride, pH 5.5).[22–26] Next, one mL of NMPs suspension (15 mg mL^{-1} in coupling buffer) was mixed with the peptide solution (1 mg of peptide substrate dissolved in 1 mL of DMSO), freshly prepared coupling agent EDC (0.57 mg mL^{-1}), and NHS (2 mg mL^{-1}).[22–26] The mixture was shaken on a rotary shaker overnight at 4 °C. Next, peptide–NMPs conjugates were collected using a magnetic separator and the supernatant was aspirated to remove uncoupled peptides. Finally, collected peptide–NMPs conjugates were washed three times with washing buffer (10 mM Tris base, 0.15 M NaCl, 0.1% (w/v) BSA, 1 mM ethylenediaminetetraacetic acid, 0.1% sodium azide, pH 7.5) and stored at 4 °C in a storage buffer.[22–27]
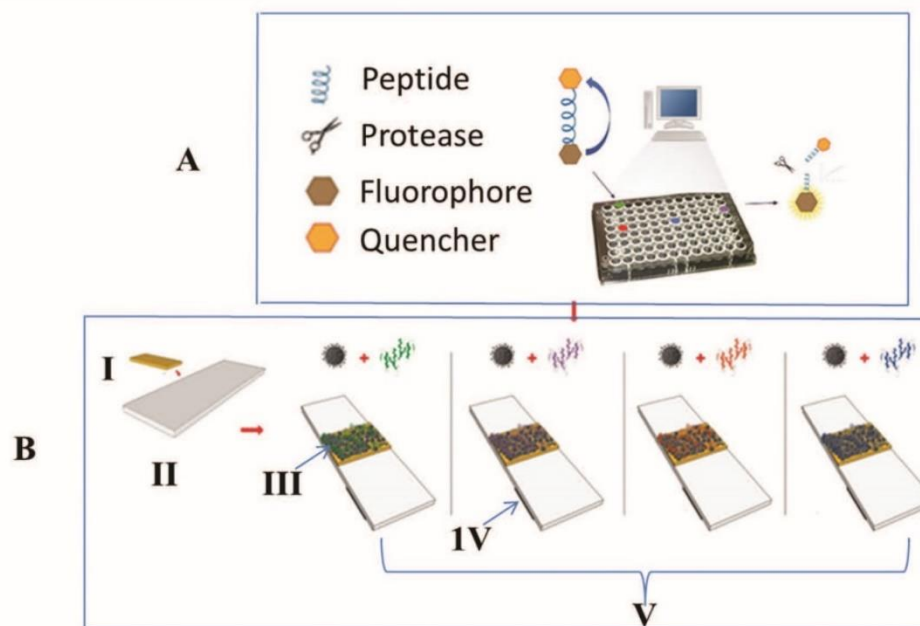

Fig. 1 Schematic overview of *Legionella* spp. detection using the peptide–MNPs probe. A Screening for peptide substrates susceptible to cleavage by *Legionella* proteases by a highthroughput method using the FRET-based dipeptide library. All peptide substrates were labeled with the FITC fluorophore at the C-terminal and KDbc quencher at the N-terminal. The proteolytic activity of different *Legionella* strains was monitored. B Colorimetric biosensors for the detection of *Legionella* strains using different peptide–NMPs conjugate probes. (I) Gold plated self-adhesive tape. (II) Solid physical support. (III) Carboxy-terminated NMPs functionalized with certain peptide substrates were immobilized over a gold sensing platform to form the sensing assay platform. (IV) Round self-adhesive magnet (1 mm in diameter) was fixed at the sensor platform backside. (V) Ready to use peptide–NMPs probe sensing platform.

2.6. Preparation of the *L. pneumophila* sensing platform

Adhesive sheet purchased from Whatman (London, UK) was coated with a thin layer of gold, which was sputtered at the School of Engineering at King Abdullah University of Science and Technology (KAUST). As shown in Fig. 1BI, the self-adhesive sheet was shaped in a specific size (1–2 mm width) and fitted over a flexible water-resistant strip (Fig. 1BII), which served as the physical support for the sensor. 10 μL of the peptide-conjugated MNP was added over the engineered gold surface and allowed to stand at room temperature until dry (Fig. 1BIII). Afterward, an external magnet (12.5 mm × 12.5 mm × 5 mm, Polarity Magnets Company, Wickford, UK) with a field strength of 3360 gauss was passed over the platform (at 10 mm distance) to remove the unbound peptide–NMPs conjugate. The color change from gold to black following peptide–NMP immobilization over the gold surface indicated the formation of a colorimetric sensor platform (Fig. 1BIII). Then, a circular self-adhesive magnet (1 mm in diameter, prepared by punching an adhesive magnet sheet (purchased from Polarity Magnets Company, Wickford, UK)) was fixed on the sensor platform backside (Fig. 1BIV) and beneath (2–3 mm) the sensing platform. This magnet will assist the collection of the cleaved peptide–NMPs-fragments. Finally, a ready-to-use peptide–NMPs probe was developed (Fig. 1BV).

3. Results and discussion

A simple paper-based protease assay was used for the detection of *Legionella* bacteria. First, we screened a large number of different peptides and selected four common peptide sequences that are specific to *Legionella* species. These selected sequences were further used for the quantitative detection of *Legionella* using the total protease from the culture supernatant. To date, several methods have been developed to detect *Legionella* bacteria. However, these assays have several drawbacks including technical difficulties, lack of sensitivity, and the possibility of false-positive results. Nanotechnology implemented biosensors have guided the development of a cost-effective and time-saving tool and can be applied on-site for the detection of pathogens.[22,23,25,26] Recently, electrochemical impedance spectroscopy-based immunosensor (EIS), a bioaffinity group sensor, has been developed to detect *Legionella* spp. in cooling towers (Table 1). This sensor successfully detected *Legionella* spp. within hours; however, the conductivity of the assay media may affect the measurements and the sensor specificity was not validated.[28] Other optical-based biosensors (Table 1) detected different concentrations of RNA from *L. pneumophila* with high spatial resolution and higher bit depth;[29] however, these sensors reported high detection limits.[29]

The majority of Legionnaires cases are caused by invasive and envasive opportunistic *L. pneumophila*. This pathogen utilizes proteases as the virulence factors to invade alveolar mucosa and subsequently cause human infection, following the inhalation of contaminated warm engineered water systems.[4,5] Remarkably, *Legionella*-mediated proteolysis may be considered valuable biomarkers for detecting the presence or absence of *Legionella* strains in hotels, hospitals, and/or other public areas for regular water monitoring and conse-

Table 1 Sensitivity comparison between commonly used methods for the detection of *Legionella* spp. and the developed biosensor

Detection techniques	LOD	Sample media (matrix)	Positivity rate	Assay time	Ref.
Culture	1 CFU mL^{-1} (for 1 L sample)	Water-BCYE agar, BPAV charcoal media	0.4%	Days	15, 17 and 33
BinaxNOW@UAT			0.8%	Hours	15, 17 and 34
PCR	10^2–10^3 CFU mL^{-1}	Water	2.7%	Hours	15, 17 and 35
Microelectrode array biosensor	10^5–10^8 CFU mL^{-1}	Water		Hours	28
Magnetic-nanoparticle conjugated peptide probe	Up to 6×10^1 CFU mL^{-1}	Water		Minutes	Current study

Table 2 FRET-based cleavage efficiency of the dipeptides by 6×10^8 CFU mL^{-1} culture supernatant of the various *Legionella* strains; *L. pneumophila* ATCC 33155, *T. micdadei* ATCC 33218, *L. anisa* ATCC 35292, *F. dumoffii* ATCC 33279, *L. pneumophila* ATCC 33152, and *F. bozemanae* ATCC 33217

Substrate	33155	33218	35292	33279	33152	33217
FITC-Ahx-L-L-K(Dabcyl)	100.00	36.67	22.80	68.13	72.20	—
FITC-Ahx-F-F-K(Dabcyl)	95.90	100.00	5.40	69.36	67.90	—
FITC-Ahx-W-W-K(Dabcyl)	52.20	19.05	28.10	100.00	100.00	12.3
FITC-Ahx-Y-Y-K(Dabcyl)	85.60	65.20	100.00	60.50	58.70	7.6
FITC-Ahx-M-M-K(Dabcyl)	7.20	0.04	4.79	32.68	33.12	6.7
FITC-Ahx-A-A-K(Dabcyl)	7.60	0.50	6.50	48.02	48.70	−3.4
FITC-Ahx-Y-y-K(Dabcyl)	2.70	5.50	—	10.86	10.90	6.4
FITC-Ahx-t-t-K(Dabcyl)	0.26	0.69	1.08	4.50	4.45	−2.9
FITC-Ahx-y-y-K(Dabcyl)	—	—	—	—	0.30	—

quent infection prevention measures.[22,23,25,26] In this work, we report the development of a simple and rapid peptide–MNPs based biosensor for the specific detection of *Legionella* spp. proteolytic activity.

3.1. Screening FRET peptide library

The proteolytic activity of different *Legionella* strains was determined by screening 115 fluorogenic dipeptide substrates.[20] Specific fluorogenic dipeptide substrates' cleavage was identi-

fied using bacterial culture supernatant by monitoring the change in the fluorescence intensity for six different *Legionella* strains. The maximum change in the fluorescence intensity was considered as 100 percent and the relative percentage change compared to the maximum was calculated. Peptidase released from all *Legionella* strains except the bozemanae strain produced a significant increase in the fluoresce intensity following the cleavage of the dimeric amino acids (L–L), (F–F), (W–W), and (Y–Y) FRET substrates. The proteolytic activity of
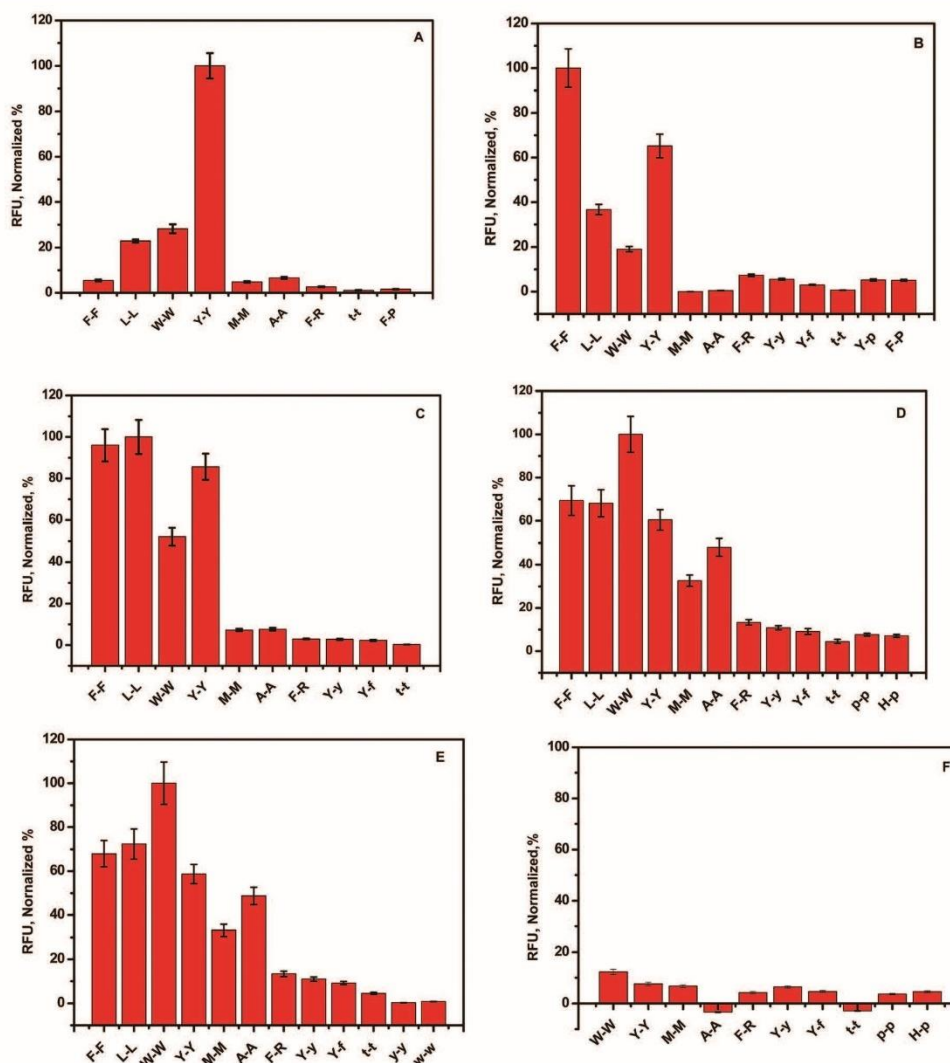

Fig. 2 Change in the fluorescence intensities of different fluorogenic peptide substrates in the presence of different *Legionella* strains culture supernatant after 30 minutes (*L. anisa* ATCC 35292 (A), *L. micdadei* ATCC 33218 (B), *L. pneumophila* ATCC 33155 (C), *F. dumoffii* ATCC 33279 (D), *L. pneumophila* ATCC 33152 (E), and *F. bozemanae* ATCC 33217 (F). All *Legionella* strains specifically cleaved L-aromatic amino acids dipeptide and LL dipeptide. No cleavage was observed with D-amino acid containing substrates.

Analyst

Legionella strains was found to specifically target L-amino acids containing dipeptides (Table 2). Notably, proteolysis was observed in the substrates containing aromatic L-amino acids (tyrosine, tryptophan, and phenylalanine) except for leucine-leucine (FITC-Ahx-LL-K(Dabcyl). On the other hand, no hydrolysis was observed in dipeptide substrates having both a D- and L-amino acid. The proteolytic activity of *Legionella* strains was stereo-specific. For example, no change in the fluorescence

Table 3 FRET assay for F–F, L–L, W–W, and Y–Y substrates in the presence of bacterial culture supernatants

Bacteria	F–F	L–L	W–W	Y–Y
L. anisa ATCC 35292	+	++	++	++++
T. micdadei ATCC 33218	++++	++	+	+++
L. pneumophilia ATCC 33155	++++	++++	++	+++
L. pneumophilia ATCC 33152	+++	+++	++++	++
F. dumoffii ATCC 33279	+++	+++	++++	++
E. coli O157:H7	—	—	—	—
S. enterica ATCC 13312	—	—	—	—
Campylobacter Jejuni ATCC 33560	—	—	—	—
F. bozemanae 33217	—	—	—	—

intensity could be detected when the y–y dipeptide substrate was examined (Table 2, the substrates having Y–Y and y–y, Fig. 2E) compared to the enantiomeric Y–Y substrate (58.7–100% fluorescence intensity change with different *Legionella* strain). Notably, *L. pneumophila* ATCC 33155 exerted efficient proteolytic activity against F–F, L–L, and Y–Y, and moderate activity against W–W (Fig. 2C), whereas the W–W substrate was cleaved efficiently by *L. pneumophila* ATCC 33152 (Fig. 2E). Moreover, *L. anisa* ATCC 35292 specifically digested Y–Y peptide, while no significant increase in the fluorescence intensity was observed with other substrates (Fig. 2A). F–F dipeptide was cleaved effectively by *L. micdadei* ATCC 33218 and moderate cleavage was detected in the Y–Y peptide. On the other hand, no significant proteolysis of L–L and W–W dipeptides was observed (Table 2 and Fig. 2B). However, in contrast to the other five species, *F. bozemanae* 33217 supernatant had no significant effect on the cleavage of any FRET substrates, which may be explained by the difference in the phenotypic characterization as well as the differences in the DNA G–C content and DNA hybridization data of *F. dumoffii* ATCC 33279 from another *Legionella* strains.[30] Furthermore, *Legionella* strain-specific cleavage of the FRET substrates were
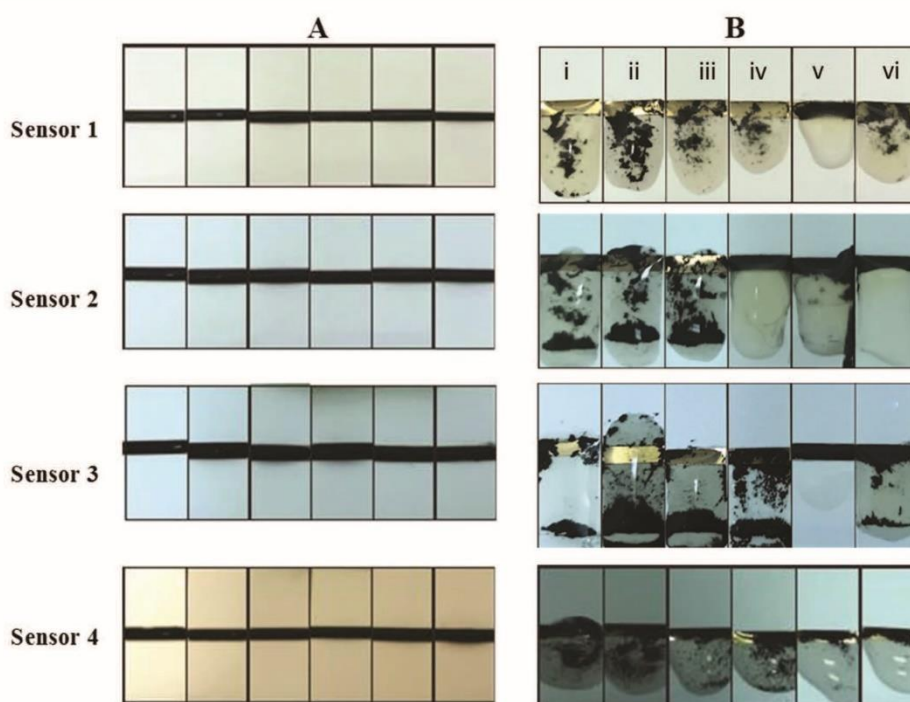

Fig. 3 Colorimetric detection of *Legionella* strains proteolytic activity using four peptide sensor nanoprobe. (A) Biosensor platform functionalized with black color peptide–NMPs conjugates. (Sensor 1) Ahx-YY-Ahx-Cys substrate covalently bound to MNPs. (Sensor 2) Ahx-WW-Ahx-Cys substrate covalently bound to MNPs. (Sensor 3) Ahx-FF-Ahx-Cys substrate covalently bound to MNPs. (Sensor 4) Ahx-LL-Ahx-Cys substrate covalently bound to MNPs. (B) Biosensor platform under the effect of (i) *L. pneumophila* ATCC 33155, (ii) *T. micdadei* ATCC 33218, (iii) *L. anisa* ATCC 35292, (iv) *F. dumoffii* ATCC 33279, (v) *L. pneumophila* ATCC 33152, and (vi) *F. bozemanae* ATCC 33217 culture supernatant (6×10^8 CFU mL^{-1}).

compared with the associated bacteria such as *E. coli*, *S. Enterica*, and *Campylobacter jejuni* (Table 3).

3.2. Biosensor structuring

Legionella protease-specific dipeptides were identified from the above FRET assay. These dipeptides were used for the paper-based protease assay. Biosensor peptide probes were prepared using L-amino acid dipeptide substrates elongated with an amino hexanoic acid Ahx-residue spacer on either terminus of the peptide (NH$_2$-Ahx-Y-Y-Ahx-Cys, NH$_2$-Ahx-W-W-Ahx-Cys, NH$_2$-Ahx-F-F-Ahx-Cys, NH$_2$-Ahx-L-L-Ahx-Cys) for easy accesability of the peptide bond in the dipeptide by the *Legionella* protease. The amine group of the substrates was coupled with carboxylic acid-functionlized NMPs to produce black colored peptide–NMPs conjugates. When the MNP-conjugated peptide was pipeted out on the golded surface, the thiol group (–SH) in the cysteine residue at the C-terminus of the substrate forms an irreversible covalent anchor with the golden platform to fabricate a colorimetric sensor.

3.3. Biosensor testing

This method aimed to visually detect the proteolytic activity of *Legionella* based on the use of specific peptide substrates by the naked eye, sandwiched between NMPs and gold platforms *via* a solid physical support. In the absence of *Legionella* protease supernatant, the gold surface is completely covered with the magnetic beads and it appears black (Fig. 3A). When the *Legionella* strains (*L. pneumophila* ATCC 33155, *L. micdadei* ATCC 33218, *L. anisa* ATCC 35292, *F. dumofii* ATCC 33279, *L. pneumophila* ATCC 33152, and *F. bozemanae* ATCC 33217 culture supernatants (prepared from a 6×10^8 CFU mL^{-1} culture)) were dripped over the fabricated peptide sensor nanoprobes, the protease in the culture supernatant digest the peptide linkage between the amino acids in the dipeptide and break the peptide bond. The proteolytic activity of the *Legionella* strains was visualized by the dissociation of the peptide–NMPs segments from the sensor surface and the consequent restoration of the sensor golden color for the positive read-out result (Fig. 3B). The cleaved peptide–NMPs segments were trapped by a paper magnet fixed under the paper support. The fabricated sensors was Ahx-Y-Y-Ahx-Cys, NH$_2$-Ahx-W-W-Ahx-Cys, and NH$_2$-Ahx-F-F-Ahx-Cys substrates were efficiently cleaved by three *Legionella* species ((i) *L. pneumophila* ATCC 33155, (ii) *L. micdadei* ATCC 33218, and (iii) *L. anisa* ATCC 35292). Sensor 1 (NH$_2$-Ahx-Y-Y-Ahx-Cys) is effectively digested by (iv) *F. dumofii* ATCC 33279 in addition

to these three species. *F. bozemanae* ATCC 33217 (vi) supernatant shows significantly less digestion on all the four sensors. However, *L. pneumophila* ATCC 33152 (v) did not cleave any of the peptides effectively compared to the other five species of *Legionella*. Compared to sensors 1, 2, and 3, sensor 4 did not effectively digest all the six species of *Legionella*. The overall results of the four sensors response to six different species interestingly show that the sensors fabricated from the dipeptide with L-amino acids having aromatic side-chain were efficiently cleaved by all the *Legionella* species family (Fig. 3B, sensor 1, sensor 2, and sensor 3). On the other hand, sensor 4 fabricated from aliphatic amino acid (NH$_2$-Ahx-L-L-Ahx-Cys) did not show a significant effect by the proteases from six different species of *Legionella* family (Fig. 3B, sensor 4). The results are in correlation with the results obtained from FRET, where the dipeptide with the aromatic side chain has high fluorescence in the presence of *Legionella* species (Fig. 2). It is clear that the L-amino acid dipeptide substrate with aromatic side chains are specifically cleaved by the *Legionella* family of bacteria.

3.4. Quantification measurement

To further explore the sensitivity of the designed sensors, target biosensing methods were implemented for the quantitative detection of *L. pneumophila* ATCC 33155, *L. micdadei*
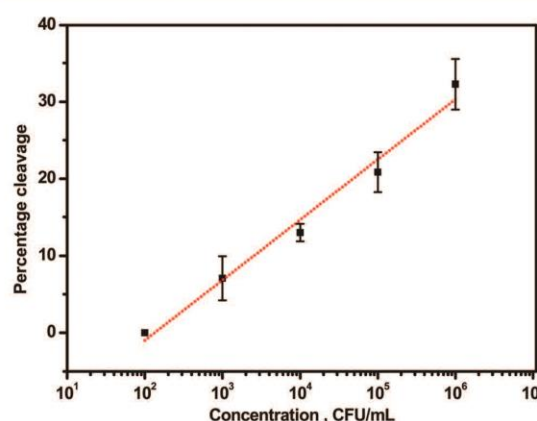

Fig. 4 The percentage cleavage of the MNP-conjugated peptides at variable concentrations of *L. pneumophila* ATCC 33152. All data show mean ± STD of triplicate measurements.

Table 4 Lower detection concentrations (6×10^x CFU mL^{-1}) of *L. pneumophila* ATCC 33155, *T. micdadei* ATCC 33218, *L. anisa* ATCC 35292, *F. dumofii* ATCC 33279, *L. pneumophila* ATCC 33152 of the colorimetric biosensors

	Bacteria	Sensor 1 (Ahx-YY-AHX-C)	Sensor 2 (Ahx-WW-AHX-C)	Sensor 3 (Ahx-FF-AHX-C)	Sensor 4 (Ahx-LL-AHX-C)
A	*L.. anisa* ATCC 35292	10^1	10^5	10^6	10^3
	T. micdadei ATCC 33218	10^1	10^7	10^1	10^5
	L. pneumophilia ATCC 33155	10^4	10^7	10^3	10^1
	F. dumofii ATCC 33279	10	10^7	10^2	10^2
	L. pneumophilia ATCC 33152	10^7	10^1	10^1	10^1

Analyst

ATCC 33218, *L. anisa* ATCC 35292, *F. dumoffii* ATCC 33279, and *L. pneumophila* ATCC 33152. Each strain was tested in various densities (Bacterial concentration (CFU mL^{-1})). The activity was examined using all the four peptide nanoprobes, namely, sensor 1 (Ahx-YY-Ahx-Cys), sensor 2 (Ahx-WW-Ahx-Cys), sensor 3 (Ahx-FF-Ahx-Cys), and sensor 4 (Ahx-LL-Ahx-Cys). The newly developed biosensors successfully detected the five different *Legionella* strains. The limit of detection (LOD) of *Legionella anisa* ATCC 35292 was 60 CFU mL^{-1} with sensor 1, followed by 6×10^3 and 6×10^5 CFU mL^{-1} with sensor 4 and sensor 2, respectively. The LODs of *L. micdadei* ATCC 33218 with sensor 1 and sensor 3 were 6×10^1 CFU mL^{-1}. However, sensors 4 and 2 show high LODs of 6×10^5 and 6×10^7 CFU mL^{-1}, respectively (Table 4). For clearer presentation, the calibration curve for *L. pneumophilia* ATCC 33155 sensor, as an example, was represented as the percentage cleavage *vs.* log concentration. The data acquisition and analysis included a computer with a data acquisition ImageJ program (developed at the National Institute of Health).[23–25] The calibration curve is depicted in Fig. 4. The LOD was calculated from the equation $\text{LOD} = \dfrac{3.3\text{SD}}{s}$, where SD is the standard deviation of the signal of blank samples in the absence of target protease and s is the slope obtained from the linear calibration curve.
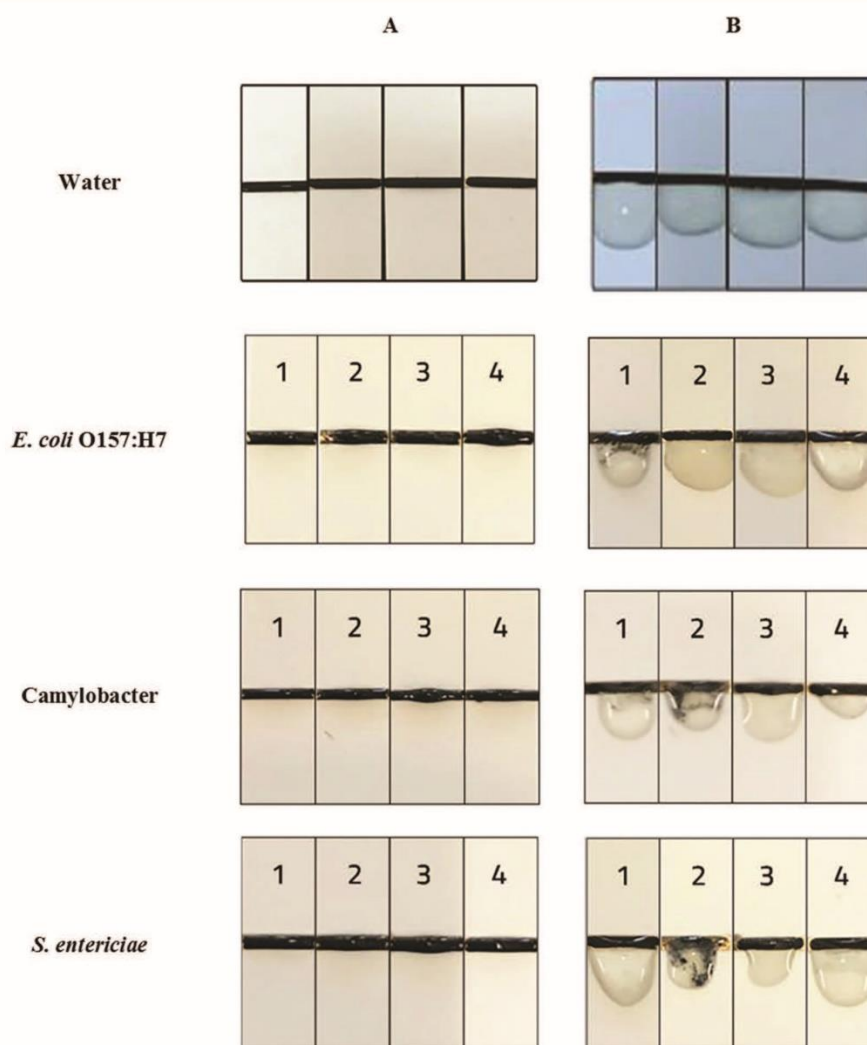

Fig. 5   Specificity of the *Legionella* colorimetric peptide nanoprobs biosensor. (A) Biosensor platform functionalized with black color peptide–NMPs conjugates. (Sensor 1) Ahx-YY-Ahx-Cys substrate covalently bound to MNPs. (Sensor 2) Ahx-WW-Ahx-Cys substrate covalently bound to MNPs, (Sensor 3) Ahx-FF-Ahx-Cys substrate covalently bound to MNPs, (Sensor 4) Ahx-LL-Ahx-Cys substrate covalently bound to MNPs. (B) *Legionella* nanoprobes (Sensor 1, Sensor 2, Sensor 3, and Sensor 4) under the effect of *E. coli* O157:H7, *Campylobacter*, and *S. entericia*.

Notably, sensor 1 (Ahx-YY-AHX-Cys) was able to detect three *Legionella* strains (*L. anisa* ATCC 35292, *L. micdadei* ATCC 33218, and *F. dumoffii* ATCC 33279) with high sensitivity (60 CFU mL^{-1}) and sensor 4 (Ahx-LL-AHX-Cys) detected both *L. pneumophilia* strains with comparable sensitivity (60 CFU mL^{-1}).

This difference in the *Legionella* strains proteolytic cleavage patterns is in agreement with that reported by Lei *et.al.*, where different *Legionella* strains had variable digestion activity on the tested synthetic peptide substrates. This may be correlated to the structural, functional, and genetic differences between the *Legionella* strains despite some observed similarities.[28]

This biosensor is simple in term of the detection reporter (showing positive readout visually), speedy in comparison with other detection methods that require minimum 2 h for PCR and few days for culturing (Table 1), sensitive with a lower limit of detection (LOD) of 60 CFU mL^{-1} for *L. anisa*, *L. micdadei*, and *F. dumoffii* using the Ahx-YY-Ahx-Cys nanoporobe, and *L. pneumophilia* using the Ahx-LL-Ahx-Cys nanoprobe (Table 4). The LOD was based on the visual evaluation of the lowest *Legionella* protease concentration incapable of restoring the biosensing platform's golden color following the cleavage of peptide–NMPs fragments. Visual detection was done side by side with the control so that any reader with normal visual capability could ascertain the LOD. A minimum of three random respondents confirmed the color change (black to yellow).

Moreover, this biosensor has the ability to specifically discriminate *Legionella* from other pathogens and so could be considered as a powerful field diagnostic tool (Fig. 5). A summary of some commonly applied assays for the detection of *Legionella* strains such as LOD, sample media (matrix), positivity rate, and assay time are presented in Table 1. To this end, the reported methods do not fully satisfy the optimal detection performance criteria for field applications and require further simplification for point-of-care testing.

3.5. Biosensor specificity and cross-reactivity

Sensor stability was validated by testing the water matrix.[31,32] As seen in Fig. 3, no reaction with water samples was detected. The sensor specificity was also evaluated using proteases extracted from another common organisms. In this study, *E. coli*, *Campylobacter*, and *S. enterica* culture supernatant proteases were used to check possible cross-reactivity (Fig. 5) against sensors prepared with each of the specific substrates. Interestingly, no significant cleavage was observed by the other bacterial culture supernatants, thus strengthening the sensors specificity. In contrast, the tested *Legionella* spp. showed significant color change. The sensor with the Ahx-WW-Ahx-Cys substrate was decolored slightly by the addition of *Campylobacter* and *Salmonella enterica* proteases, indicating that there is an insignificant cross-reactivity by these species. However, the other species have no effect on the sensors. Thus, the developed biosensors are a promising detection tool for *Legionella* spp. because of their low cost, specificity, and rapidity.

4. Conclusions

Herein, we have selected *Legionella* specific dipeptide fluorogenic substrates by FRET methods. The selected dipeptides were employed for the fabrication of the paper-based biosensors. The new calorimetric biosensors were able to detect the *Legionella* species, *Legionella anisa*, *Legionella micdadei*, and *Fluoribacter dumoffii* as low as 60 CFU mL^{-1} using the Ahx-YY-AHX-Cys nanoporobe, and detected *L. pneumophilia* using the Ahx-LL-AHX-Cys nanoprobe with comparable sensitivity within minutes and with high specificity. The cross-reactivity test confirms that there is no interference from the other closely related bacterial species on the sensor. This portable disposable platform confers several advantages for use onsite in hotels, hospitals, and other public areas for regular water monitoring. It allows fast and proper water treatment without the need for sample processing.

Conflicts of interest

All authors declare no conflict of interest.

Acknowledgements

References

1 A. Levcovich, T. Lazarovitch, J. Moran-Gilad, C. Peretz, E. Yakunin, L. Valinsky and M. Weinberger, *BMC Infect. Dis.*, 2016, **16**, 75.

2 M. Swanson and B. Hammer, *Annu. Rev. Microbiol.*, 2000, **54**, 567–613.

3 D. W. Fraser, T. R. Tsai, W. Orenstein, W. E. Parkin, H. J. Beecham, R. G. Sharrar, J. Harris, G. F. Mallison, S. M. Martin and J. E. McDade, *N. Engl. J. Med.*, 1977, **297**, 1189–1197.

4 E. I. Azhar, A. M. Ashshi, A. H. Asghar, S. Z. Bukhari, T. A. Zafar and H. A. Jukdar, *Prof. Med. J.*, 2010, **17**, 479–482.

5 L. H. Bajrai, E. I. Azhar, M. Yasir, P. Jardot, L. Barrassi, D. Raoult, B. La Scola and I. Pagnier, *Int. J. Syst. Evol. Microbiol.*, 2016, **66**, 4367–4371.

6 H. Tronel and P. Hartemann, *Lett. Appl. Microbiol.*, 2009, **48**, 653–656.

7 H. Whiley and M. Taylor, *Crit. Rev. Microbiol.*, 2016, **42**, 65–74.

8 M. Steinert, U. Hentschel and J. Hacker, *FEMS Microbiol. Rev.*, 2002, **26**, 149–162.

9 J. W. Winn, F. Glavin, D. Perl, J. L. Keller, T. Andres, T. Brown, C. Coffin, J. Sensecqua, L. Roman and J. Craighead, *Arch. Pathol. Lab. Med.*, 1978, **102**, 344–350.

96

10 M. R. Thompson, R. D. Miller and B. H. Iglewski, *Infect. Immun.*, 1981, **34**, 299–302.

11 L. A. Dreyfus and B. Iglewski, *Infect. Immun.*, 1986, **51**, 736–743.

12 J. Conlan, A. Baskerville and L. Ashworth, *Microbiology*, 1986, **132**, 1565–1574.

13 J. Rosenfeld, F. Kueppers, T. Newkirk, R. Tamada, J. Meissler Jr. and T. Eisenstein, *FEMS Microbiol. Lett.*, 1986, **37**, 51–58.

14 M. G. Keen and P. S. Hoffman, *Infect. Immun.*, 1989, **57**, 732–738.

15 D. J. Chen, G. W. Procop, S. Vogel, B. Yen-Lieberman and S. S. Richter, *J. Clin. Microbiol.*, 2015, **53**, 3474–3477.

16 A. Parr, E. A. Whitney and R. L. Berkelman, *J. Public Health Manage. Pract.*, 2015, **21**, E17.

17 A. Peci, A.-L. Winter and J. B. Gubbay, *Front. Public Health*, 2016, **4**, 175.

18 T. Avni, A. Bieber, H. Green, T. Steinmetz, L. Leibovici and M. Paul, *J. Clin. Microbiol.*, 2016, **54**, 401–411.

19 C. Moliner, C. Ginevra, S. Jarraud, C. Flaudrops, M. Bedotto, C. Couderc, J. Etienne and P.-E. Fournier, *J. Med. Microbiol.*, 2010, **59**, 273–284.

20 W. E. Kaman, I. Voskamp-Visser, D. M. de Jongh, H. P. Endtz, A. van Belkum, J. P. Hays and F. J. Bikker, *Anal. Biochem.*, 2013, **441**, 38–43.

21 W. E. Kaman, N. E. Arkoubi-El Arkoubi, S. Roffel, H. P. Endtz, A. van Belkum, F. J. Bikker and J. P. Hays, *PLoS One*, 2013, **8**, e81428.

22 S. Alhogail, G. A. R. Y. Suaifan and M. Zourob, *Biosens. Bioelectron.*, 2016, **86**, 1061–1066.

23 G. A. R. Y. Suaifan and M. Zourob, *Microchim. Acta*, 2019, **186**, 230.

24 G. A. R. Y. Suaifan, S. Alhogail and M. Zourob, *Biosens. Bioelectron.*, 2017, **92**, 702–708.

25 G. A. R. Y. Suaifan, S. Alhogail and M. Zourob, *Biosens. Bioelectron.*, 2017, **90**, 230–237.

26 S. Wignarajah, G. A. R. Y. Suaifan, S. Bizzarro, F. J. Bikker, W. E. Kaman and M. Zourob, *Anal. Chem.*, 2015, **87**, 12161–12168.

27 G. A. R. Y. Suaifan, C. Esseghaier, A. Ng and M. Zourob, *Analyst*, 2013, **138**, 3735–3739.

28 K. F. Lei and P. H. Leung, *Microelectron. Eng.*, 2012, **91**, 174–177.

29 S. Filion-Côté, P. J. Roche, A. M. Foudeh, M. Tabrizian and A. G. Kirk, *Rev. Sci. Instrum.*, 2014, **85**, 093107.

30 A. Brown, G. Garrity and R. Vickers, *Int. J. Syst. Evol. Microbiol.*, 1981, **31**, 111–115.

31 G. A. R. Y. Suaifan, S. Alhogail and M. Zourob, *Biosens. Bioelectron.*, 2017, **92**, 702–708.

32 G. A. R. Y. Suaifan, S. Alhogail and M. Zourob, *Biosens. Bioelectron.*, 2017, **90**, 230–237.

33 S. Bonetta, C. Pignata, S. Bonetta, L. Meucci, D. Giacosa, E. Marino, I. Gorrasi, G. Gilli and E. Carraro, *Chemosphere*, 2018, **210**, 550–556.

34 L. Deforges, P. Legrand, J. Tankovic, C. Brun-Buisson, P. Lang and C.-J. Soussy, *Clin. Infect. Dis.*, 1999, **29**, 953–954.

35 S. Jespersen, O. S. Søgaard, M. J. Fine and L. Østergaard, *Scand. J. Infect. Dis.*, 2009, **41**, 425–432.

97

[SAA 5]

On site visual detection of *Porphyromonas gingivalis* related periodontitis by using a magnetic-nanobead based assay for gingipains protease biomarkers

Sahar Alhogail, Ghadeer A. R. Y. Suaifan, Sergio Bizzarro, Wendy E. Kaman, Floris J. Bikker, Karina Weber, Dana Cialla-May, Jürgen Popp & Mohammed Zourob

	Sahar Alhogail	Mohammed Zourob
Konzeption des Forschungsansatzes	X	
Planung der Untersuchungen	X	X
Datenerhebung	X	
Datenanalyse und – interpretation	X	
Schreiben des Manuskripts	X	
Vorschlag Anrechnung Publikationsäquivalente	1,0	

ORIGINAL PAPER

CrossMark

On site visual detection of *Porphyromonas gingivalis* related periodontitis by using a magnetic-nanobead based assay for gingipains protease biomarkers

Sahar Alhogail[1] · Ghadeer A. R. Y. Suaifan[2] · Sergio Bizzarro[3] · Wendy E. Kaman[4,5] · Floris J. Bikker[4] · Karina Weber[6,7,8] · Dana Cialla-May[6,7,8] · Jürgen Popp[6,7,8] · Mohammed Zourob[9,10]

Abstract

Porphyromonas gingivalis (P. gingivalis) is a pathogen causing periodontitis. A rapid assay is described for the diagnosis of periodontal infections related to *P. gingivalis*. The method is making use of gingipains, a group of *P. gingivalis* specific proteases as a detection biomarker. Magnetic-nanobeads were labeled with gingipain-specific peptide substrates and immobilized on a gold biosensing platform via gold-thiol linkage. As a result of this, the color of the gold layer turns black. Upon cleavage of the immobilized substrates by gingipains, the magnetic-nanobeads-peptide fragments were attracted by a magnet so that the golden surface color becomes visible again. This assay is highly sensitive and specific. It is capable of detecting as little as 49 $CFU \cdot mL^{-1}$ of *P. gingivalis* within 30 s. Examination of periodontitis patients and healthy control saliva samples showed the potential of the assay. The simplicity and rapidity of the assay makes it an effective point-of-care device.

Keywords *Porphyromonas gingivalis* · Periodontal diseases · Colorimetric assay · Magnetic nanoparticles · Biosensor · Gingivitis · Diagnosis · Point of care

Introduction

Periodontal diseases are inflammatory diseases of microbial etiology affecting tooth supporting tissues [1]. Periodontal diseases comprise a wide range of inflammatory conditions that affect the supporting structures of the teeth such as the gingiva, bone and periodontal ligament, which may lead to tooth loss and contribute to systemic inflammation [2]. Gingivitis is characterized by the inflammation of the gums without loss of connective tissue attachment or bone. Gingivitis is a prerequisite for periodontitis, but does not necessarily lead to periodontitis [2] which affects approximately 7–15% of the adults in the Western world [3]. Periodontitis involves progressive loss of the alveolar bone around the

✉ Mohammed Zourob
mzourob@alfaisal.edu

1 Department of Medical Technology, College of Applied Medical Sciences, King Saud University, Riyadh, Saudi Arabia

2 Department of Pharmaceutical Sciences, Faculty of Pharmacy, The University of Jordan, Amman 11942, Jordan

3 Department of Periodontology, Academic Centre for Dentistry Amsterdam, University of Amsterdam and VU UniversityAmsterdam, Gustav Mahlerlaan 3004, 1081 LA Amsterdam, The Netherlands

4 Department of Oral Biochemistry, Academic Centre for Dentistry Amsterdam, University of Amsterdam and VU University Amsterdam, Gustav Mahlerlaan 3004, 1081 LA Amsterdam, The Netherlands

5 Department of Medical Microbiology and Infectious Diseases, Erasmus Medical Center, Wytemaweg 80, 3015 CE Rotterdam, The Netherlands

6 Institute of Physical Chemistry and Abbe Center of Photonics, Friedrich Schiller University Jena, Helmholtzweg 4, 07743 Jena, Germany

7 InfectoGnostics Research Campus Jena, Center for Applied Research, Philosophenweg 7, 07743 Jena, Germany

8 Leibniz Institute of Photonic Technology, Albert-Einstein-Straße 9, 07745 Jena, Germany

9 Faisal Specialist Hospital and Research Center, Zahrawi Street, Al Maather, Riyadh 12713, Saudi Arabia

10 Department of Chemistry, Alfaisal University, Al Zahrawi Street, Al Maather, Al Takhassusi Rd, Riyadh 11533, Saudi Arabia

Springer

teeth, and if left untreated, can lead to the loosening and subsequent loss of teeth. Epidemiological studies have linked periodontitis to other systemic illness such as atherosclerosis, cardiovascular diseases and rheumatoid arthritis [4, 5].

The microbiota of the human oral mucosa consists of a myriad bacterial species that normally exists in commensal harmony with the host [6]. In case of periodontitis a specific bacterial group, named as "red complex", including *Porphyromonas gingivalis*, *Tannerella forsythia* and *Treponema denticola,* show to be one of the factor that may be involved in the periodontaldisease [7]. Of these bacteria *P. gingivalis* participates intensively in the initiation and progression of this diseases.It invades teeth supporting tissues and evades the host defense mechanisms causing periodontitis [8]. It is armed with a plethora of virulence factors such as lipopolysaccharide (LPS), proteases such as gingipains, peptidyl arginine deiminase, hemagglutinins, fimbriae and other outer membrane proteins [3, 9, 10]. These virulence proteins facilitate *P. gingivalis* survival in the periodontal pocket, and contribute to the destruction of the teeth supportive tissues.

The current understanding of periodontitis pathogenesis suggests that gingipain proteases have an important role in the onset and progression of the disease [11]. This is because gingipains, which are trypsin-like cysteine proteases, account for at least 85% of the general proteolytic activity displayed by *P. gingivalis* [11, 12].

Up to date, many methods have been developed to diagnose periodontal diseases. Some of which include subjective observational indices, which are based on criteria such as bleeding on probing, measuring pocket depth, attachment loss and radiographic evidence of bone loss [7]. However, these methods are not capable to identify pathogens involved [11]. Alternative diagnostic methods available for identifying periodontal pathogens include culture-based, nucleic acid-based and antibody-based assays [13–16]. The advantages and disadvantages of these methods are summerized in Table 1.

More recently, research was being conducted on using the gingipains activity as biomarker for periodontitis. For example, Kaman et al. have developed highly specific fluorogenic protease substrates for the detection of *P. gingivalis* in situ. Applying the substates in a laboratory setting revealed that the substrates had a sensitivity up to 95% and a specificity up to 100% [11]. Alternatively, protease substrates were developed to detect human proteases which are involved in periodontitis, including cathepsin G and elastase. Althought the sensitivity and specificity of these protease substrates were low, the use of magnetic nanobeads to detect their proteolytic breakdown appeared promising [18].

In line with the latter study, the goal of this study was to develop a *P. gingivalis* specific test using magnetic nanoparticle technology. Ideally, such a test can serve as a low-cost

Table 1   Common *P. gingivalis* detection techniques

Detection method	Advantage	Disadvantage	Reference
Culture	Detecting and quantify oral cavities microbiota to create an antibiogram; has the ability to specifically distinguish between species	Time-consuming; laborious; has relatively low level of sensitivity	[14–16]
PCR	Reliable; able to detect low numbers of bacterial cells	Costly; laborious technique; bacterial DNA needs to be extracted and isolated from the sample; Crossreactivity with other (unknown) species may occur as the oral and subgingival microbiota is extensive and diverse	[14–16]
Antibody-based	High specificity; quantitative; applicable for multiplexing assays	Complex sample preparation; high instrument cost; requires trained personnel	[17]

and specific colorimetric chair-side assay which can aid the dentist to diagnose periodontal diseases.

Materials and methods

Magnetic-nanobeads with a mean diameter of 50 nm (according to manufacturer) and surface-coated with primary carboxylic groups was purchased from TurboBeads (Zurich, Switzerland). *N*-Hydroxysuccinimide (NHS), 1-(3-Dimethylaminopropyl)-3-Ethyl-Carbodiimide (EDC), greiner multiwell plate sealing film (A 5596) and pH test strips 0–14 pH, resolution: 1.0 pH unit (P4786) were purchased from Sigma-Aldrich (Dorset, UK). Magnetic sheets self adhesive A4 (Product Code: 15000SHEETA4) was purchased from Polarity Magnets Company (Wickford, UK). Peptide substrate (NH$_2$-Ahx-Arg-DLys-Ahx-Cys) was synthesised by Pepmic Co., Ltd. (Suzhou, China) with >98% purity. Brain Heart Infusion (BHI) medium and Trypticase Soy Agar (TSA) were purchased from Bio- Trading (Mijdrecht, The Netherlands).

100

Preparation of *P. gingivalis* culture supernatant

P. gingivalis culture supernatant containing secreted proteases was prepared as described previously [11]. In brief, *P. gingivalis* W50 was grown in BHI medium supplemented with 1 µg mL^{-1} hemin and 0.5 µg mL^{-1} menadione (Sigma, Zwijndrecht, The Netherlands) under anaerobic conditions at 37 °C for 72 h. The number of bacteria was determined by plating 10-fold serial dilutions on TSA plates. Following, plates were incubated at 37 °C under anaerobic conditions and enumerated after 3 days. The pure bacterial culture was serial diluted in culture broth (10^8, 10^7, 10^6, 10^5, 10^4, 10^3,10^2 and 10 CFU / mL), centrifuged for 10 min at 10,000 x *g* and filtered through 0.22 µm sterile filter (Millipore, Amsterdam, The Netherlands). Samples were used directly or stored at −20 °C for later use. The specificity testing was carried out by using culture supernatants from, 10^6 CFU / mL *Fusobacterium nucleatum* ATCC 33693 and 10^6 CFU / mL *T. forsythia* ATCC 43037. These bacterial strains were grown in 15 mL BHI medium under anaerobic conditions at 37 °C [11]. Next, the bacteria were pelleted by centrifugation for 10 min at 10,000 x *g* and the supernatant, containing secreted proteases, was sterilized by filtration through an 0.22 µm sterile filter (Millipore, Amsterdam, The Netherlands). Samples were stored at −20 °C for later use.

Saliva spiking

Commercially purchased human saliva (Lee Biosolutions Inc., St Louis, Missouri, USA) was spiked with *P. gingivalis*, *F. nucleatum* and *T. forsythia* pure culture supernatants (1:1 aliquots ratio). Saliva spiked with broth was used as a negative control to verify that the commercially purchased saliva does not react with the peptide labelled magnetic-nanobeads. The experiments were conducted in triplicate.

Preperation of peptide labeled magnetic-nanobeads

Magnetic-nanobeads suspension (15 mg/mL, Turbobeads, Zurich, Switzerland) was dispersed in an ultrasonic bath (Grant, XUBA3 model, Spain) for 5 min, then collected using a magnet separator and washed three times with the coupling saline buffer (10 mM potassium phosphate, 0.15 M sodium chloride, pH 5.5). Next, 1 mL of the peptide substrate (1.0 mg mL^{-1}, 'NH$_2$-Ahx-Arg-DLys-Ahx-Cys [11]', >98% %, Pepmic Co. Ltd., Suzhou, China), EDC (0.57 mg mL^{-}1, Sigma-Aldrich, UK) and NHS (12 µg/mL, Sigma-Aldrich, UK) were added to 30 mg /mL magnetic-nanobeads suspension in coupling buffer. The mixture was then shaken gently at room temperature for 24 h. Next, magnetic-nanobeads were collected using the magnet separator and the supernatant was discarded. The collected peptide labeled magnetic-nanobeads were then washed three times with washing buffer (10 mM Tris base, 0.15 M sodium chloride, 0.1% (*w/v*) bovine serum albumin, 1 mM ethylenediaminetetraacetic acid, 0.1% sodium azide, pH 7.5) and stored in washing buffer at 4 °C for later use [19, 20] (Fig. 1a).

Preparation of *P. gingivalis* assay platform

Greiner multiwell plate sealing film (A 5596, Sigma-Aldrich, UK) was coated with gold at the school of Engineering at Cranfield University, United Kingdom. The coated sheet was then chopped into small rectangular pieces (1 mm × 2 mm). Each piece was lodged over a solid support to bestow assay platform base (Fig. 1b). Afterwards, 20 µL of the peptide labeled magnetic-nanobeads suspension was dropped over the gold platform and set aside at room temperature till dryness (Fig. 1c). A gingipain-specific peptide substrate was covalently bound to the carboxylated magnetic-nanobeads by an amide linkage on one hand and to the gold platform via disulfide linkage handled by the cystine residue thiol on the other hand. During substrate synthesis, the lysine amino terminal was blocked to avoid incorrect coupling. The substrate sequence did not contain any carboxy terminal which may lead to polymerization. However, noncovalent adsorption of the labeled magnetic-nanobeads over the gold platform unavoidably occured, thus, a magnet (12.5 mm × 12.5 mm × 5 mm, Polarity Magnets Company, Wickford, UK) with a field strength of 3360 gauss and 573 gauss at 1 mm and 10 mm distance, respectively, was passed over the platform from a distance of 3–5 mm to remove the noncovalently adsorbed labeled magnetic-nanobeads. Later, a 2 mm diameter adhesive circle magnet (prepared by punching an adhesive magnet sheet purchased from Polarity Magnets Company, Wickford, UK) was fixed on the platform backside beneath (2–3 mm) the sensing platform as shown in Fig. 1d.

Measurement of gingipain proteolytic activity

In this colorimetric detection method, the probe was aimed to detect the proteolytic activity of gingipains as a diagnostic biomarker for periodontitis using a specific peptide substrate. *P. gingivalis* culture media was dropped over the functionalized (self-assembled monolayer (SAM)) platform triggering magnetic-nanobeads cleavage (Fig. 1e). The permanent magnet which was stacked at the back of the strip attracted the released magnetic-nanobeads prompting visual observation for a qualitative evaluation of the tested samples. Quantitative evaluation was tested by using different *P. gingivalis* concentrations with the following CFU values; 4.5×10^8 CFU/ mL, 4.5×10^7 CFU/ mL, 4.5×10^6 CFU/ mL, 4.5×10^5 CFU/ mL, 4.5×10^4 CFU/ mL, 4.5×10^3 CFU/ mL, 4.5×10^2 CFU/ mL, 45 CFU/ mL and 4.5 CFU/ mL.

Fig. 1 Schematic overview of *P. gingivalis* protease detection assay. **a** Preparation of peptide labeled magnetic-nanobeads; **b** Immobilization of peptide labeled magnetic nano-beads over assay gold platform; **c** Ready to use assay platform; **d** Back view of ready to use assay platform; **e** Detection assay
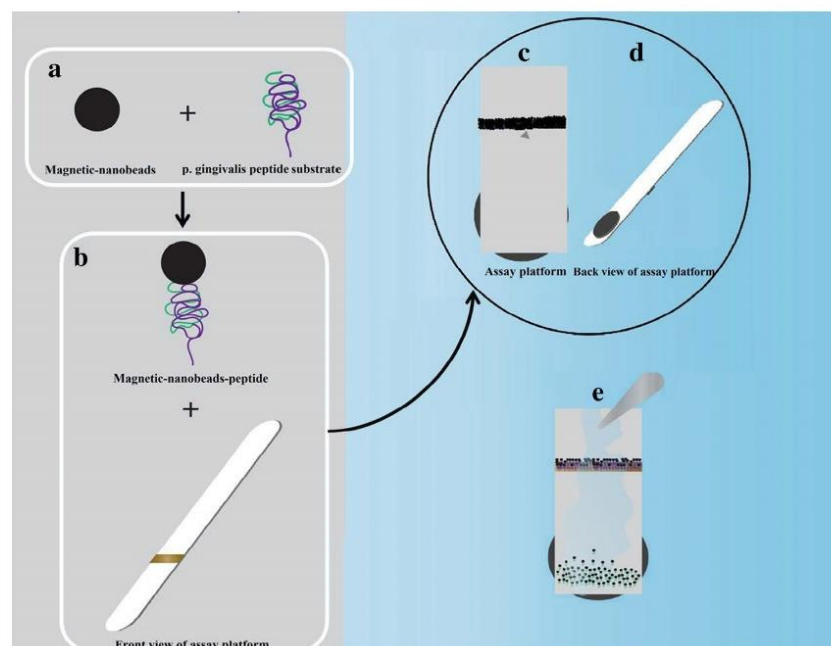
Moreover, a quantitative measurement of the disappearance of magnetic-nanobeads peptide fragment and appearance of golden color was achieved by analyzing the images using ImageJ (National Institute of Health) [21].

Testing of periodontitis patient's samples

To test the clinical application of the constructed method for *P. gingivalis* related infections detection in situ [22], gingival crevicular fluid attained from patients suffering from periodontitis were examined. This study was approved by the Institutional Ethical Board of the Academic Medical Center of Amsterdam, The Netherlands, and informed consent was obtained from all donors. All patients' samples showed positive periodontitis results by standard qPCR method performed at the Department of Periodontology, VU University Amsterdam. Patients' samples were examined using the designed assay. The experiments were conducted in triplicate.

Results and discussion

P. gingivalis is an invasive and evasive opportunistic oral pathogen [3, 23]. It invades periodontal tissues and evades the host defense mechanisms. It utilizes a panel of virulence factors such as gingipain proteases which play a critical role in periodontal inflammation [6]. Therefore, the *P. gingivalis* specific gingipains are considered biomarkers for periodontal diseases [24]. At present, nanotechnology

bioapplication in diagnostic analytical techniques, in particular those capable of identifying proteases activity, as a disease biomarker were very attractive due to their high specificity and sensitivity [22, 25–32]. The ultimate goal of this study was to develop a low-cost diagnostic tool for *P. gingivalis* related periodontitis measuring gingipain protease activity.

Detection assay using *P. gingivalis* protease culture supernatant

The proteolytic activity of *P. gingivalis* culture supernatant, and thus gingipain presence, was detected by dripping culture supernatant over the functionalized assay platform (Fig. 1). Cleavage of the specific peptide bond by the proteases leads to dissociation of the magnetic-nanobeads-peptide fragments, away from the detection platform surface due to the subsequent attraction by an external magnet. As a result, the golden color of the detecting platform is restored and can be observed by the nakedeye (Fig. 1d). Kaman et al., reported that peptide substrates containing single D-amino acids have a high specificity (up to 100%). In addition, the effect of spacer Ahx moiety length on the detection sensitivity was evaluated in our previous work [33]. Significant improvement in sensitivity was observed when the spacer length on each termini of the substrate sequence was from 4 to 8 carbons. Thus, the current study substrate was designed to have a spacer length on each terminus within the optimum length required, *i.e.* 6

102

Fig. 2 Colorimetric *P. gingivalis* protease sensor probe under the effect of varying concentrations of *P. gingivalis* culture supernatant. **a** Before; and **b** after application of the samples
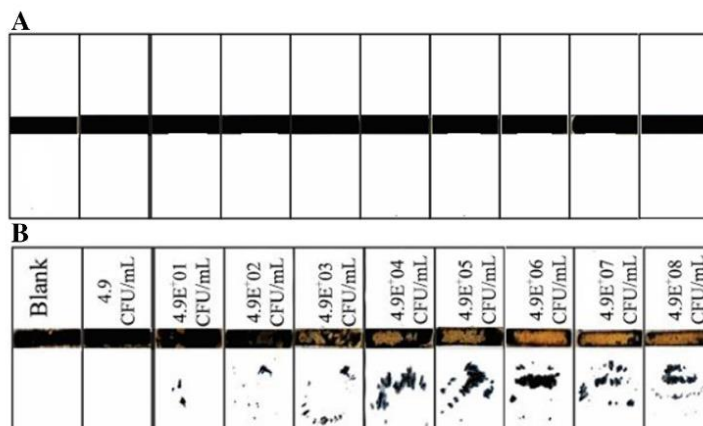
carbon via hexyl moiety. The amount of the peptide substrate required for peptide-magnetic-nanoparticles conjugation step was optimized in our previous work to achieve optimal monolayer performance and stability [26].

To test the sensitivity of the assay, serial diluted *P. gingivalis* culture was prepared and spotted onto the assay platform. Figures 1b and 2a showed the results before and after sample application, respectively. It was observed that there is a gradual increase in the visible golden color area which is proportional to the *P. gingivalis* concentration. This is related to the activity of the secreted proteases which results in the cleavage of the magnetic-nanobeads-peptide fragments. The designed technique

showed a limit of detection (LOD) of 49 CFU/ mL within 30 s. This technique exhibited higher sensitivity and shorter response time in comparison to the work with the FRET-based assay [11]. This is mainly due to the amplification of the signal; using the magnetic-nanobeads in the assay rather than using the organic fluorescent dyes. Currently, other researchers had pointed up an immunochromatographic device with monoclonal antibodies against *P. gingivalis* outer membrane protein (OMP) 40 (HBP35) for semi-quantification of *P. gingivalis* in subgingival plaque [34]. Another research group demonstrated a portable electrochemical DNA sensor linked to PCR. A comparison of assays lower limit of

Table 2 New trends for the detection of *P. gingivalis* related periodontitis

Method	Sample	Detection limit (CFU mL^{-1})	Advantages	Disadvantages	Year Ref
Magnetic-nanobeads protease based assay	Saliva	49	Feasible; highly sensitive; high specificity; applicable for "on-site" detection; visual read out of the results; benefit clinical diagnosis of periodontal disease	Requires minimal detection platform manipulation	Current Work 2018
Immunochromatography based device DK13-PG-001	GCF Saliva	10^4	Requires minimal sample manipulation; easy-to-read results; feasible for chair-side detection; benefit clinical diagnosis of periodontal disease	Needs trained personnel and instrument to read out the result	[9, 14, 34]
Electrochemical DNA sensor linked with PCR	GCF Saliva	10^4	Measurement principle is simple; easy and can be applied to other targets; Suitable for primary screening of periodontal bacteria.	Need trained personnel and instrument to read out the result	[35]
FRET	GCF Saliva	10^5	Easy to perform; does not require enzyme pre-enrichment and purification steps; specific; offers the potential for development into a chairside test; bacteria as a source of the enzymes need not necessarily be viable as long as there is bacteria-derived enzyme activity	Requires fluorimeter to read out the results	[11]

Fig. 3 Graph shows the quantitative data using ImageJ software in buffer and in saliva for various concentrations of bacteria; Cleaved area is defined as the area of the restored golden platform color after sample application; Total area is defined as the total area of the black color platform before application
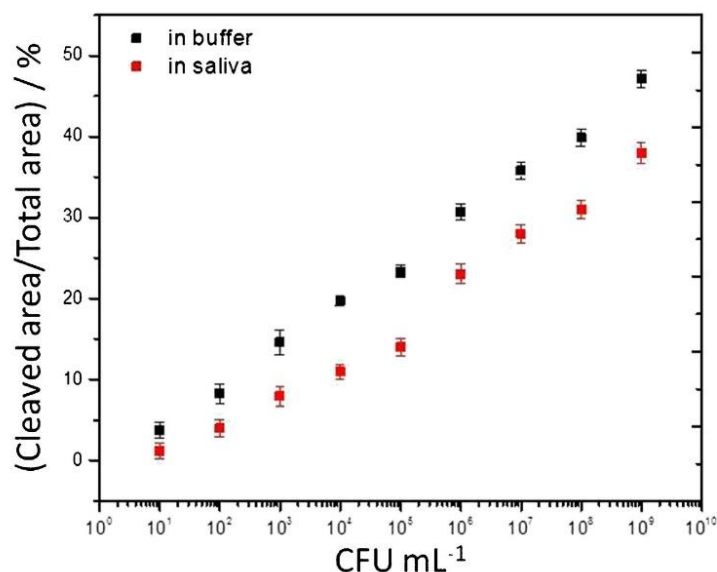
detection (LOD), advantages and disadvantages are summarized in Table 2.

Spiked saliva testing

The feasibility of the current assay in *P. gingivalis*-related periodontitis as a diagnostic device was examined by using spiked saliva as an oral non-invasive diagnostic fluid. Varying *P. gingivalis* concentrations were spiked into the purchased saliva in a 1:1 aliquots ratio and applied to the functionalized biosensor. Figure 3 shows the quantitative data (detection responses) for various bacterial concentrations in buffer and saliva. Clearly, a gradual increase in the visible golden area with the increase of bacterial concentration was observed (Fig. 3). Unspiked saliva samples were used as a negative control and showed no cleavage of the magnetic-nanobeads-peptide fragments, no disruption of the SAM layer and no significant change in the platform color. In principle, the designed assay appears suitable for the analysis of patients' specimens at the site of collection. This enables the dental practitioner to perform an "on-site" test, to identify the periodontal pathogen *P. gingivalis* and to execute a proper treatment protocol.

Patient sample testing

To evaluate the performance characteristics of the designed assay in a clinical setting, the technique was tested with *P. gingivalis* patient CGF samples. Accordingly, 3 specimens from patients diagnosed with *P. gingivalis*-related periodontitis were tested. The presence of *P. gingivalis* was confirmed by positive cultures and qPCR as described previously [11].

Notably, the platform golden color was restored and can be observed by bare eye (Fig. 4). Furthermore, the assay results were positive and comparable with culturing technique.
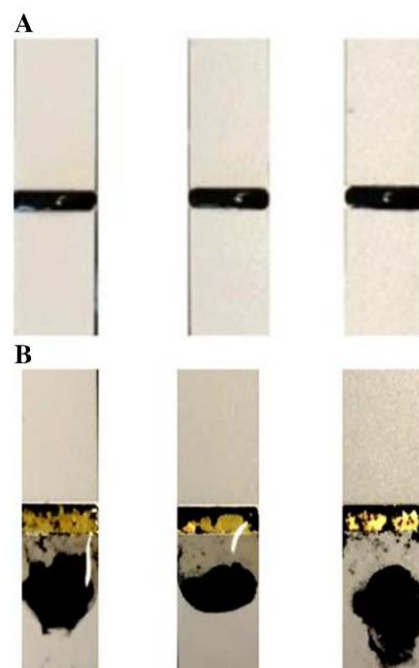

Fig. 4 Example of the colorimetric *P. gingivalis* protease biosensor with patient material; **a** Before adding the periodontitis patient sample; and **b** after addition of saliva from *P. gingivalis* related periodontis patients.
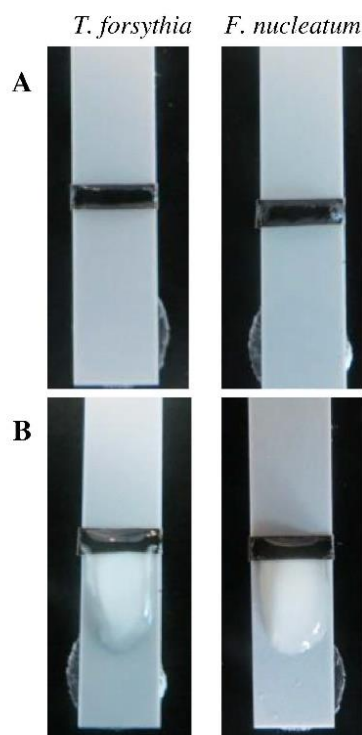
104

Fig. 5 Cross-reactivity study of the *P. gingivalis* protease biosensor with *T. forsythia* and *F. nucleatum* culture supernatants **a** Before application of the culture; and **b** after application of the culture

Cross-reactivity studies

Likewise, the specificity of the detection assay in the presence of other saliva pathogens proteases such as *F. nucleatum* (10^6 CFU / mL) and *T. forsythia* (10^6 CFU / mL) was assessed. The assay showed no disruption of the detecting platform and no appearance of the gold color (Fig. 5). These results confirm that the current assay is specific towards the detection of *P. gingivalis* and has no cross-reactivity with the other oral pathogens tested in vitro.

Conclusions

P. gingivalis proteases showed significant interest being one of the promising biomarkers associated with periodontal diseases. In this article, a novel and low-cost analytical assay capable of detecting *P. gingivalis* proteases were pointed up, using magnetic nanobeads covalently linked with a gingipain specific peptide substrate. The sensor was tested with serial diluted *P. gingivalis* culture, saliva spiked samples and patient material. The detection limit of the assay was 49 CFU/mL and the presence of *P. gingivalis* was detected within 30 s.

Noteworthy, *P. gingivalis* protease detection was based on the appearance of the gold platform color which can be observed visually. This assay can be performed "on site" by non-skilled personnel without the requirement of expensive instrumentation. However, future work must be conducted to proof method selectivity and precision by using independent methods such as HPLC to measure the substrate concentration before and after gingipain application. In addition certified reference material should be used as assay control.

Compliance with ethical standards

The author(s) declare that they have no competing interests.

References

1. Armitage GC, Svanberg GK, Löe H (1977) Microscopic evaluation of clinical measurements of connective tissue attachment levels. J Clin Periodontol 4:173–190
2. Kretschmar S, Yin L, Roberts F, London R, Flemmig TT, Arushanov D, Kaiyala K, Chung WO (2012) Protease inhibitor levels in periodontal health and disease. J Periodontal Res 47: 228–235
3. Bostanci N, Belibasakis GN (2012) Porphyromonas gingivalis: an invasive and evasive opportunistic oral pathogen. Fems Microbiol Lett 333:1–9
4. Zhang B, Elmabsout AA, Khalaf H, Basic VT, Jayaprakash K, Kruse R, Bengtsson T, Sirsjö A (2013) The periodontal pathogen Porphyromonas gingivalis changes the gene expression in vascular smooth muscle cells involving the TGFbeta/Notch signalling pathway and increased cell proliferation. BMC Genomics 14:770. https://doi.org/10.1186/1471-2164-14-770
5. Ogrendik M (2013) Rheumatoid arthritis is an autoimmune disease caused by periodontal pathogens. Int J Gen Med 6:383–386. https://doi.org/10.2147/IJGM.S45929
6. Mysak J, Podzimek S, Sommerova P, Lyuya Mi Y, Bartova J, Janatova T, Prochazkova J, Duskova J (2014) Porphyromonas gingivalis: major periodontopathic pathogen overview. J Immunol Res 2014:476068. https://doi.org/10.1155/2014/476068
7. Highfied J (2009) Diagnosis and classification of periodontal disease. Aust Dent J 54(supplement s1):S11–S26 View at Publisher View at Google Scholar
8. O'Brien-Simpson NM, Veith PD, Dashper SG, Reynolds EC (2004) Antigens of bacteria associated with periodontitis. Periodontol 2000 35:101–134. https://doi.org/10.1111/j.0906-6713.2004.003559.x
9. Lamont RJ, Jenkinson HF (1998) Life below the gum line: pathogenic mechanisms of Porphyromonas gingivalis. Microbiol Mol Biol Rev 62:1244–1263
10. Robertson PB, Lantz M, Marucha PT, Kornman KS, Trummel CL, Holt SC (1982) Collagenolytic activity associated with Bacteroides species and Actinobacillus actinomycetemcomitans. J Periodontal Res 17:275–283
11. Kaman WE, Galassi F, de Soet JJ, Bizzarro S, Loos BG, Veerman EC, van Belkum A, Hays JP, Bikker FJ (2012) Highly specific protease-based approach for detection of porphyromonas gingivalis in diagnosis of periodontitis. J Clin Microbiol 50:104–112. https://doi.org/10.1128/JCM.05313-11
12. Kah YH, Keang PS, Kok GC (2016) *Porphyromonas gingivalis*: an overview of Periodontopathic pathogen below the gum line. Front Microbiol 7:53

13. Galassi F, Kaman WE, Anssar Moin D, van der Horst J, Wismeijer D, Crielaard W, Laine ML, Veerman ECI, Bikker FJ, Loos BG (2012) Comparing culture, real-time PCR and fluorescence resonance energy transfer technology for detection of Porphyromonas gingivalis in patients with or without peri-implant infections. J Periodontal Res 47:616–625

14. Choe Y, Leonetti F, Greenbaum DC, Lecaille F, Bogyo M, Brömme D, Ellman JA, Craik CS (2006) Substrate profiling of cysteine proteases using a combinatorial peptide library identifies functionally unique specificities. J Biol Chem 281:12824–12832

15. Kuboniwa M, Sakanaka A, Hashino E, Bamba T, Fukusaki E, Amano A (2016) Prediction of periodontal inflammation via metabolic profiling of saliva. J Dent Res 95:1381–1386

16. Jervøe-Storm PM, AlAhdab H, Koltzscher M, Fimmers R, Jepsen S (2010) Quantification of periodontal pathogens by paper point sampling from the coronal and apical aspect of periodontal lesions by real-time PCR. Clin Oral Investig 14:533–541

17. O'Brien-Simpson NM, Burgess K, Lenzo JC, Brammar GC, Darby IB, Reynolds EC (2017) Rapid chair-side test for detection of Porphyromonas gingivalis. J Dent Res 96(6):618–625

18. Wignarajah S, Suaifan G, Bikker F, Kaman W, Zourob M (2015) Colorimetric assay for the detection of typical biomarkers for periodontitis using a magnetic nanoparticle biosensor. Anal Chem 87: 12161–12168

19. Zourob M (2017) Biosensor using magnetic particles for pathogen detection. Google patents 20170038373

20. Zourob M, Suaifan G (2017) Paper based magnetic nanoparticles biosensor for rapid prostate specific antigen detection. WSEAS Trans Biol Biomed 14:2224–2902

21. Rajwa B, Mcnally HA, Varadharajan P, Sturgis J, Robinson JP (2004) AFM/CLSM data visualization and comparison using an open-source toolkit. Microsc Res Tech 64(2):176–184

22. Suaifan G, Esseghaier C, Ng A, Zourob M (2012) Wash-less and highly sensitive assay for prostate specific antigen detection. Analyst 137:5614–5619

23. Bostanci N, Belibasakis GN (2012) Porphyromonas gingivalis: an invasive and evasive opportunistic oral pathogen. FEMS Microbiol Lett 333(1):1–9

24. Watanabe H, Hattori S, Katsuda S, Nakanishi I, Nagai Y (1990) Human neutrophil elastase: degradation of basement membrane components and immunolocalization in the tissue. J Biochem 108:753–759

25. Esseghaier C, Suaifan G, Ng A, Zourob M (2014) One-step assay for optical prostate specific antigen detection using magnetically engineered responsive thin film. J Biomed Nanotechnol 10:1123–1129

26. Suaifan, G (2017) Colorimetric biosensors for bacterial detection. In: Ahmed MU, Zourob M, Tamiya E (ed) Food biosensors. The Royal Society of Chemistry, pp 182–202

27. Suaifan G, Alhogail S, Zourob M (2017) Rapid and low-cost biosensor for the detection of Staphylococcus aureus. Biosens Bioelectron 90:230–237

28. Suaifan G, Jaber D, Shehadeh MB, Zourob M (2017) Proteinases as biomarkers in breast cancer prognosis and diagnosis. Mini Rev Med Chem 17(7):583–592

29. Alhogail S, Suaifan G, Zourob M (2016) Rapid colorimetric sensing platform for the detection of Listeria monocytogenes foodborne pathogen. Biosens Bioelectron 86:1061–1066

30. Suaifan G, Alhogail S, Zourob M (2016) Paper-based magnetic nanoparticle-peptide probe for rapid and quantitative colorimetric detection of Escherichia coli O157:H7. Biosens Bioelectron 92: 702–708

31. Suaifan G, Esseghaier C, Ng A, Zourob M (2013) Ultra-rapid colorimetric assay for protease detection using magnetic nanoparticle-based biosensors. Analyst 138:3735–3739

32. Suaifan G, Shehadeh M, Al-Ijel H, Ng A, Zourob M (2013) Recent progress in prostate-specific antigen and HIV proteases detection. Expert Rev Mol Diagn 13:707–718

33. Esseghaier C, Ng AF, Zourob M (2013) A novel and rapid assay for HIV-1 protease detection using magnetic bead mediation. Biosens Bioelectron 41:335–341

34. Imamura K, Takayama S, Saito A, Inoue E, Nakayama Y, Ogata Y, Shirakawa S, Nagano T, Gomi K, Morozumi T, Akiishi K, Watanabe K, Yoshie H (2015) Evaluation of a novel immunochromatographic device for rapid and accurate clinical detection of Porphyromonas gingivalis in subgingival plaque. J Microbiol Methods 117:4–10

35. Yamanaka K, Sekine S, Uenoyama T, Wada M, Ikeuchi T, Saito M, Yamaguchi Y, Tamiya E (2014) Quantitative detection for Porphyromonas gingivalis in tooth pocket and saliva by portable electrochemical DNA sensor linked with PCR. Electroanalysis 26(12):2686–2692

[SAA 6]

Rapid Colorimetric Detection of *Pseudomonas aeruginosa* in Clinical Isolates Using a Magnetic Nanoparticle Biosensor

Sahar Alhogail, Ghadeer A.R.Y. Suaifan, Floris J. Bikker, Wendy E. Kaman, Karina Weber, Dana Cialla-May, Jürgen Popp, and Mohammed M. Zourob.

	Sahar Alhogail	**Mohammed Zourob**
Konzeption des Forschungsansatzes	X	
Planung der Untersuchungen	X	X
Datenerhebung	X	
Datenanalyse und – interpretation	X	
Schreiben des Manuskripts	X	
Vorschlag Anrechnung Publikationsäquivalente	1,0	

ACS OMEGA

Article

http://pubs.acs.org/journal/acsodf

Rapid Colorimetric Detection of *Pseudomonas aeruginosa* in Clinical Isolates Using a Magnetic Nanoparticle Biosensor

Sahar Alhogail,[†,‡] Ghadeer A.R.Y. Suaifan,[§] Floris J. Bikker,[∥] Wendy E. Kaman,[∥,⊥] Karina Weber,[#,¶,▽] Dana Cialla-May,[#,¶,▽] Jürgen Popp,[#,¶,▽] and Mohammed M. Zourob*[,‡,○]

[†]Department of Clinical Laboratory Science, King Saud University, Ad Diriyah District, 11433 Riyadh, Kingdom of Saudi Arabia

[‡]Department of Chemistry, Alfaisal University, Al Zahrawi Street, Al Maather, Al Takhassusi Road, 11533 Riyadh, Saudi Arabia

[§]Department of Pharmaceutical Sciences, Faculty of Pharmacy, The University of Jordan, 11942 Amman, Jordan

[∥]Department of Oral Biochemistry, Academic Centre for Dentistry Amsterdam, University of Amsterdam and VU University Amsterdam, Gustav Mahlerlaan 3004, 1081 LA Amsterdam, The Netherlands

[⊥]Department of Medical Microbiology and Infectious Diseases, Erasmus Medical Center, Wytemaweg 80, 3015 CE Rotterdam, The Netherlands

[#]Institute of Physical Chemistry and Abbe Center of Photonics, Friedrich Schiller University Jena, Helmholtzweg 4, 07743 Jena, Germany

[¶]InfectoGnostics Research Campus Jena, Center for Applied Research, Philosophenweg 7, 07743 Jena, Germany

[▽]Leibniz Institute of Photonic Technology, Albert-Einstein-Straße 9, 07745 Jena, Germany

[○]King Faisal Specialist Hospital and Research Center, Zahrawi Street, Al Maather, Riyadh 12713, Saudi Arabia

ABSTRACT: A rapid, sensitive, and specific colorimetric biosensor based on the use of magnetic nanoparticles (MNPs) was designed for the detection of *Pseudomonas aeruginosa* in clinical samples. The biosensing platform was based on the measurement of *P. aeruginosa* proteolytic activity using a specific protease substrate. At the N-terminus, this substrate was covalently bound to MNPs and was linked to a gold sensor surface via cystine at the C-terminus of the substrates. The golden sensor appears black to naked eyes because of the coverage of the MNPs. However, upon proteolysis, the cleaved peptide−MNP moieties will be attracted by an external magnet, revealing the golden color of the sensor surface, which can be observed by the naked eye. In vitro, the biosensor was able to detect specifically and quantitatively the presence of *P. aeruginosa* with a detection limit of 10^2 cfu/mL in less than 1 min. The colorimetric biosensor was used to test its ability to detect in situ *P. aeruginosa* in clinical isolates from patients. This biochip is anticipated to be useful as a rapid point-of-care device for the diagnosis of *P. aeruginosa*-related infections.
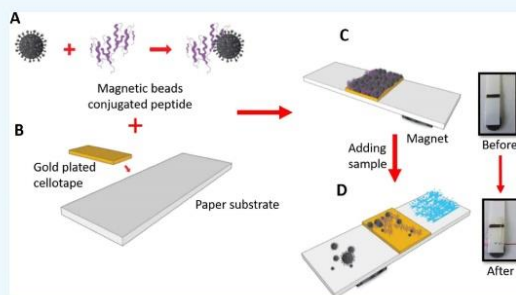
1. INTRODUCTION

Pseudomonas aeruginosa is an opportunistic pathogen[1] which is involved in various nosocomial diseases such as respiratory tract infections,[2,3] urinary tract infections,[4] wound infections,[5] and bacteremia.[6] *P. aeruginosa* was identified as the second infectious pathogen isolated from patients with hospital-associated pneumonia (HAP).[7] Therefore, rapid and proper diagnosis is essential to enable timely treatment in order to reduce the risk of mortality. Accordingly, the American Thoracic Society (ATS) and the Infectious Diseases Society of America (IDSA) issued guidelines for the management of HAP and emphasized on the importance of "quantitative cultures" for specific HAP diagnosis without deleterious consequences.[8]

Conventional diagnostic methods are based on culturing and require at least 24 h to report the results, reducing the chance of appropriate and successful treatment.[3,8] Alternatively, rapid quantitative detection methods based on real-time polymerase chain reaction (PCR)[9−11] and enzyme-linked immunosorbent assays[12] were developed to detect *P. aeruginosa* in HAP clinical specimens. In these methods, results were obtained within a few hours with high specificity and sensitivity. However, these methods are costly and laborious and require handling by highly skilled personnel. Bacterial enzymes, such as proteases, are ideally suited as biomarkers for quick and sensitive

108

identification of micro-organisms in clinical samples.[13] Many of these enzymes are released into the surrounding microenvironment and are accessible for detection based on sensitive fluorogenic and/or colorimetric substrates.[14−17] Recently, a specific peptide substrate was identified to detect the activity of the *P. aeruginosa* specific LasA protease, of which the expression appears to be mediated by the Las and Rhl quorum sensing (QS) systems.[13,18,19] In this study, this *P. aeruginosa* specific peptide substrate was coupled to magnetic nanoparticles (MNPs) to be utilized in a rapid and specific colorimetric biosensor.

2. RESULTS AND DISCUSSION

P. aeruginosa is considered the second most prevalent nosocomial bacterium in hospital environments and can contaminate medical equipment.[1] Its infection is challenging due to its resistance to a large number of antibiotics.[20] Therefore, there is a high-demand for the development of rapid and early detection method in clinical samples to guide therapeutic treatment.

Kaman et al.[13] designed and evaluated a fluorogenic substrate as a potential tool to detect the virulence of *P. aeruginosa*. This *P. aeruginosa* specific protease substrate was utilized in the development of the paper-based colorimetric assay. In brief, hexanoic acid (Ahx) linkers were attached to both terminals of the peptide sequence (Gly-Gly-Gly) to enhance the protease accessibility to the peptide substrate near the sensor surface. Then, a cysteine amino acid was linked to the C-terminal, allowing the gold−thiol interaction and resulting in the formation of a self-assembled monolayer (SAM) of *P. aeruginosa* peptide−MNPs onto the gold sensor surface. The N-terminal of the peptide was attached to the MNPs.

2.1. Testing the *P. aeruginosa* Protease Biosensor.
Initially, the fabricated sensor was examined to detect the proteolytic activity of *P. aeruginosa* protease by incubating 10^7 cfu/mL over the functionalized gold sensor surface. Upon proteolysis, the peptide segment−MNP moiety was released and collected by a circle shaped magnet placed at the back of the sensor strip. This results in revealing the golden color of the sensor surface, which is visible to the naked eye. Then, this biosensing method was applied for quantitative detection of *P. aeruginosa*. Accordingly, different concentrations of *P. aeruginosa* 4.5×10^7, 4.5×10^6, 4.5×10^5, 4.5×10^4, 4.5×10^3, 4.5×10^2, and 4.5×10 cfu/mL were added over the functionalized gold sensor. Results in Figures 1 and 2 show the gradual increase in the visible bare gold area with increasing bacteria concentration. This is explained by the ability of the higher protease enzyme concentration to dissociate the
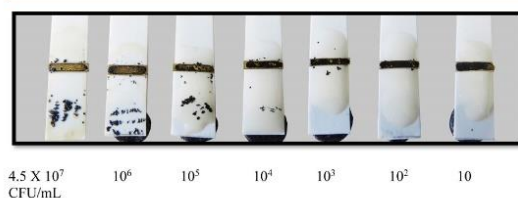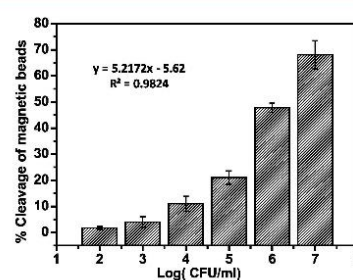

Figure 2. Dose response of the sensor under the effect of various concentrations of *P. aeruginosa*.

peptide−MNP moiety faster than the lower concentrations. Moreover, to validate the colorimetric biosensor, a negative blank [brain heart infusion (BHI) broth only] with no protease was incubated with the sensor and showed no cleavage (Figure 2). Results confirmed the ability of the fabricated biosensor to detect *P. aeruginosa*.

The developed colorimetric biosensor exhibited a limit of detection of 10^2 cfu/mL within one min time. This detection limit was determined by identifying the lowest protease concentration, capable of cleaving the covalently attached peptide black MNP moiety, which in turn revealed the sensors' golden surface area. The negative blank (BHI broth only) showed no change in colors, as the sensor demonstrated no disruption of the SAM layer (Figure 1).

This colorimetric detection method provided better detection limit in a shorter time than the previously reported fluorescent dye including the lipid vesicle method, which was reported by Thet et al.[21] Although, their method managed to correctly discriminate 40 clinical isolates of two pathogens, *P. aeruginosa* and *Staphylococcus aureus* (*S. aureus*), their method was used only for qualitative measurements. Another method developed to provide quantitative detection of *P. aeruginosa* was reported by Tang et al.[22] This method is based on the use of magnetic enrichment and magnetic separation methodology and managed to detect as low as 10 cfu/mL. Dong et al.[1] managed to develop a ten times more potent polymerase spiral reaction method with a lower detection limit of 2.3 pg/μL[1] within 60 min. Tang et al.[23] shortened the procedure time for DNA extraction to detection and retained a lower detection limit of 10 cfu/mL based on magnetic enrichment and nested PCR. All above mentioned methods are complex and require the use of centralized labs, instrumentation, and trained personnel. In addition, the PCR techniques are not suitable for bed-side routine testing, unlike the colorimetric assay described in this study which is approved to be cheap, simple, rapid, and sensitive. Furthermore, it does not require expensive equipment and trained personnel. It is to be mentioned that sensor stability in addition to the amount of a substrate−MNP composite was optimized in our previous work to achieve optimal monolayer performance.[16,17,24−26]

2.2. Specificity of the Sensor.
The biosensor specificity was examined in the presence of two other pathogenic microbes: *Listeria monocytogenes* (*L. monocytogenes*), and *S. aureus*. Figure 3 shows the results of the *P. aeruginosa* sensors with *L. monocytogenes* and *S. aureus*, respectively. The sensor showed no disruption of the SAM layer and no significant change in the sensor surface golden color upon incubation with
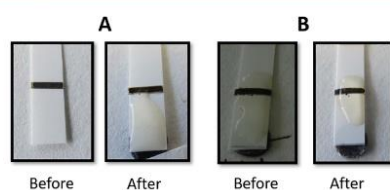

4.5 × 10⁷ CFU/mL   10⁶   10⁵   10⁴   10³   10²   10

Figure 1. Colorimetric *P. aeruginosa* proteases sensor probe tested with different concentrations of *P. aeruginosa* ranging from 4.5×10^7 to 4.5×10 cfu/mL.

Figure 3. *P. aeruginosa* sensor specificity (A) *L. monocytogenes* before and after application and (B) *S. aureus* before and after application.

L. monocytogenes and *S. aureus*, showing sufficient specificity to detect *P. aeruginosa*.

2.3. Detection of *P. aeruginosa* in Clinical Isolates.
The clinical applicability of the developed biosensors was tested using 20 *P. aeruginosa* clinical isolates (among which sputum, ear, and wound). These samples were previously analyzed by conventional culture and PCR methods at King Faisal Specialist Hospital microbiology laboratory. These samples were incubated with the fabricated biosensor and all showed positive results, with a clear cleavage of the peptide–MNPs moiety, with a consequent appearance of the sensor golden surface color (Figure 4). Notably, the differences in cleavage intensity between tested samples were attributed to the difference in the number of colonies of *P. aeruginosa*. A negative control proved no cleavage of the peptide–MNPs moiety without any disruption of the SAM layer. The experiments were conducted in triplicate.

3. CONCLUSIONS
This study demonstrated the ability of the designed colorimetric biosensor to detect *P. aeruginosa* protease in clinical samples. The assay was simple, rapid, sensitive, and specific and does not require any labeling or amplification steps. Furthermore, it does not require sample pretreatment or preconcentration and so can be applicable for onsite use by clinicians. This low-cost colorimetric biosensor was based on the use of specific substrate–MNPs, which were covalently attached to the gold sensor surface. This biosensing configuration is amenable for a qualitative and semi quantitative detection of *P. aeruginosa* proteases. The limit of detection was as low as 10^2 cfu/mL within one min. In conclusion, this biosensor presented a valuable onsite diagnostic tool to improve the control of potential risk infections caused by *P. aeruginosa*.

4. MATERIALS AND METHODS
4.1. Materials and Reagents.
Carboxyl-terminated beads (50 nm diameter), *N*-hydroxysuccinimide (NHS), 1-(3-dimethylaminopropyl)-3-ethyl-carbodiimide (EDC), and the plastic pH indicator strip were purchased from Sigma-Aldrich (Dorset, UK). Self-adhesive magnet sheets were purchased from Polarity Magnets Company (Wickford, Essex, UK). The *P. aeruginosa* peptide substrate NH2-Ahx-Gly-Gly-Gly-Ahx-Cys was synthesized by Pepmic Co. Ltd (Suzhou, China). BHI broth and agar were purchased from SDA, Oxoid Ltd (Basingstoke, UK). Sterile filters (0.22 μm) were obtained from Millipore (Watford, UK). The wash/storage buffer (10 mM Tris base, 150 mM sodium chloride, 0.1% (w/v) bovine serum albumin, 1 mM ethylenediaminetetraacetic acid, 0.1% sodium azide, pH 7.5) and the coupling buffer (10 mM potassium phosphate, 0.15 M sodium chloride, pH 5.5) were prepared from chemicals of analytical grade.

4.2. Bacteria Culture and Protease Preparation.
P. aeruginosa (ATCC 15692), *S. aureus* (ATCC 25923), and *L. monocytogenes* (ATCC 19115) were individually cultured on BHI agar plates for 24 h at 37 °C. Subsequently, a single colony from each bacterium was grown in 5 mL BHI medium and incubated at 37 °C for 16 h to provide the primary bacterial culture (PBC) stock. Then, each bacterial concentration PBC was pelted by centrifugation at 3000*g* for 10 min, and the culture supernatant was filtered to obtain *P. aeruginosa* crude protease solution to be used later in sensitivity and specificity studies. Also, the bacterial count was analyzed via a spread-plate technique by plating 10-fold serial dilutions from each bacterial concentration on BHI plates and then incubating at 37 °C overnight.

4.3. Clinical Isolates and Protease Preparation.
Twenty clinical isolates of *P. aeruginosa* were collected from King Faisal Specialist Hospital bacterial biobank in Riyadh kingdom at Saudi Arabia. The bibliographic data of the sources were not reviled to us. The samples were as follows: 12 from sputum, 3 from ear, 1 from wound, and 4 from different (unregistered) sites. The specimens were examined in King Faisal Specialist Hospital microbiology lab for complete identification and antibiotic susceptibility testing. Clinical
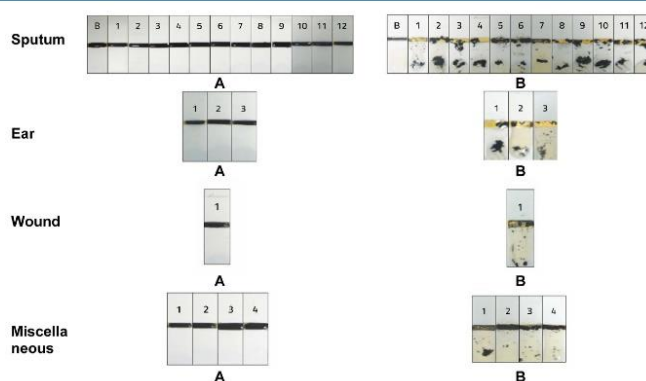

Figure 4. Biosensing of *P. aeruginosa* in clinical samples from King Faisal Specialist Hospital microbiology laboratory. Sensor before (A) and after (B) clinical sample application.

isolates were then stored at −70 °C. After which, samples were thawed and recultured, and a single colony from each clinical isolate was grown in 5 mL BHI medium and incubated at 37 °C for 16 h to provide the PBC stock which was then centrifuged to pellet bacteria. Consequently, culture supernatant containing secreted proteases was added dropwise over the constructed biosensor to examine its applicability.

4.4. Preparation of the Substrate−MNP Composite.

The carboxylated MNP suspension (1 mL) was mixed with the peptide substrate (1.0 mg/mL), EDC (0.57 mg/mL) and NHS (12 µg/mL). The mixture was shaken gently on a rotary shaker at room temperature for 24 h. The substrate−MNP composites were isolated using a magnet separator and washed three times, using a washing buffer to remove uncoupled components (Scheme 1A). Finally, the conjugate was dispersed in a storage buffer and stored at 4 °C until further use.[24,27]

Scheme 1. Fabrication of the *P. aeruginosa* Functional Sensor; (A) Conjugation of the Peptide Substrate to the Magnetic Beads; (B) Sticking the Gold Plated Cellotape on the Paper Solid Support; (C) Self-Assembly of the Magnetic Beads Conjugated Peptides to the Sensor Surface; and (D) Application of the Test Sample and Color Change Observation
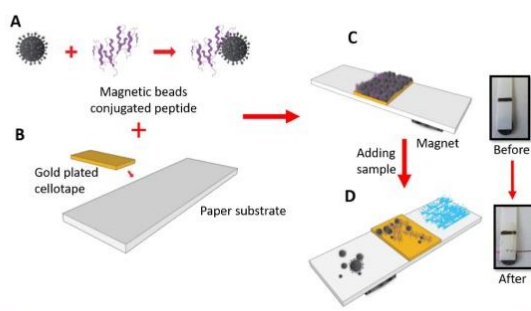
4.5. Biosensing Platform Preparation and Functionalization.

Self-adhesive sheets were purchased from Whatman (London, U.K.) and coated with gold using a sputtering machine in the clean room at KAUST-KSA. The gold-coated sheet was cut into rectangular pieces (4 mm × 2 mm) and stacked over the plastic strip at a specified distance 3 mm. This plastic strip was used as a physical support for the whole biofunctionalization process as well as the *P. aeruginosa* protease detection and quantification sensor (Scheme 1B).

The biosensing gold surface was functionalized with a layer of the black color substrate−MNPs composite. At the beginning, the substrate−MNPs composite suspension was mounted over the gold sensor surface and allowed to stand at room temperature for 30 min for dryness (Scheme 1C). Subsequently, an external magnet (12.5 × 12.5 × 5 mm) with a field strength of 3360 and 573 G at 1 and 10 mm distance, respectively, was passed over the functionalized strip to remove any unattached substrate−MNPs conjugates. At this stage, the sensor surface golden color is masked and turned black (Scheme 1C). After that, a round paper magnet was fixed on the strip back, 2−3 mm distance below the sensor platform.

4.6. Biosensing of *P. aeruginosa* Proteases.

Culture medium supernatant solution containing *P. aeruginosa* crude proteases was added dropwise on the functionalized black

color sensor surface. During the enzymatic cleavage reaction, the paper magnet attracted the cleaved peptide segment−MNPs, prompting a visual observation of the sensor golden color for a qualitative evaluation of the tested samples (Scheme 1D). Moreover, a quantitative evaluation was performed by using different counts of *P. aeruginosa* 4.5×10^7, 4.5×10^6, 4.5×10^5, 4.5×10^4, 4.5×10^3, 4.5×10^2, and 4.5×10 cfu/mL.

4.7. Quantitative Measurements.

The images of the sensors were taken and saved as JPEG format and processed using the ImageJ software, which was developed by the National Institute of Health[28] to calculate the quantitative data. The concentration was calculated by dividing the cleaved area (yellow color) to the total black sensor area. The quantitation was tested using different bacteria concentrations. Experiments were conducted in triplicate.

■ AUTHOR INFORMATION

Corresponding Author
*E-mail: mzourob@alfaisal.edu.

ORCID ⓘ
Karina Weber: 0000-0003-4907-8645
Jürgen Popp: 0000-0003-4257-593X
Mohammed M. Zourob: 0000-0003-2187-1430

Notes
The authors declare no competing financial interest.

■ REFERENCES

(1) Dong, D.; Zou, D.; Liu, H.; Yang, Z.; Huang, S.; Liu, N.; He, X.; Liu, W.; Huang, L. Rapid detection of Pseudomonas aeruginosa targeting the toxA gene in intensive care unit patients from Beijing, China. *Front. Microbiol.* **2015**, *6*, 1100.

(2) Pereira, S. G.; Cardoso, O. Mobile genetic elements of Pseudomonas aeruginosa isolates from hydrotherapy facility and respiratory infections. *Clin. Microbiol. Infect.* **2014**, *20*, O203−O206.

(3) Feizabadi, M. M.; Majnooni, A.; Nomanpour, B.; Fatolahzadeh, B.; Raji, N.; Delfani, S.; Habibi, M.; Asadi, S.; Parvin, M. Direct detection of Pseudomonas aeruginosa from patients with healthcare associated pneumonia by real time PCR. *Infect. Genet. Evol.* **2010**, *10*, 1247−1251.

(4) Mittal, R.; Aggarwal, S.; Sharma, S.; Chhibber, S.; Harjai, K. Urinary tract infections caused by Pseudomonas aeruginosa: a minireview. *J. Infect. Public Health* **2009**, *2*, 101−111.

(5) Altoparlak, U.; Aktas, F.; Celebi, D.; Ozkurt, Z.; Akcay, M. N. Prevalence of metallo-beta-lactamase among Pseudomonas aeruginosa and Acinetobacter baumannii isolated from burn wounds and in vitro activities of antibiotic combinations against these isolates. *Burns* **2005**, *31*, 707−710.

(6) Kang, C.-I.; Sung, H.; kim, H.; kim, S.; Park, S.; Choe, Y.; Oh, M.; Kim, E.; Choe, K. Pseudomonas aeruginosa Bacteremia: Risk Factors for Mortality and Influence of Delayed Receipt of Effective Antimicrobial Therapy on Clinical Outcome. *Clin. Infect. Dis.* **2003**, *15*, 745−751.

(7) Anuj, S. N.; Whiley, D. M.; Kidd, T. J.; Bell, S. C.; Wainwright, C. E.; Nissen, M. D.; Sloots, T. P. Identification of Pseudomonas aeruginosa by a duplex real-time polymerase chain reaction assay targeting the ecfX and the gyrB genes. *Diagn. Microbiol. Infect. Dis.* **2009**, *63*, 127−131.

(8) American Thoracic Society and Infectious Diseases Society of America. Guidelines for the management of adults with hospital-

111

acquired, ventilator-associated, and healthcare-associated pneumonia. *Am. J. Respir. Crit. Care Med.* **2005**, *171*, 388−416.

(9) Mackay, I. M. Real-time PCR in the microbiology laboratory. *Clin. Microbiol. Infect.* **2004**, *10*, 190−212.

(10) Huang, Q.; Hu, Q.; Li, Q. Identification of 8 foodborne pathogens by multicolor combinational probe coding technology in a single real-time PCR. *Clin. Chem.* **2007**, *53*, 1741−1748.

(11) Aghamollaei, H.; Moghaddam, M. M.; Kooshki, H.; Heiat, M.; Mirnejad, R.; Barzi, N. S. Detection of Pseudomonas aeruginosa by a triplex polymerase chain reaction assay based on lasI/R and gyrB genes. *J. Infect. Public Health* **2015**, *8*, 314−322.

(12) Mauch, R. M.; Rossi, C.; Ribeiro, A.; Nolasco da Silva, M.; Levy, C. Assessment of IgG antibodies to Pseudomonas aeruginosa in patients with cystic fibrosis by an enzyme-linked immunosorbent assay (ELISA). *Diagn. Pathol.* **2014**, *9*, 158.

(13) Kaman, W. E.; Arkoubi-El Arkoubi, N. E.; Roffel, S.; Endtz, H. P.; van Belkum, A.; Bikker, F. J.; Hays, J. P. Evaluation of a FRET-Peptide Substrate to Predict Virulence in Pseudomonas aeruginosa. *PLoS One* **2013**, *8*, No. e81428.

(14) Alhogail, S.; Suaifan, G. A. R. Y.; Zourob, M. Rapid colorimetric sensing platform for the detection of Listeria monocytogenes foodborne pathogen. *Biosens. Bioelectron.* **2016**, *86*, 1061−1066.

(15) Alhogail, S.; Suaifan, G.; Bizzarro, S.; Kaman, W.; Bikker, F.; Weber, K.; Cialla-May, D.; Popp, J.; Zourob, M. On site visual detection of Porphyromonas gingivalis related periodontitis by using a magnetic-nanobead based assay for gingipains protease biomarker. *Mikrochim. Acta* **2018**, *185*, 149.

(16) Suaifan, G. A. R. Y.; Alhogail, S.; Zourob, M. Rapid and low-cost biosensor for the detection of Staphylococcus aureus. *Biosens. Bioelectron.* **2017**, *90*, 230−237.

(17) Suaifan, G. A. R. Y.; Alhogail, S.; Zourob, M. Paper-based magnetic nanoparticle-peptide probe for rapid and quantitative colorimetric detection of Escherichia coli O157: H7. *Biosens. Bioelectron.* **2017**, *92*, 702−708.

(18) Girard, G.; Bloemberg, G. V. Central role of quorum sensing in regulating the production of pathogenicity factors in Pseudomonas aeruginosa. *Future Microbiol.* **2008**, *3*, 97−106.

(19) Brint, J. M.; Ohman, D. E. Synthesis of multiple exoproducts in Pseudomonas aeruginosa is under the control of RhlR-RhlI, another set of regulators in strain PAO1 with homology to the autoinducer-responsive LuxR-LuxI family. *J. Bacteriol.* **1995**, *177*, 7155−7163.

(20) Loveday, H. P.; Wilson, J. A.; Kerr, K.; Pitchers, R.; Walker, J. T.; Browne, J. Association between healthcare water systems and Pseudomonas aeruginosa infections: a rapid systematic review. *J. Hosp. Infect.* **2014**, *86*, 7−15.

(21) Thet, N. T.; Hong, S. H.; Marshall, S.; Laabei, M.; Toby, A.; Jenkins, A. Visible, colorimetric dissemination between pathogenic strains of Staphylococcus aureus and Pseudomonas aeruginosa using fluorescent dye containing lipid vesicles. *Biosens. Bioelectron.* **2013**, *41*, 538−543.

(22) Tang, Y.; Zou, J.; Ma, C.; Ali, Z.; Li, Z.; Li, X.; Ma, N.; Mou, X.; Deng, Y.; Zhang, L.; Li, K.; Lu, G.; Yang, H.; He, N. Highly sensitive and rapid detection of Pseudomonas aeruginosa based on magnetic enrichment and magnetic separation. *Theranostics* **2013**, *3*, 85−92.

(23) Tang, Y.; Ali, Z.; Zou, J.; Yang, K.; Mou, X.; Li, Z.; Deng, Y.; Lu, Z.; Ma, C.; Shah, M. A. A.; Elingarami, S.; Yang, H.; He, N. Detection of Pseudomonas aeruginosa based on magnetic enrichment and nested PCR. *J. Nanosci. Nanotechnol.* **2014**, *14*, 4886−4890.

(24) Suaifan, G. A. R. Y.; Esseghaier, C.; Ng, A.; Zourob, M. Wash-less and highly sensitive assay for prostate specific antigen detection. *Analyst* **2012**, *137*, 5614−5619.

(25) Suaifan, G. A. R. Y.; Esseghaier, C.; Ng, A.; Zourob, M. Ultra-rapid colorimetric assay for protease detection using magnetic nanoparticle-based biosensors. *Analyst* **2013**, *138*, 3735−3739.

(26) Suaifan, G. A. R. Y.; Zourob, M. Portable paper-based colorimetric nanoprobe for the detection of Stachybotrys chartarum using peptide labeled magnetic nanoparticles. *Microchim. Acta* **2019**, *186*, 230.

(27) Suaifan, G. A. R. Y.; Shehadeh, M.; Al-Ijel, H.; Ng, A.; Zourob, M. Recent progress in prostate-specific antigen and HIV proteases detection. *Expert Rev. Mol. Diagn.* **2013**, *13*, 707−718.

(28) Rajwa, B.; McNally, H. A.; Varadharajan, P.; Sturgis, J.; Robinson, J. P. AFM/CLSM data visualization and comparison using an open-source toolkit. *Microsc. Res. Tech.* **2004**, *64*, 176−184.

Curriculum vita   personal

NAME: SAHAR ALHOGAIL

- ADRESS: 02 Mesameh st Al Rehmaneyah

  - P.O.Box 230106

  - Riyadh 11321

  - Saudi Arabia

  - Tel : +966505214451

  - Email: salhogail@ksu.edu.sa

EDUCATION & QUALIFICATION

- High school: ALMANARATE INTERNATIONAL SCHOOL 1991
- BSc: Clinical laboratory science Applied Medical Science Collage, Clinical Laboratory, King Saud University Riyadh Saudi Arabia 1995.
- Master Degree: Clinical laboratory science Applied Medical Science Collage, Clinical Laboratory, King Saud University Riyadh Saudi Arabia 2004.
- IELTS: (6.5) 2012.
- 2ND YAER Phd student Cranfield University 2015.
- Training at institution of food Research Norich Research Park Colony September 2015.

WORK & EXPERIENCE

- 1997- 2004 Demonstrator at Collage of Applied Medical Science, Clinical Laboratory, King Saud University Riyadh Kingdom of Saudi Arabia.
- 2004 to date lecturer at Collage of Applied Medical Science, Clinical Laboratory, King Saud University Riyadh Kingdom of Saudi Arabia.

- 1998- 2000 teaching analytical chemistry for enzymology Lab at Collage of Applied Medical Science for undergraduates at Clinical Laboratory, King Saud University Riyadh Kingdom Of Saudi Arabia

- 1999-2001 Teaching biochemistry & Environmental Lab at Collage of Applied Medical Science, Clinical Laboratory, King Saud University Riyadh Kingdom Of Saudi Arabia

- 2000 – 2013 mycology Lab for master student and microbiology topics for undergraduate at Collage of Applied Medical Science, Clinical Laboratory, King Saud University Riyadh Kingdom of Saudi Arabia.

- 2014- 2015 PhD student at Cranfield university.

- 2015 -2021 lecturer at King Saud University and continue my research of nanoparticles.

- 2018-2020 Supervisor of the Internship Committee.

- 2017-2021 join Jena university to continue PhD

PRESENTATION:

- 8 May 2014 presentation at Carnfield University under the title of Developing of rapid nano sensor for pathogen detection .

- 15 Jan 2015 presentation at Carnfield University under the title of Development of diagnostic tools for oral pathogens .

- 20 Apr 2015 presentation at king Alfisal University under the title of Developing paper based sensing plat form *for P.gingivalis.* .

- 10 Mar 2016 presentation at king Saud university under the title of Developing of rapid nano sensor for bacterial detection .

- 23 Feb 2017 presentation at King Abdullaziz City for Science and Technology under the title of Review on the recent developing sensors using nanomagnetic particles.

- 10 Mar 2019 presentation at Alfaisal University under the title of Rapid papper based assay for *Listeria monocytogenes.*

- M. Zourob, Sahar Alhogail, Ghadeer Suifan, 'Recent development in pathogens detetcion' Ifran, Nano Micro and Biotechnology conference, Ifrane, Morocco, 26-28 Oct 2014.

- *Sahar Alhogail, Ghadeer Suaifan, Mohammed Zourob,* Rapid and Low-cost Nanobiosensor for Pathogens Detection, Dubai, UAE, 4th Nano Today 6-10 Dec 2015.

- *Sahar Alhogail, Ghadeer Suaifan, Mohammed Zourob,* Rapid and low-cost paper-based nanobiosensor for pathogens detection, Gothenburg, Sweden, 2527 May 2016.

114

CONFERENCE CONTRIBUTIONS

- 4^Th Nano Today conference 6-10 December 2015 Dubai.
- Saudi Society of Clinical Laboratory Sciences 2017.
- Saudi Society for clinical microbiology and infectious disease marsh 2017   Jeddah Saudi Arabia.
- Congress biosensors conference 12-15 June 2018 Miami.
- Saudi Society of Clinical Laboratory Sciences 2019.
- MENA International conference on Biosensors 2021.

POSTER PRESENTATION

- Development of low cost and portable bacterial detection platform.   Presented at King Abdullah University for Science and Technology 2015.
- Development of low cost and portable bacterial detection platform. Presented at Biosensors 2016 from 25-27 may Gothenburg Sweden.

PUBLICATIONS

1. Rapid colorimetric sensing platform for the detection of *Listeria monocytogenes* foodborne pathogen. Sahar Alhogail, Ghadeer A. R. Y. Suaifan, Mohammed Zourob. Biosens Bioelectron. 2016 Dec 15;86:1061-1066.

2. Rapid and low-cost biosensor for the detection of *Staphylococcus aureus.* Ghadeer A. R. Y. Suaifan, Sahar Alhogail, Mohammed Zourob. Biosens Bioelectron. 2017 Apr 15;90:230-237.

3. Paper-based magnetic nanoparticle-peptide probe for rapid and quantitative colorimetric detection of *Escherichia coli O157:H7*. Ghadeer A. R. Y. Suaifan, Sahar Alhogail, Mohammed Zourob. Biosens Bioelectron. 2017 Jun 15;92:702-708.

4. Simple and rapid peptide nanoprobe biosensor for the detection of *Legionellaceae.* Sahar Alhogail, Raja Chinnappan, Majeda Alrifai, Ghadeer A. R. Y. Suaifan, Floris J. Bikker, Wendy E. Kaman, Karina Weber, Dana Cialla-May, Jürgen Popp, Mohamed B. Alfageeh, K. Al-Kattan, Mohammed M. Zourob. Analyst. 2021 Jun 7;146(11):3568-3577.

5. On site visual detection of *Porphyromonas gingivalis* related periodontitis by using a magnetic-nanobead based assay for gingipains protease biomarkers. Sahar Alhogail, Ghadeer A. R. Y. Suaifan, Sergio Bizzarro, Wendy E. Kaman, Floris J. Bikker, Karina Weber, Dana Cialla-May, Jürgen Popp, Mohammed Zourob. Mikrochim Acta. 2018 Feb 1;185(2):149.

6. Rapid colorimetric detection of *Pseudomonas aeruginosa* in clinical isolates using a magnetic nanoparticle biosensor. Sahar Alhogail, Ghadeer A. R. Y. Suaifan, Floris J. Bikker, Wendy E. Kaman, Karina Weber, Dana Cialla-May, Jürgen Popp, Mohammed M. Zourob. *ACS Omega*. 2019;4(26):21684-21688.